Hadron Spectroscopy at COMPASS

Boris Grube
for the COMPASS Collaboration

CERN

On leave of absence from
Physik-Department E18
Technische Universität München,
Garching, Germany

Hadron Physics with High-Momentum Hadron Beams at J-PARC
Tsukuba, 16. Jan 2013

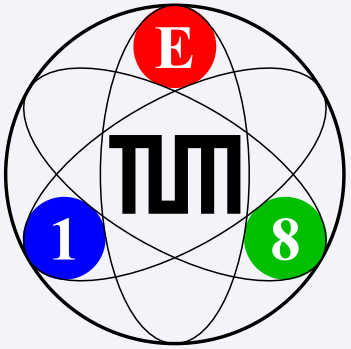

The COMPASS Physics Program

COmmon **M**uon and **P**roton **A**pparatus for **S**tructure and **S**pectroscopy

Goal

- Study non-perturbative QCD
- Probe structure and dynamics of hadrons

Chiral dynamics

- $\pi\gamma$ and $K\gamma$ reactions (Primakoff)
- π and K polarizabilities

Hadron spectroscopy

- Mass spectrum of hadrons
- Gluonic excitations

Nucleon structure

- Helicity and transversity PDFs
- $k_\perp$-dependent PDFs
- Generalized PDFs

The COMPASS Physics Program

COmmon **M**uon and **P**roton **A**pparatus for **S**tructure and **S**pectroscopy

Goal

- Study non-perturbative QCD
- Probe structure and dynamics of hadrons

Chiral dynamics

- $\pi\gamma$ and $K\gamma$ reactions (Primakoff)
- π and K polarizabilities

Hadron spectroscopy

- Mass spectrum of hadrons
- Gluonic excitations

Nucleon structure

- Helicity and transversity PDFs
- $k_\perp$-dependent PDFs
- Generalized PDFs

The COMPASS Physics Program

COmmon **M**uon and **P**roton **A**pparatus for **S**tructure and **S**pectroscopy

Goal

- Study non-perturbative QCD
- Probe structure and dynamics of hadrons

Chiral dynamics

- $\pi\gamma$ and $K\gamma$ reactions (Primakoff)
- π and K polarizabilities

Hadron spectroscopy

- Mass spectrum of hadrons
- Gluonic excitations

Nucleon structure

- Helicity and transversity PDFs
- $k_\perp$-dependent PDFs
- Generalized PDFs

The COMPASS Physics Program

COmmon **M**uon and **P**roton **A**pparatus for **S**tructure and **S**pectroscopy

Goal

- Study non-perturbative QCD
- Probe structure and dynamics of hadrons

Chiral dynamics

- $\pi\gamma$ and $K\gamma$ reactions (Primakoff)
- π and K polarizabilities

Hadron spectroscopy

- Mass spectrum of hadrons
- Gluonic excitations

Nucleon structure

- Helicity and transversity PDFs
- $k_\perp$-dependent PDFs
- Generalized PDFs

Outline

1. Introduction

2. Search for spin-exotic mesons in π^- diffraction
   - PWA of $\pi^-\pi^+\pi^-$ system
   - PWA of $\pi^-\eta$ and $\pi^-\eta'$ from final states
   - PWA of $\pi^-\pi^+\pi^-\pi^+\pi^-$ decay channel

3. Search for scalar glueballs in central production
   - PWA of $\pi^+\pi^-$ system

Outline

The COMPASS Experiment at the CERN SPS

Experimental Setup

NIM A **577**, 455 (2007)

Fixed-target experiment

- Two-stage spectrometer
- Large acceptance over wide kinematic range
- Electromagnetic and hadronic calorimeters
- Beam and final-state particle ID (CEDARs, RICH)

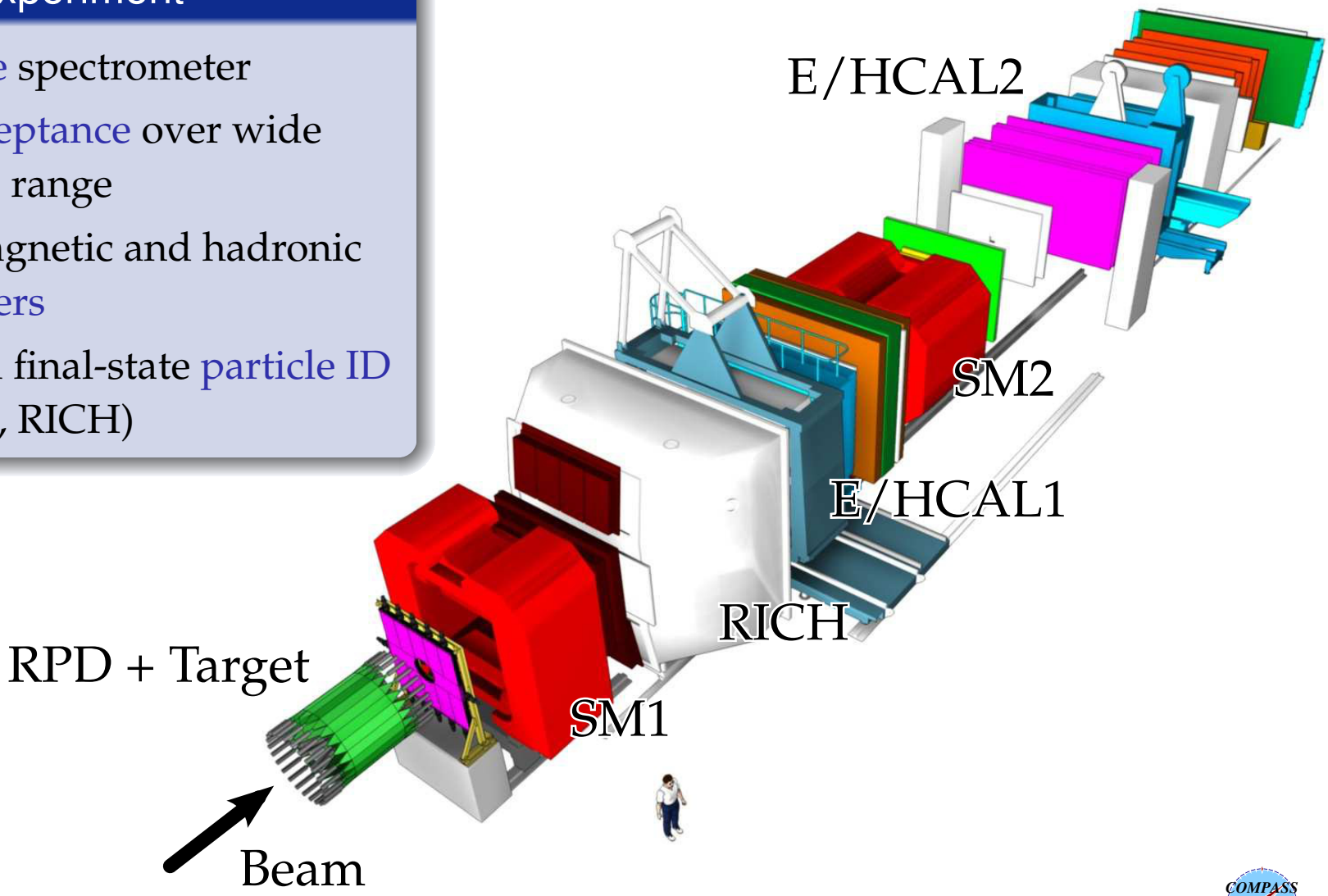

The COMPASS Experiment at the CERN SPS

Experimental Setup

NIM A **577**, 455 (2007)

Fixed-target experiment

- Two-stage spectrometer
- Large acceptance over wide kinematic range
- Electromagnetic and hadronic calorimeters
- Beam and final-state particle ID (CEDARs, RICH)

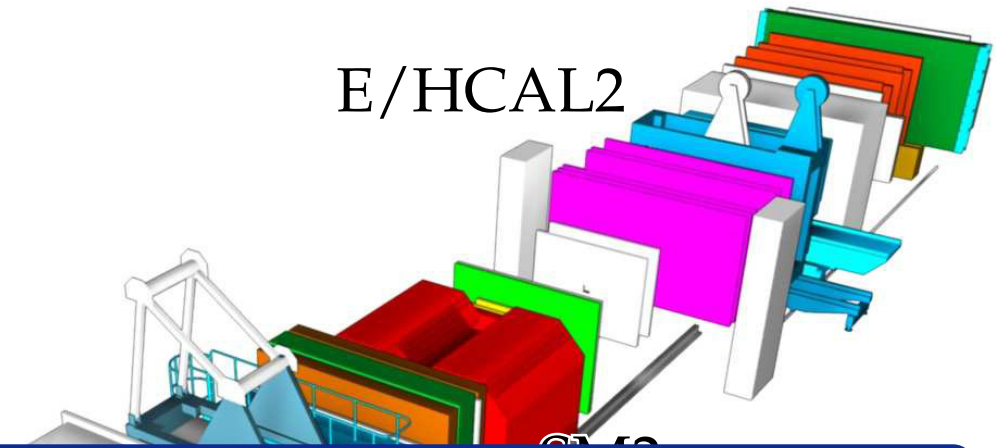

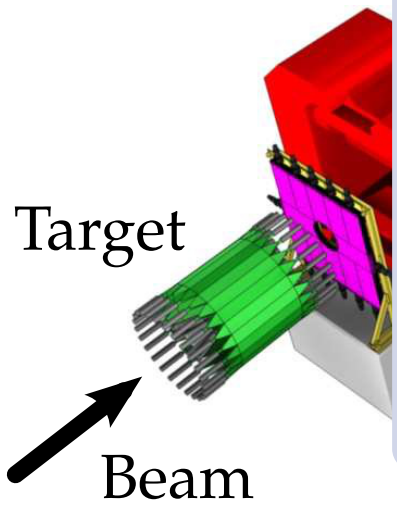

Beam parameters

- 400 GeV/c primary p from SPS
  - $1.5 \cdot 10^{12}$ sec^{-1} on Be target
  - Duty cycle: 20-30 %
- Secondary h beam through M2 beam line NIM **A 343** (1994) 351
  - At 190 GeV/c: up to $4 \cdot 10^7$ sec^{-1} (limited by radio protection)

The COMPASS Experiment at the CERN SPS

Experimental Setup

NIM A **577**, 455 (2007)

Fixed-target experiment

- Two-stage spectrometer
- Large acceptance over wide kinematic range
- Electromagnetic and hadronic calorimeters
- Beam and final-state particle ID (CEDARs, RICH)

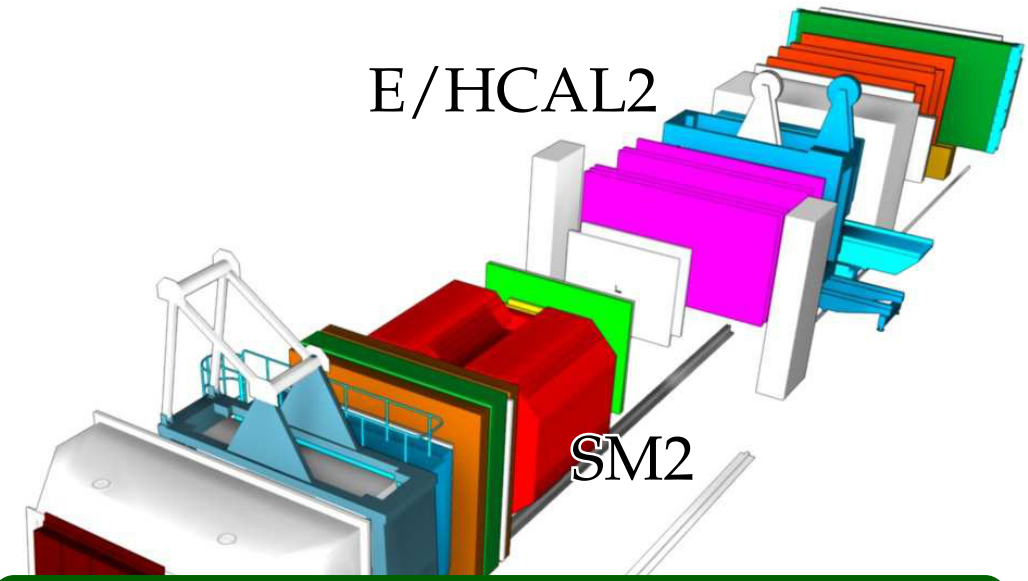

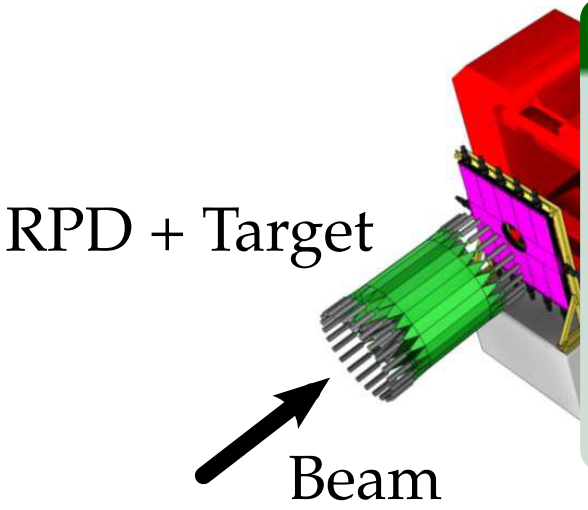

Hadron spectroscopy 2008-09, 2012

- 190 GeV/c secondary hadron beams
  - h^- **beam:** 97 % π^-, 2 % K^-, 1 % $\bar{p}$
  - h^+ **beam:** 75 % p, 24 % π^+, 1 % K^+
- Various targets: $\ell\mathbf{H_2}$, Ni, **Pb**, W
- $>$ 1 PByte of data per year

Mesons in the Constituent Quark Model

Spin-parity rules for bound $q\bar{q}$ system

- Quark spins couple to total intrinsic spin $S = 0$ (singlet) or 1 (triplet)
- Relative orbital angular Momentum $\vec{L}$ and total spin $\vec{S}$ couple to meson spin $\vec{J} = \vec{L} + \vec{S}$
- Parity $P = (-1)^{L+1}$
- Charge conjugation $C = (-1)^{L+S}$
- **Forbidden J^{PC}: $0^{--}, 0^{+-}, 1^{-+}, 2^{+-}, 3^{-+}, \ldots$**
- Extension to charged mesons via G parity: $G = (-1)^{L+S+I}$

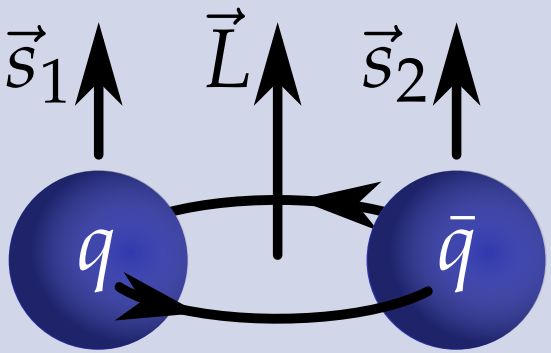

QCD allows for **states beyond the CQM**

- Hybrids $|q\bar{q}g\rangle$, glueballs $|gg\rangle$, multi-quark states $|q^2\bar{q}^2\rangle, \ldots$
- **Physical mesons:** superposition of all allowed basis states
- "Exotic" mesons have quantum numbers forbidden for $|q\bar{q}\rangle$
  - Particularly interesting: J^{PC}-exotic states

Mesons in the Constituent Quark Model

Spin-parity rules for bound $q\bar{q}$ system

- Quark spins couple to total intrinsic spin $S = 0$ (singlet) or 1 (triplet)
- Relative orbital angular Momentum $\vec{L}$ and total spin $\vec{S}$ couple to meson spin $\vec{J} = \vec{L} + \vec{S}$
- Parity $P = (-1)^{L+1}$
- Charge conjugation $C = (-1)^{L+S}$
- **Forbidden J^{PC}: $0^{--}, 0^{+-}, 1^{-+}, 2^{+-}, 3^{-+}, \ldots$**
- Extension to charged mesons via G parity: $G = (-1)^{L+S+I}$

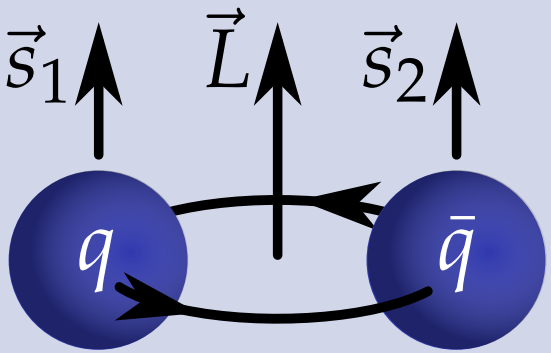

QCD allows for **states beyond the CQM**

- Hybrids $|q\bar{q}g\rangle$, glueballs $|gg\rangle$, multi-quark states $|q^2\bar{q}^2\rangle, \ldots$
- **Physical mesons:** superposition of all allowed basis states
- "Exotic" mesons have quantum numbers forbidden for $|q\bar{q}\rangle$
  - Particularly interesting: J^{PC}-exotic states

Mesons in the Constituent Quark Model

Spin-parity rules for bound $q\bar{q}$ system

- Quark spins couple to total intrinsic spin $S = 0$ (singlet) or 1 (triplet)
- Relative orbital angular Momentum $\vec{L}$ and total spin $\vec{S}$ couple to meson spin $\vec{J} = \vec{L} + \vec{S}$
- Parity $P = (-1)^{L+1}$
- Charge conjugation $C = (-1)^{L+S}$

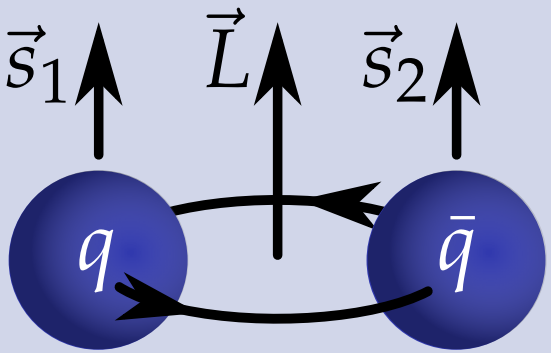

- **Forbidden J^{PC}: $0^{--}, 0^{+-}, 1^{-+}, 2^{+-}, 3^{-+}, \ldots$**
- Extension to charged mesons via G parity: $G = (-1)^{L+S+I}$

QCD allows for **states beyond the CQM**

- Hybrids $|q\bar{q}g\rangle$, glueballs $|gg\rangle$, multi-quark states $|q^2\bar{q}^2\rangle, \ldots$
- **Physical mesons:** superposition of all allowed basis states
- "Exotic" mesons have quantum numbers forbidden for $|q\bar{q}\rangle$
  - Particularly interesting: J^{PC}-exotic states

Mesons in the Constituent Quark Model

Spin-parity rules for bound $q\bar{q}$ system

- Quark spins couple to total intrinsic spin $S = 0$ (singlet) or 1 (triplet)
- Relative orbital angular Momentum $\vec{L}$ and total spin $\vec{S}$ couple to meson spin $\vec{J} = \vec{L} + \vec{S}$
- Parity $P = (-1)^{L+1}$
- Charge conjugation $C = (-1)^{L+S}$

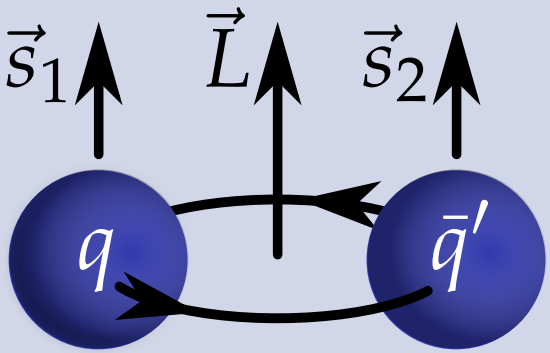

- **Forbidden J^{PC}: $0^{--}, 0^{+-}, 1^{-+}, 2^{+-}, 3^{-+}, \ldots$**
- Extension to charged mesons via G parity: $G = (-1)^{L+S+I}$

QCD allows for **states beyond the CQM**

- Hybrids $|q\bar{q}g\rangle$, glueballs $|gg\rangle$, multi-quark states $|q^2\bar{q}^2\rangle, \ldots$
- **Physical mesons:** superposition of all allowed basis states
- "Exotic" mesons have quantum numbers forbidden for $|q\bar{q}\rangle$
  - Particularly interesting: J^{PC}-exotic states

Mesons in the Constituent Quark Model

Spin-parity rules for bound $q\bar{q}$ system

- Quark spins couple to total intrinsic spin $S = 0$ (singlet) or 1 (triplet)
- Relative orbital angular Momentum $\vec{L}$ and total spin $\vec{S}$ couple to meson spin $\vec{J} = \vec{L} + \vec{S}$
- Parity $P = (-1)^{L+1}$
- Charge conjugation $C = (-1)^{L+S}$

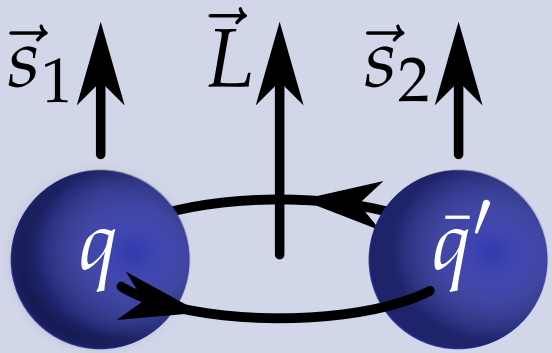

- **Forbidden J^{PC}: $0^{--}, 0^{+-}, 1^{-+}, 2^{+-}, 3^{-+}, \ldots$**
- Extension to charged mesons via G parity: $G = (-1)^{L+S+I}$

QCD allows for **states beyond the CQM**

- Hybrids $|q\bar{q}g\rangle$, glueballs $|gg\rangle$, multi-quark states $|q^2\bar{q}^2\rangle, \ldots$
- **Physical mesons:** superposition of all allowed basis states
- "Exotic" mesons have quantum numbers forbidden for $|q\bar{q}\rangle$
  - Particularly interesting: J^{PC}-exotic states

Light-Meson Spectrum in Lattice QCD

State-of-the-art light-meson spectrum

Dudek, PRD 84 (2011) 074023

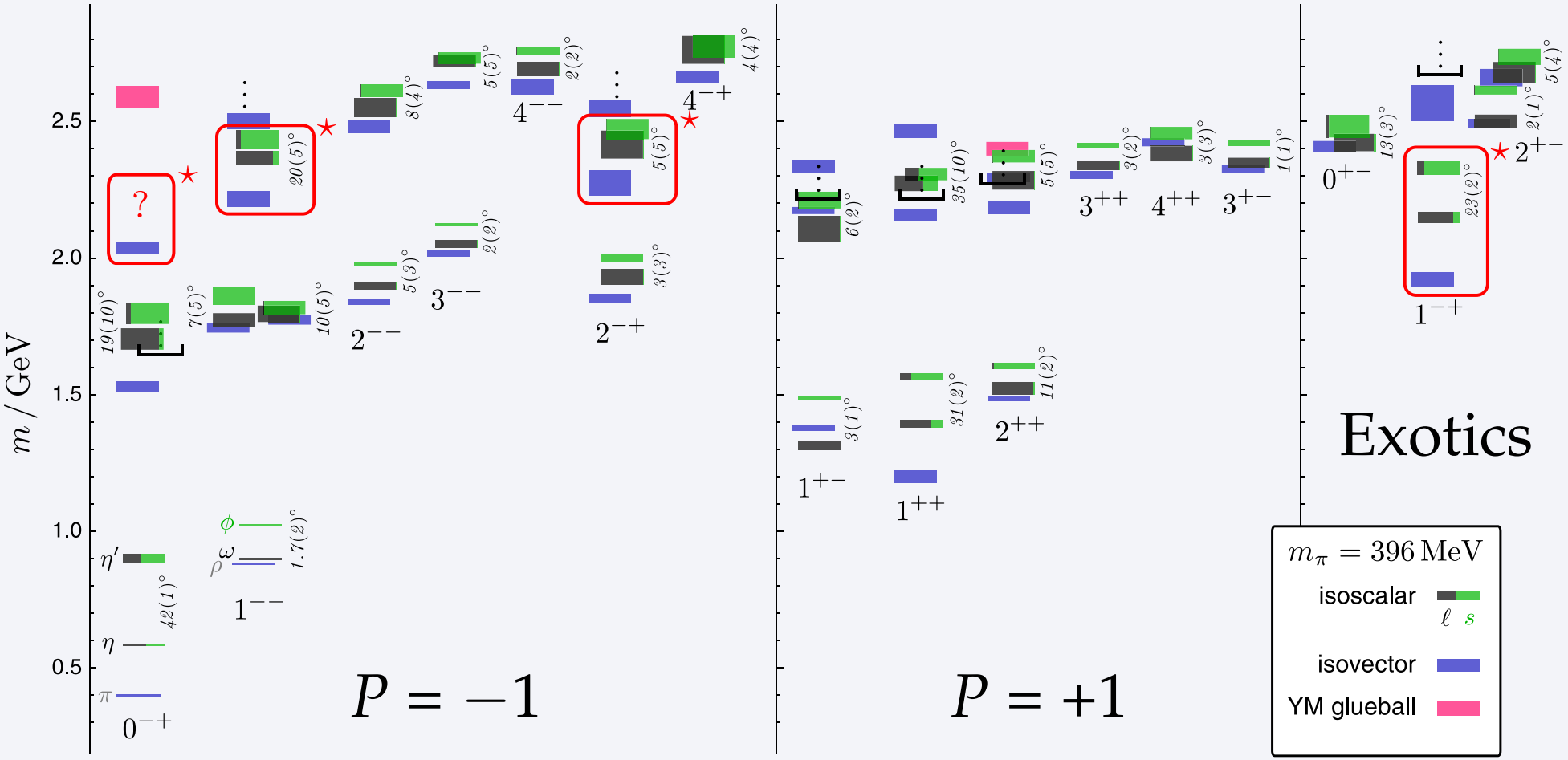

- Resonance widths and decay modes still very difficult

Outline

Production of Hadrons in Diffractive Dissociation

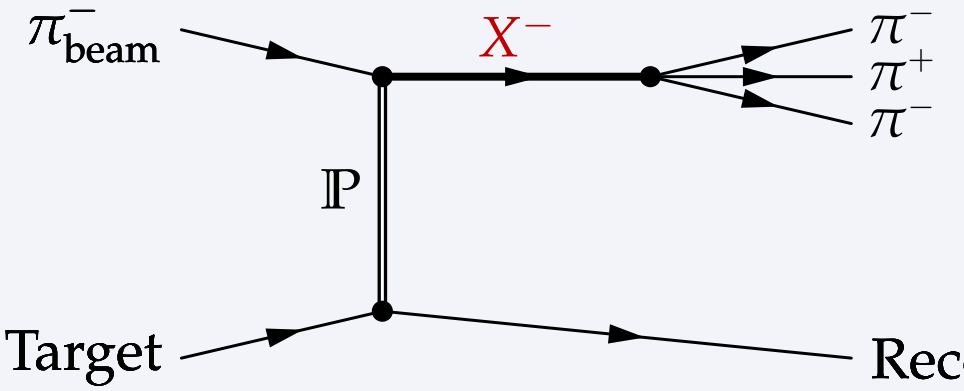

- Soft scattering of beam hadron off nuclear target (remains intact)
  - Beam particle is excited into intermediate state X
  - X decays into n-body final state
- High $\sqrt{s}$ and low t': Pomeron exchange dominates strong interaction
- Rich spectrum: large number of overlapping and interfering X
- **Goal:** use kinematic distribution of final-state particles to
  - Disentangle all resonances X
  - Determine their mass, width, and quantum numbers
- **Method:** partial-wave analysis (PWA)

Production of Hadrons in Diffractive Dissociation

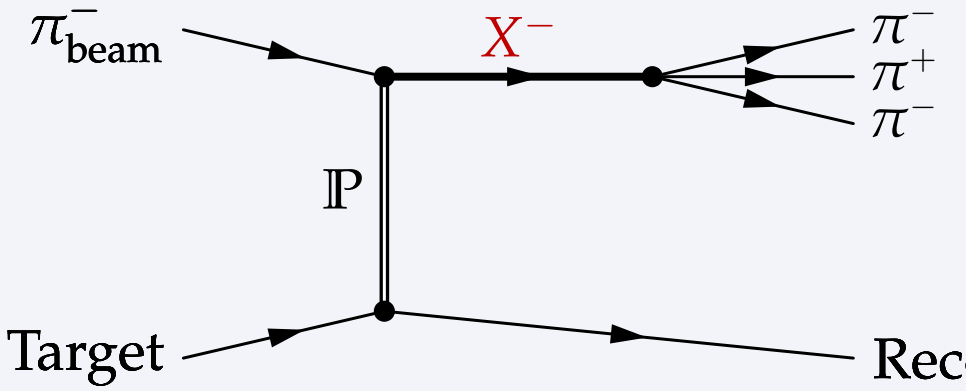

- Soft scattering of beam hadron off nuclear target (remains intact)
  - Beam particle is excited into intermediate state X
  - X decays into n-body final state
- High $\sqrt{s}$ and low t': Pomeron exchange dominates strong interaction
- Rich spectrum: large number of overlapping and interfering X
- **Goal:** use kinematic distribution of final-state particles to
  - Disentangle all resonances X
  - Determine their mass, width, and quantum numbers
- **Method:** partial-wave analysis (PWA)

Production of Hadrons in Diffractive Dissociation

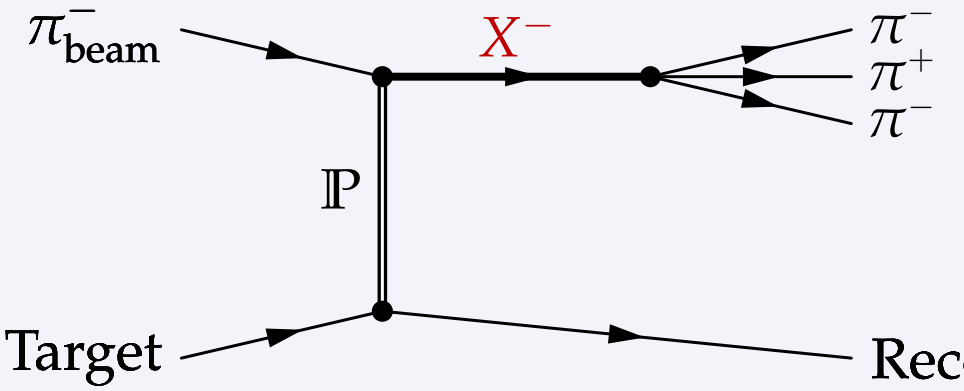

- Soft scattering of beam hadron off nuclear target (remains intact)
  - Beam particle is excited into intermediate state X
  - X decays into n-body final state
- High $\sqrt{s}$ and low t': Pomeron exchange dominates strong interaction
- Rich spectrum: large number of overlapping and interfering X
- **Goal:** use kinematic distribution of final-state particles to
  - Disentangle all resonances X
  - Determine their mass, width, and quantum numbers
- **Method:** partial-wave analysis (PWA)

Diffractive Dissociation of π^- into $\pi^-\pi^+\pi^-$ Final State

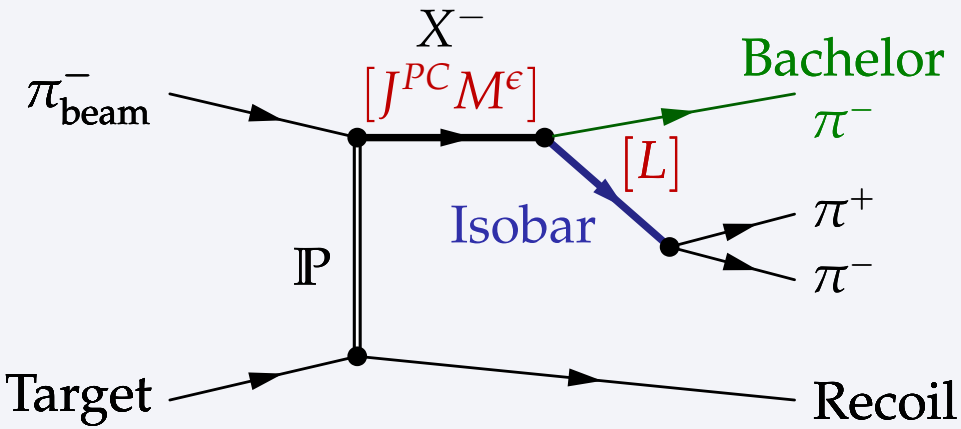

Isobar model: X^- decay is chain of successive two-body decays

- **"Wave":** unique combination of isobar and quantum numbers
- Full wave specification (in reflectivity basis): $J^{PC}M^{\epsilon}[\text{isobar}]L$

Fit model: $\sigma(m_X,\tau) = \sigma_0 \left|\sum_{\text{waves}} T_{\text{wave}}(m_X)\, A_{\text{wave}}(m_X,\tau)\right|^2$

- Calculable decay amplitudes $A_{\text{wave}}(m_X,\tau)$
- Transition amplitudes $T_{\text{wave}}(m_X)$ determined from multi-dimensional fit to final-state kinematic distributions taking into account interference effects

Diffractive Dissociation of π^- into $\pi^-\pi^+\pi^-$ Final State

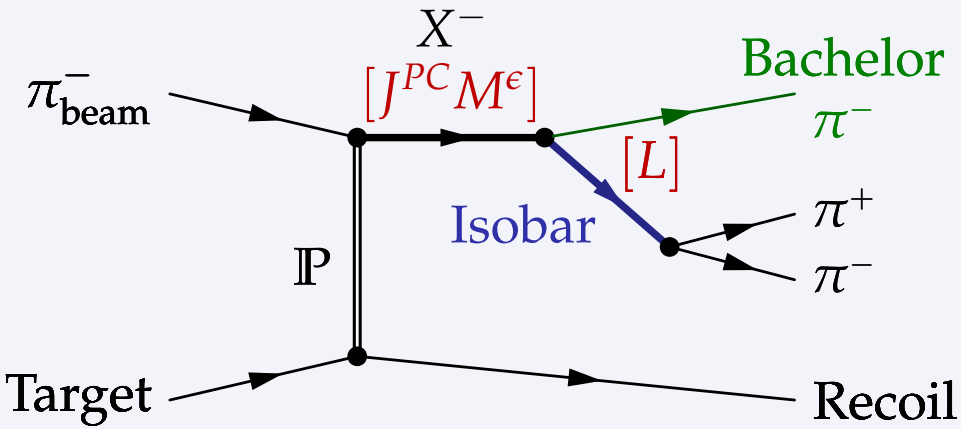

Isobar model: X^- decay is chain of successive two-body decays

- **"Wave":** unique combination of isobar and quantum numbers
- Full wave specification (in reflectivity basis): $J^{PC}M^{\epsilon}[\text{isobar}]L$

Fit model: $\sigma(m_X,\tau) = \sigma_0 \left|\sum_{\text{waves}} T_{\text{wave}}(m_X)\, A_{\text{wave}}(m_X,\tau)\right|^2$

- Calculable decay amplitudes $A_{\text{wave}}(m_X,\tau)$
- Transition amplitudes $T_{\text{wave}}(m_X)$ determined from multi-dimensional fit to final-state kinematic distributions taking into account interference effects

PWA of $\pi^- p \to \pi^-\pi^+\pi^- p_{\text{slow}}$

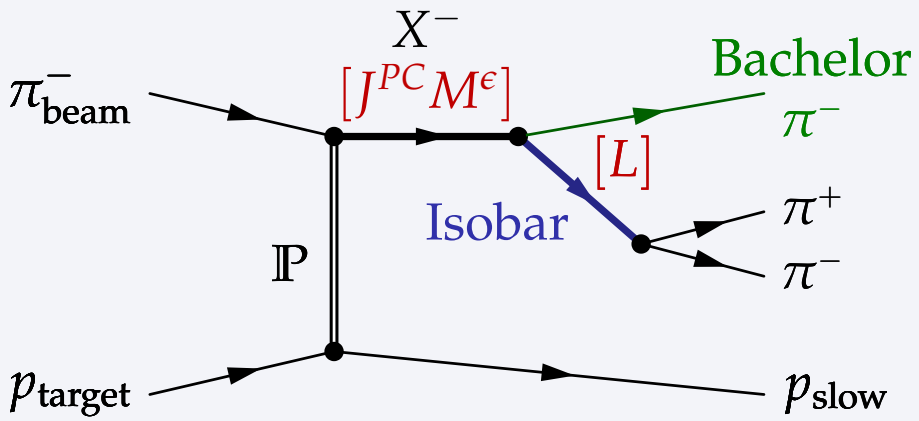

- 190 GeV/c negative hadron beam: 97 % π^-, 2 % K^-, 1 % $\bar{p}$
- Liquid hydrogen target
- Recoil proton p_{slow} measured by RPD
- Kinematic range $0.1 < t' < 1.0\ (\text{GeV}/c)^2$

PWA of $\pi^- p \to \pi^-\pi^+\pi^- p_{\text{slow}}$

World's largest 3π data set: $\approx$**50 M exclusive events**

- Challenging analysis
  - Needs precise understanding of apparatus
  - Model deficiencies become visible

PWA of $\pi^- p \to \pi^-\pi^+\pi^- p_{\text{slow}}$

World's largest 3π data set: $\approx$**50 M exclusive events**

- Challenging analysis
  - Needs precise understanding of apparatus
  - Model deficiencies become visible

$\pi^-\pi^+\pi^-$ invariant mass distribution

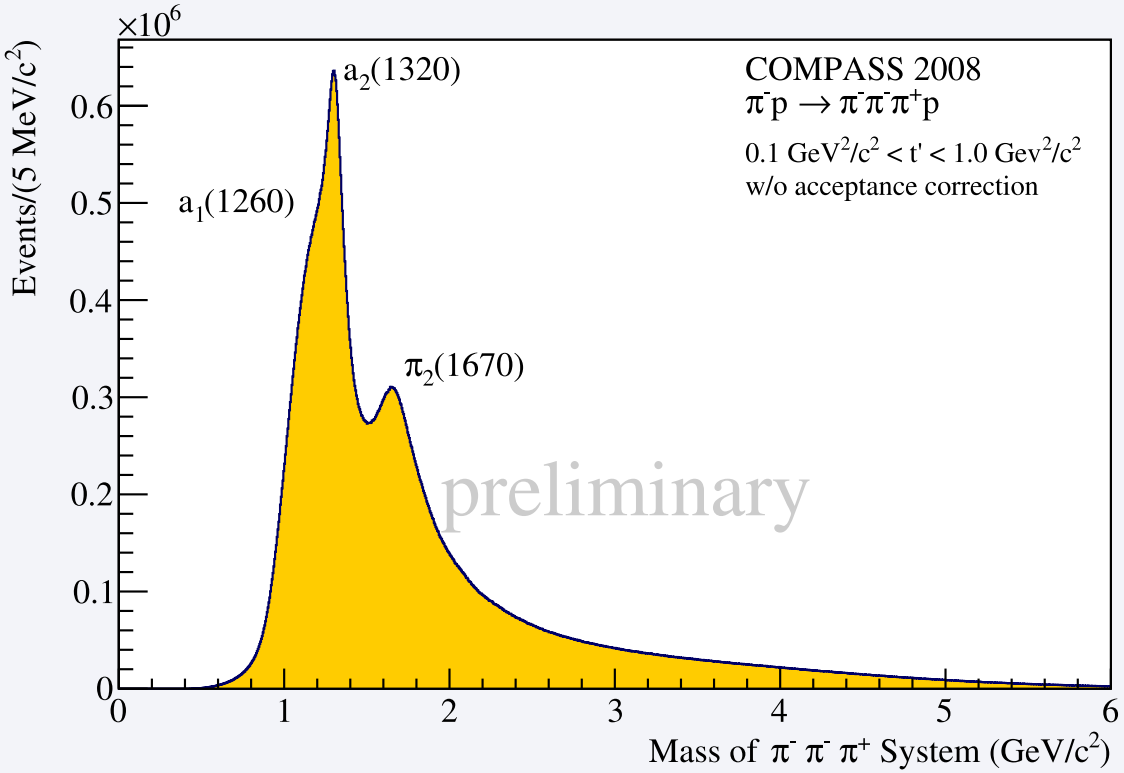

PWA of $\pi^- p \to \pi^-\pi^+\pi^- p_{\text{slow}}$

World's largest 3π data set: $\approx$50 M exclusive events

- Challenging analysis
  - Needs precise understanding of apparatus
  - Model deficiencies become visible

$\pi^-\pi^+\pi^-$ invariant mass distribution

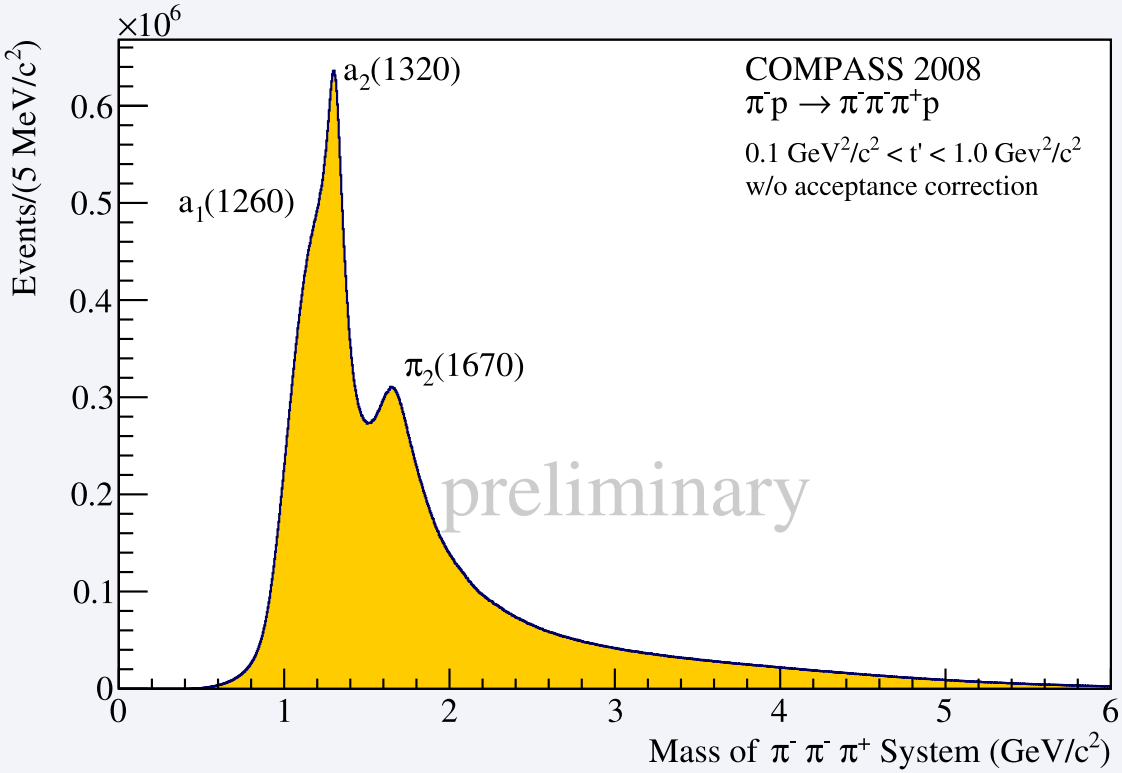

Dalitz plot for $\pi_2(1670)$ region

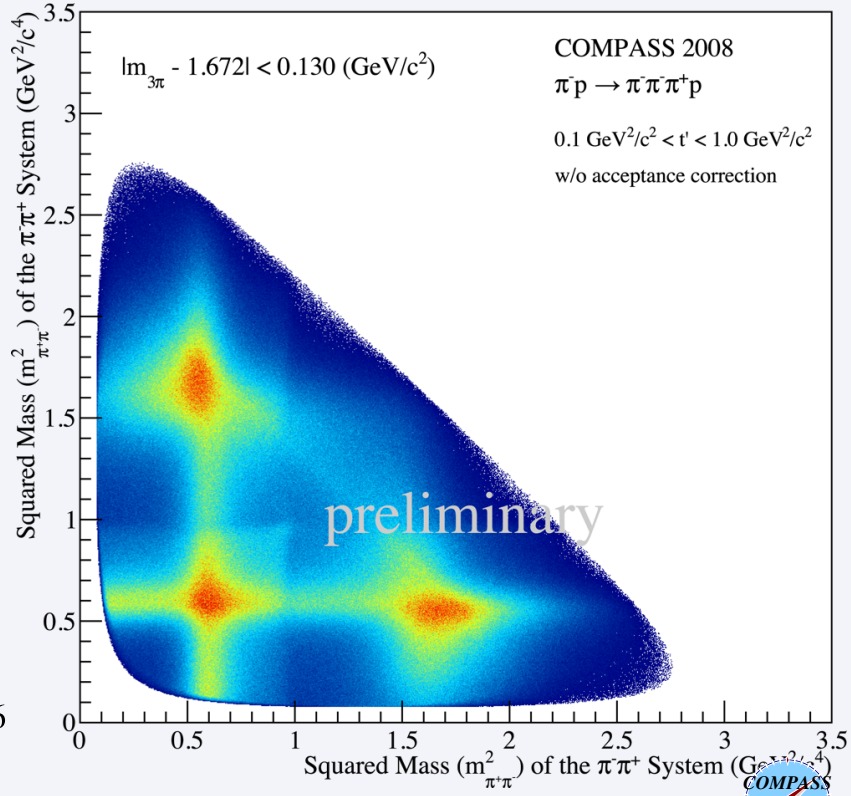

PWA of $\pi^- p \to \pi^-\pi^+\pi^- p_{\text{slow}}$

$\pi^-\pi^+\pi^-$ invariant mass spectrum

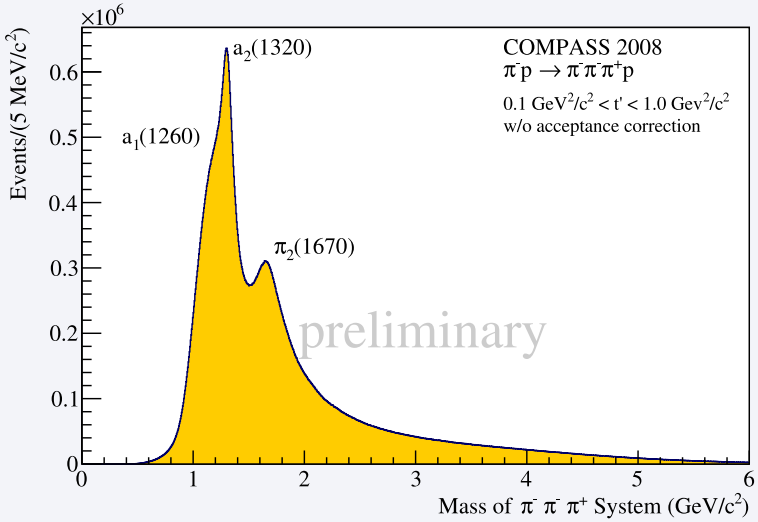

PWA of $\pi^- p \to \pi^-\pi^+\pi^- p_{\text{slow}}$

$\pi^-\pi^+\pi^-$ invariant mass spectrum

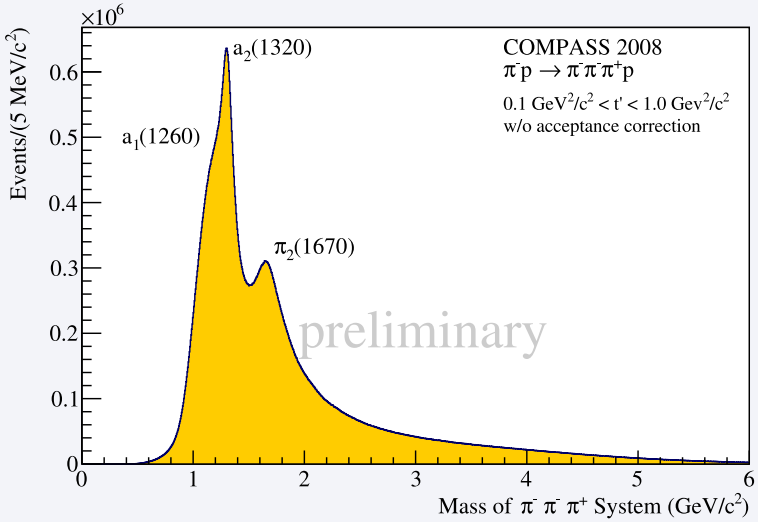

$1^{++}\,0^+\,[\rho\pi]S$: $a_1(1260)$

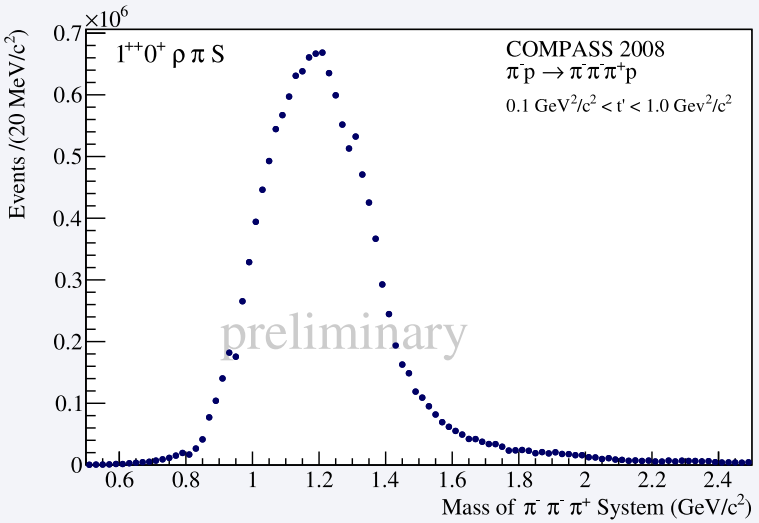

PWA of $\pi^- p \to \pi^-\pi^+\pi^- p_{\text{slow}}$

$\pi^-\pi^+\pi^-$ invariant mass spectrum

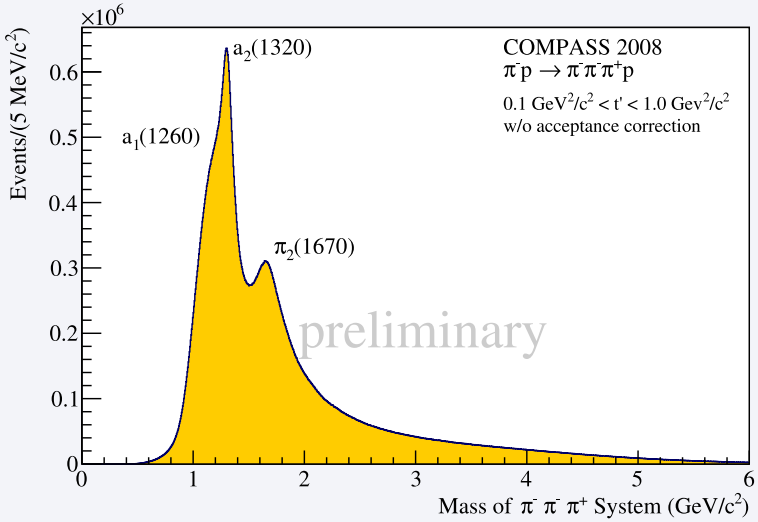

$1^{++}\,0^+\,[\rho\pi]S$: $a_1(1260)$

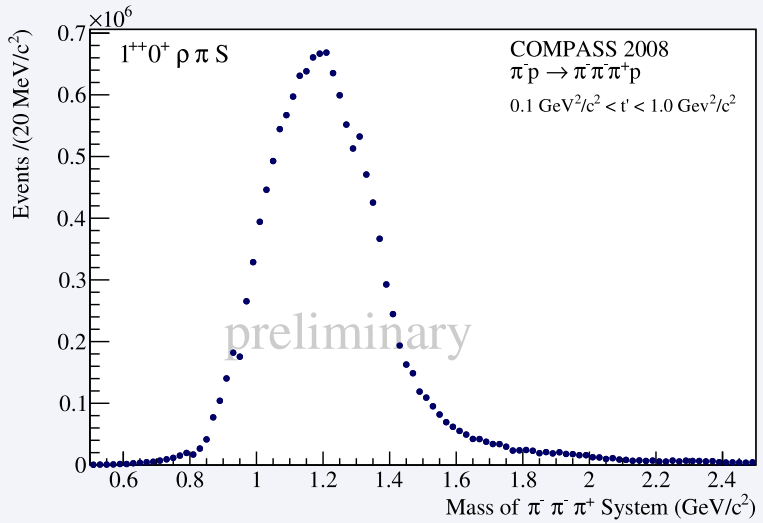

$2^{++}\,1^+\,[\rho\pi]D$: $a_2(1320)$

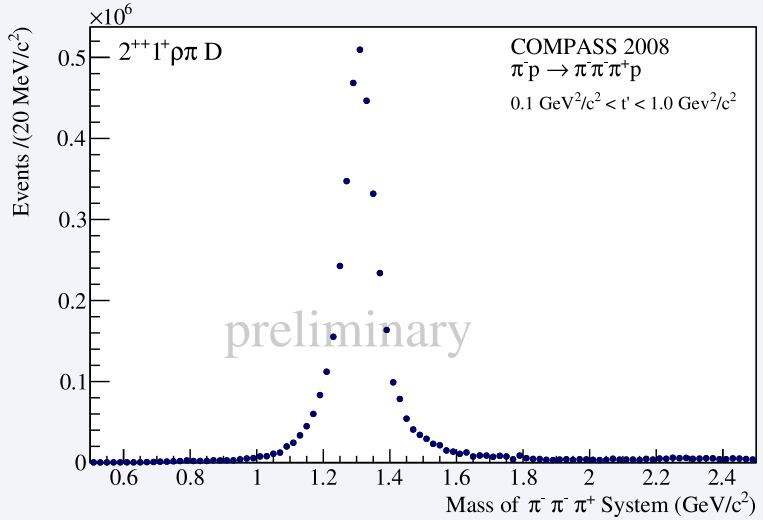

PWA of $\pi^- p \to \pi^-\pi^+\pi^- p_{\text{slow}}$

$\pi^-\pi^+\pi^-$ invariant mass spectrum

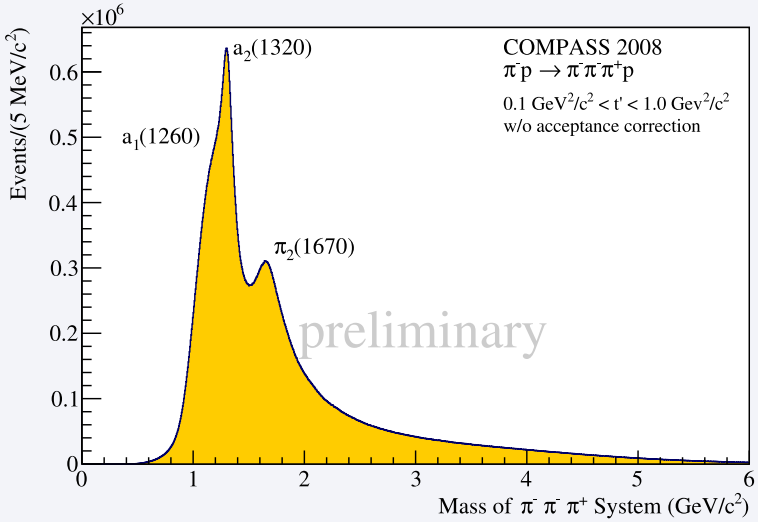

$1^{++}\,0^+\,[\rho\pi]S$: $a_1(1260)$

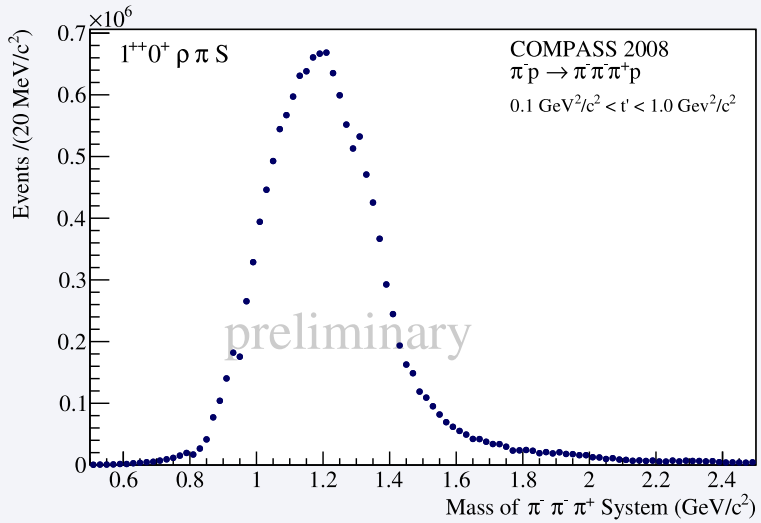

$2^{-+}\,0^+\,[f_2\pi]S$: $\pi_2(1670)$

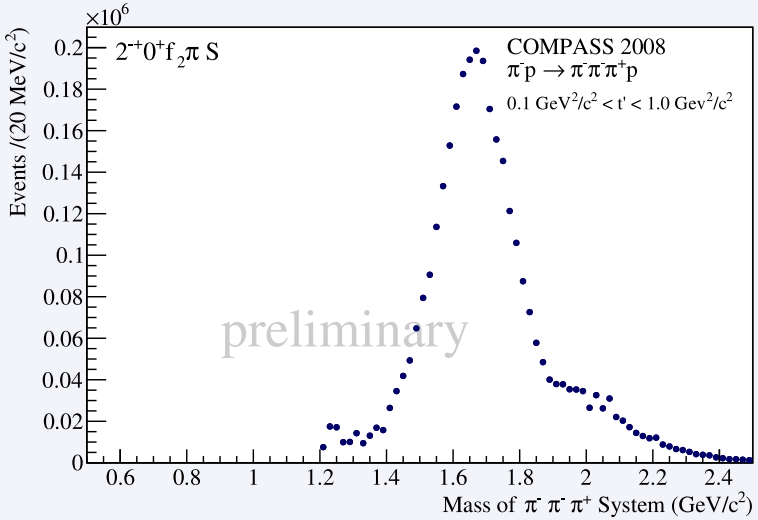

$2^{++}\,1^+\,[\rho\pi]D$: $a_2(1320)$

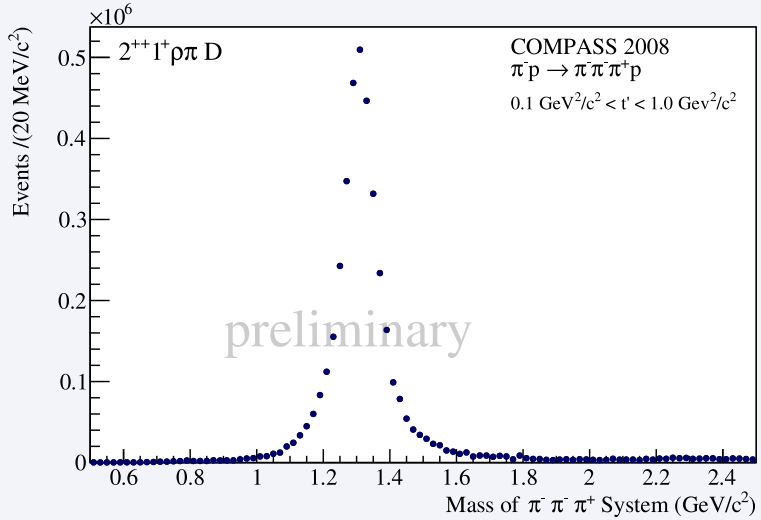

PWA of $\pi^- p \to \pi^-\pi^+\pi^- p_{\text{slow}}$

$\pi^-\pi^+\pi^-$ invariant mass spectrum

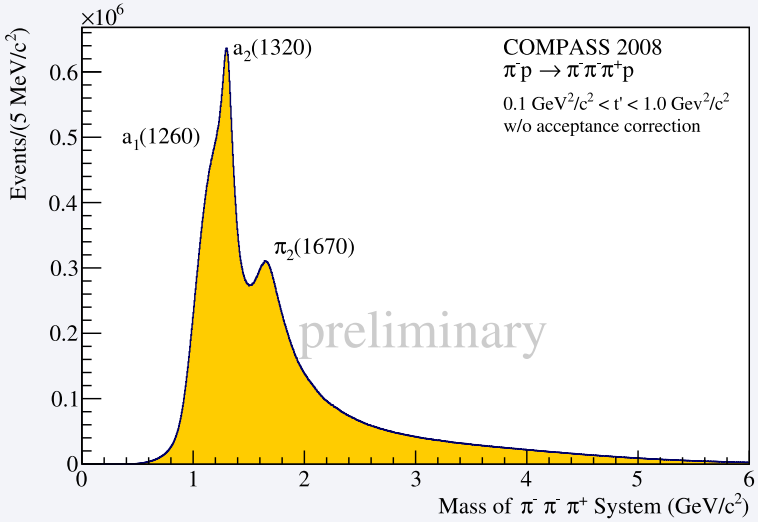

$2^{-+}\,0^+\,[f_2\pi]S$: $\pi_2(1670)$

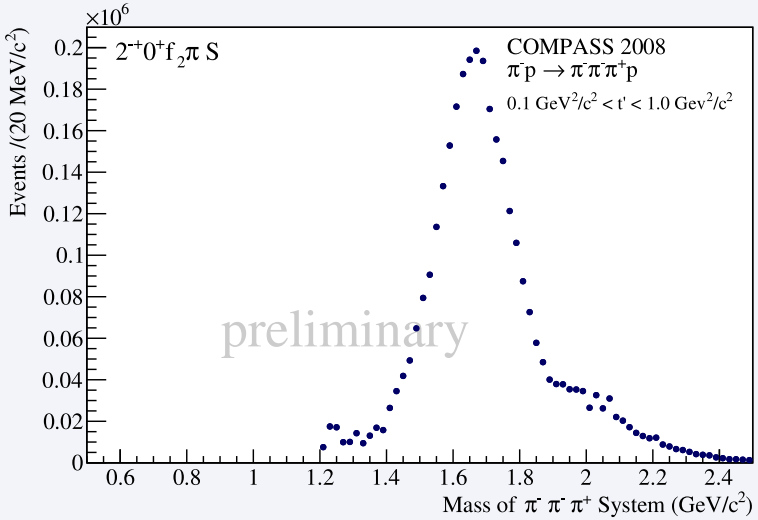

Cf. data from 2004 pilot-run

PRL **104** (2010) 241803

$2^{-+}\,0^+\,[f_2\pi]S$: $\pi_2(1670)$

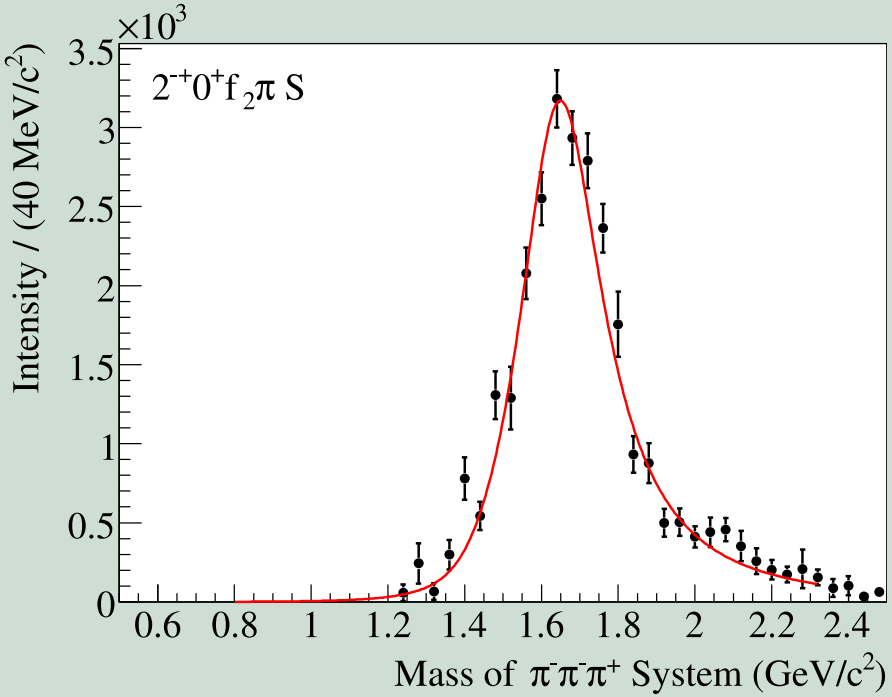

- 420 000 events
- Pb target

PWA of $\pi^- p \to \pi^-\pi^+\pi^- p_{\text{slow}}$

$2^{++}\,2^+\,[\rho\pi]D$: $a_2(1320)$

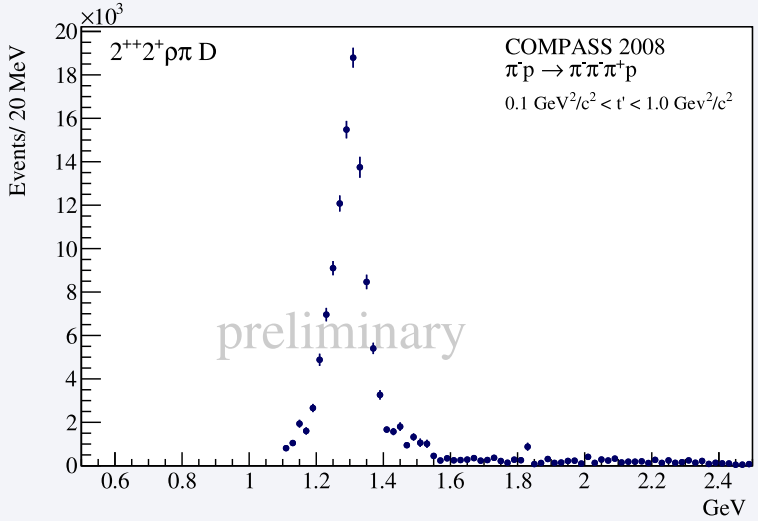

PWA of $\pi^- p \to \pi^-\pi^+\pi^- p_{\text{slow}}$

$2^{++}\,2^+\,[\rho\pi]D$: $a_2(1320)$

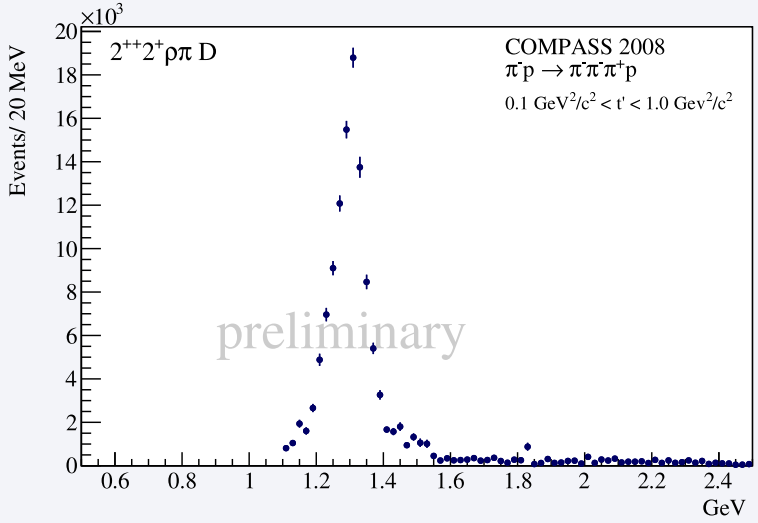

$4^{++}\,1^+\,[f_2\pi]F$: $a_4(2040)$

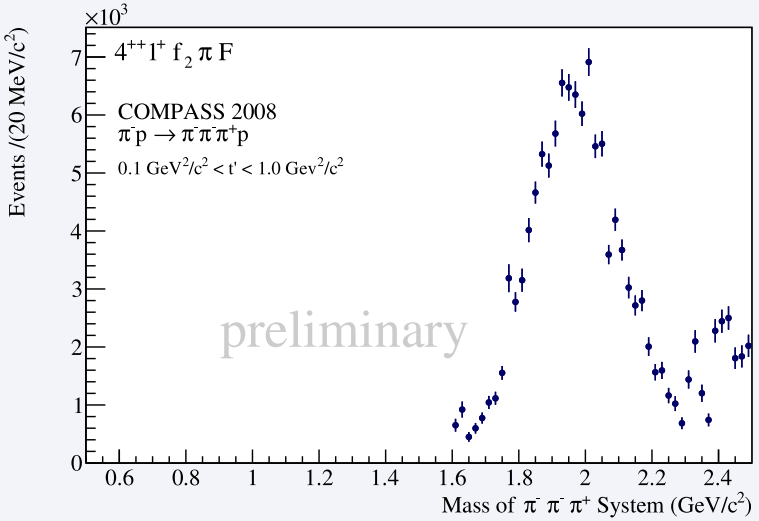

PWA of $\pi^- p \to \pi^-\pi^+\pi^- p_{\text{slow}}$

$2^{++}\,2^+\,[\rho\pi]D$: $a_2(1320)$

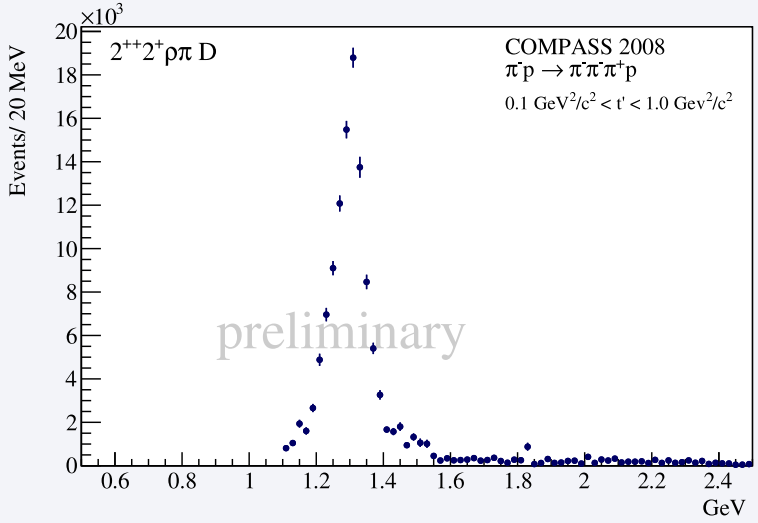

$4^{++}\,1^+\,[f_2\pi]F$: $a_4(2040)$

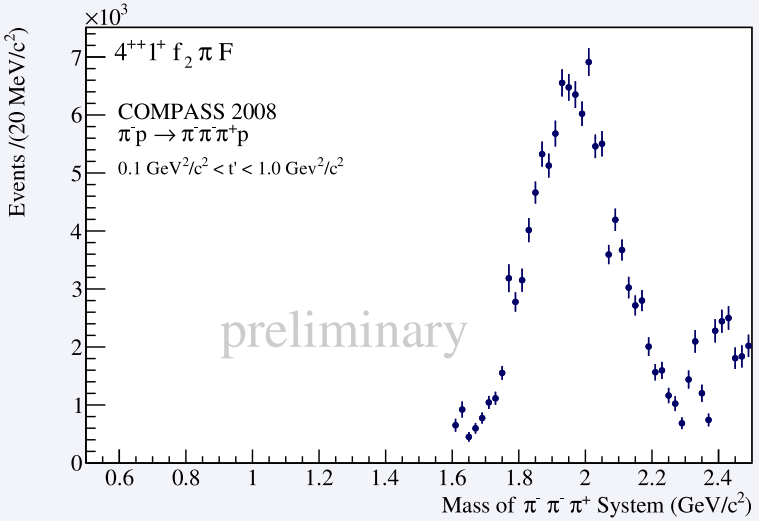

$4^{++}\,1^+\,[\rho\pi]G$: $a_4(2040)$

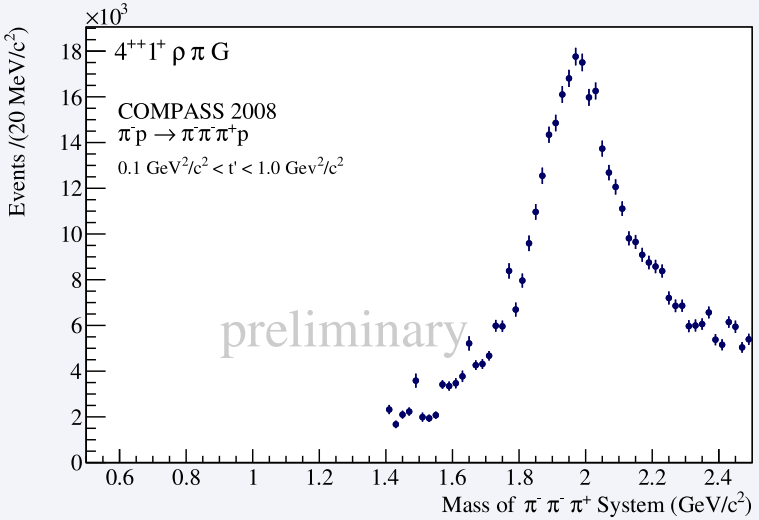

PWA of $\pi^- p \to \pi^-\pi^+\pi^- p_{\text{slow}}$

$2^{++}\,2^+\,[\rho\pi]D$: $a_2(1320)$

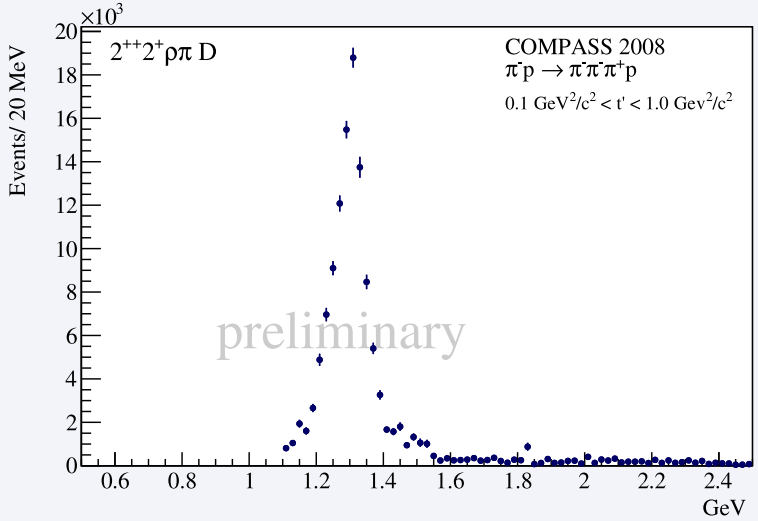

$4^{++}\,1^+\,[f_2\pi]F$: $a_4(2040)$

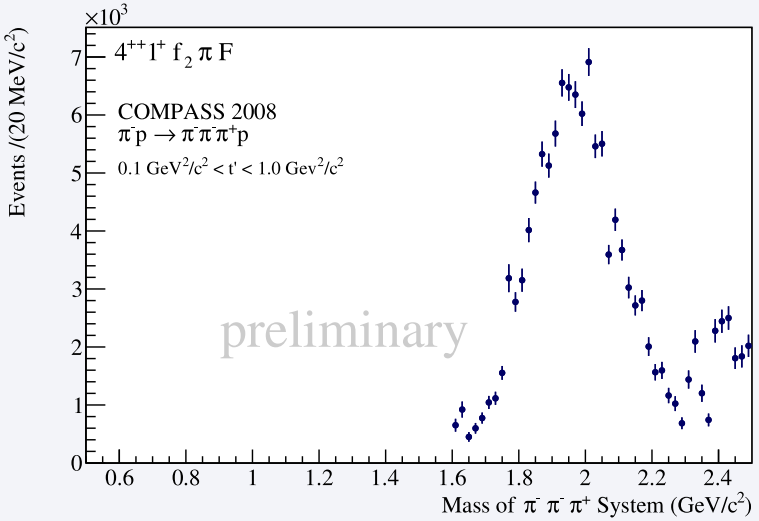

$0^{-+}\,0^+\,[f_0(980)\pi]S$: $\pi(1800)$

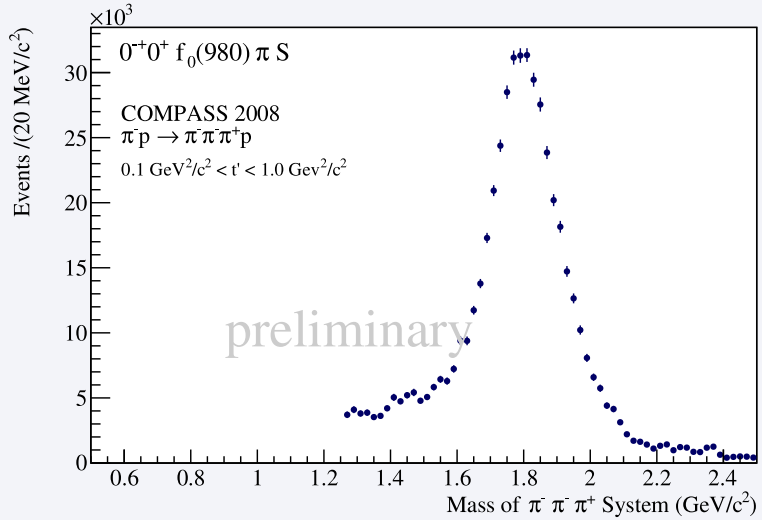

$4^{++}\,1^+\,[\rho\pi]G$: $a_4(2040)$

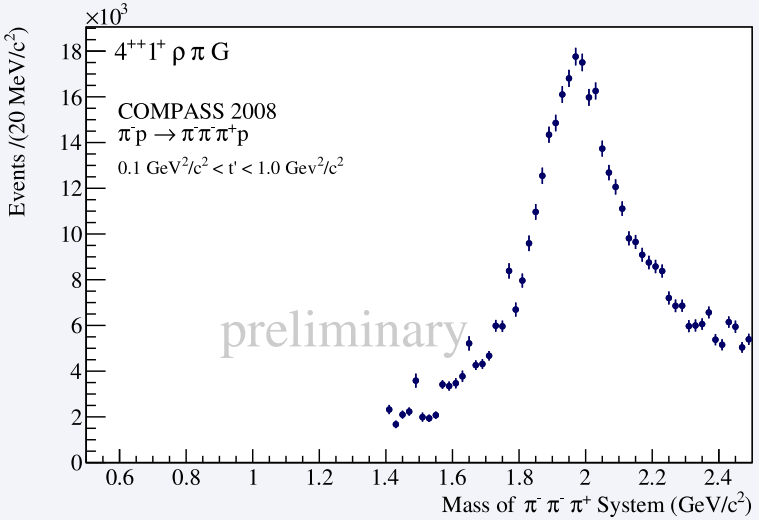

PWA of $\pi^- p \to \pi^-\pi^+\pi^- p_{\text{slow}}$

Spin-exotic $1^{-+}\,1^+\,[\rho\pi]P$

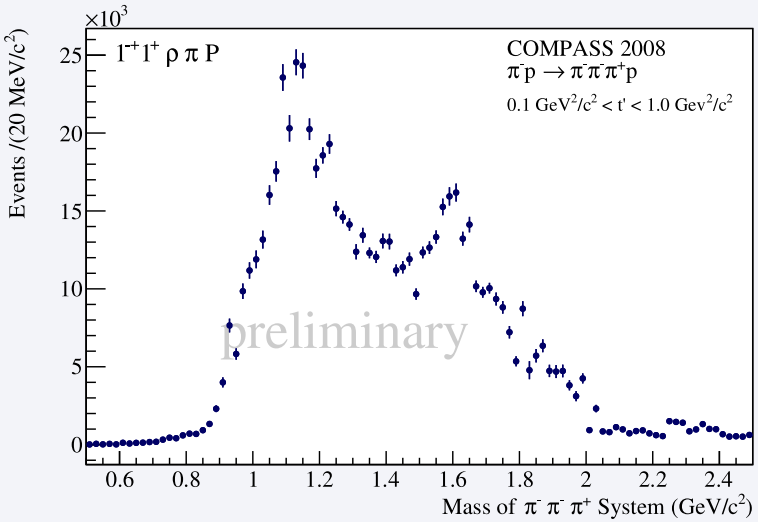

- Structure around 1.1 GeV/c^2 unstable w.r.t. fit model
- Stable enhancement around 1.6 GeV/c^2
- Phase motion w.r.t. to tail of $a_1(1260)$
- Phase locked w.r.t. $\pi_2(1670)$
- Ongoing analysis

PWA of $\pi^- p \to \pi^-\pi^+\pi^- p_{\text{slow}}$

Spin-exotic $1^{-+}\,1^+\,[\rho\pi]P$

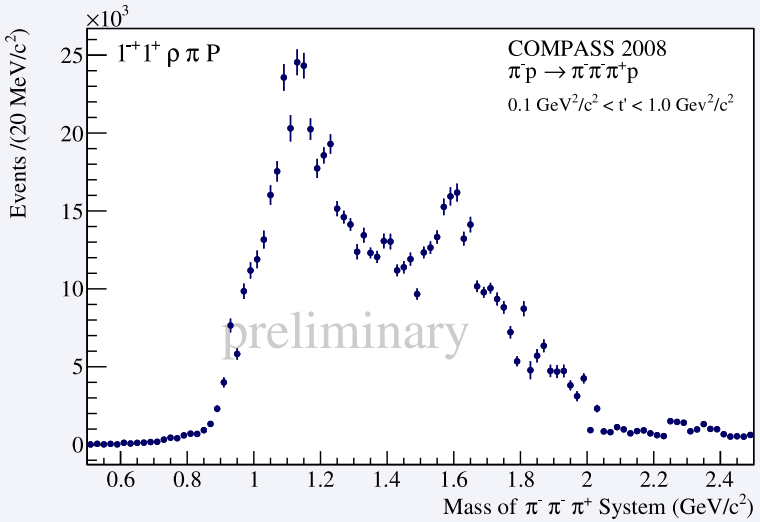

$1^{++}\,0^+\,[\rho\pi]S$: $a_1(1260)$

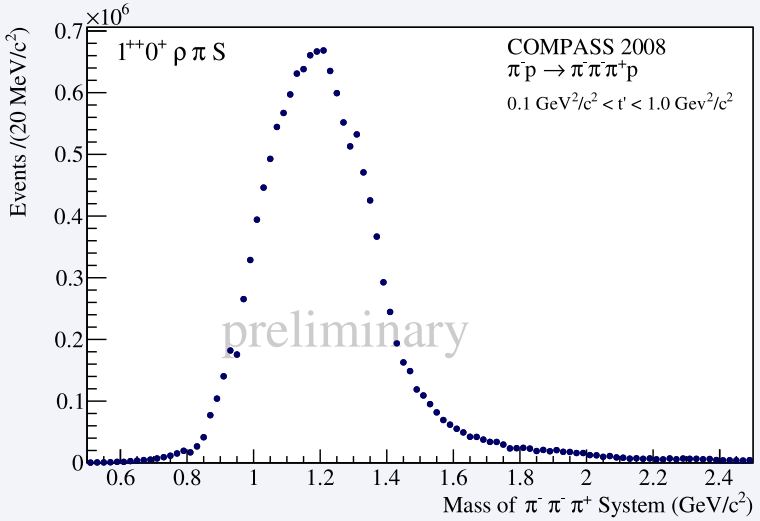

$1^{-+}\,1^+\,[\rho\pi]P - 1^{++}\,0^+\,[\rho\pi]S$

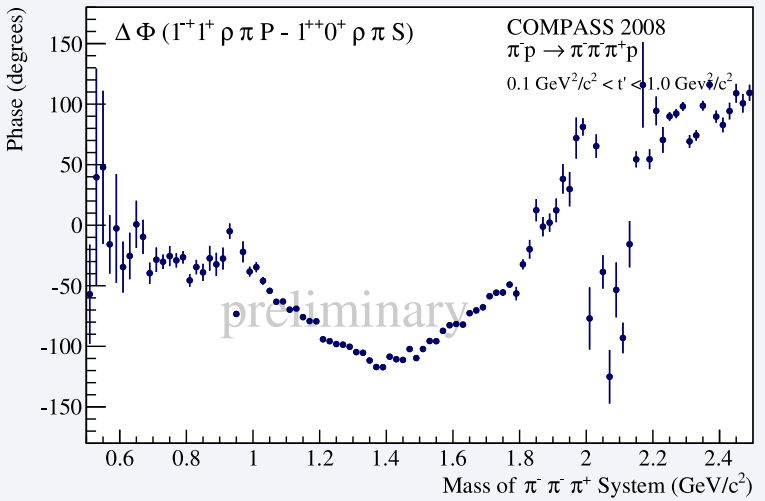

- Structure around 1.1 GeV/c^2 unstable w.r.t. fit model
- Stable enhancement around 1.6 GeV/c^2
- Phase motion w.r.t. to tail of $a_1(1260)$
- Phase locked w.r.t. $\pi_2(1670)$
- Ongoing analysis

PWA of $\pi^- p \to \pi^-\pi^+\pi^- p_{\text{slow}}$

Spin-exotic $1^{-+}1^+[\rho\pi]P$

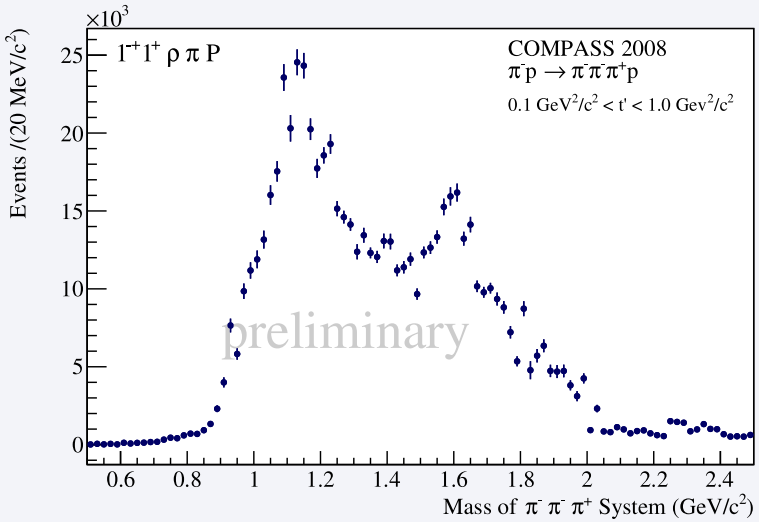

$2^{-+}0^+[f_2\pi]S$: $\pi_2(1670)$

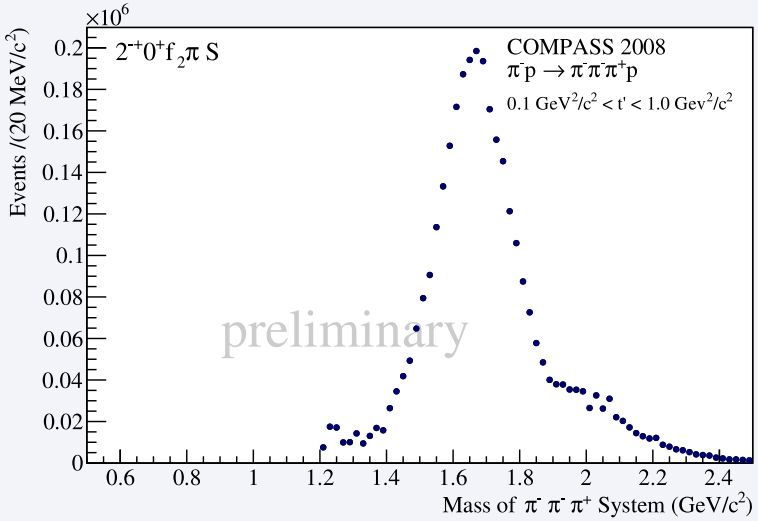

$1^{-+}1^+[\rho\pi]P - 2^{-+}0^+[f_2\pi]S$

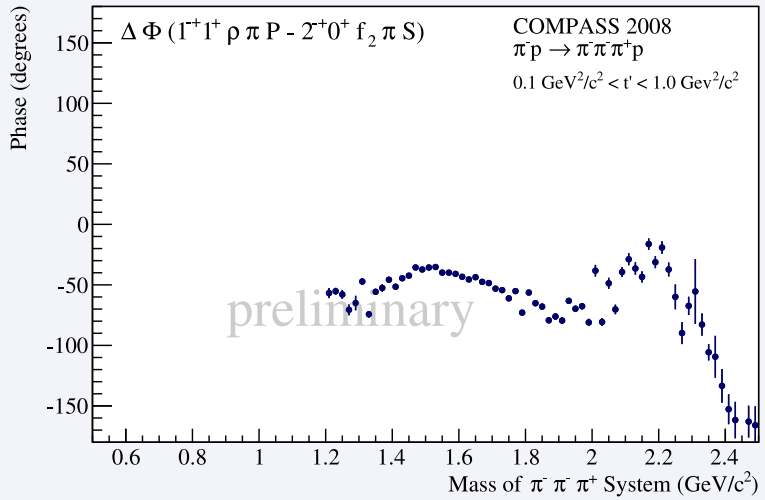

- Structure around 1.1 GeV/c^2 unstable w.r.t. fit model
- Stable enhancement around 1.6 GeV/c^2
- Phase motion w.r.t. to tail of $a_1(1260)$
- Phase locked w.r.t. $\pi_2(1670)$
- Ongoing analysis

PWA of $\pi^- p \to \pi^-\pi^+\pi^- p_{\text{slow}}$

Summary

- Data described by model consisting of 52 waves + incoherent isotropic background
  - Isobars: $(\pi\pi)_{S-\text{wave}}$, $f_0(980)$, $\rho(770)$, $f_2(1270)$, $f_0(1500)$ and $\rho_3(1690)$

Understanding of small waves is work in progress

- Intensity in spin-exotic $1^{-+}1^+ [\rho\pi]P$ wave
  - Interpretation in terms of resonances still unclear
- Significant contributions from non-resonant Deck-like processes
  - Inclusion into fit model
- Exploit t'-dependence of partial-wave amplitudes
  - PWA in narrow $m_{\pi^-\pi^+\pi^-}$ and t' bins
- Improvements of wave set and isobar parameterization

PWA of $\pi^- p \to \pi^-\pi^+\pi^- p_{\text{slow}}$

Summary

- Data described by model consisting of 52 waves + incoherent isotropic background
  - Isobars: $(\pi\pi)_{S-\text{wave}}$, $f_0(980)$, $\rho(770)$, $f_2(1270)$, $f_0(1500)$ and $\rho_3(1690)$

Understanding of small waves is work in progress

- Intensity in spin-exotic $1^{-+}\,1^+\,[\rho\pi]P$ wave
  - Interpretation in terms of resonances still unclear
- Significant contributions from non-resonant Deck-like processes
  - Inclusion into fit model
- Exploit t'-dependence of partial-wave amplitudes
  - PWA in narrow $m_{\pi^-\pi^+\pi^-}$ and t' bins
- Improvements of wave set and isobar parameterization

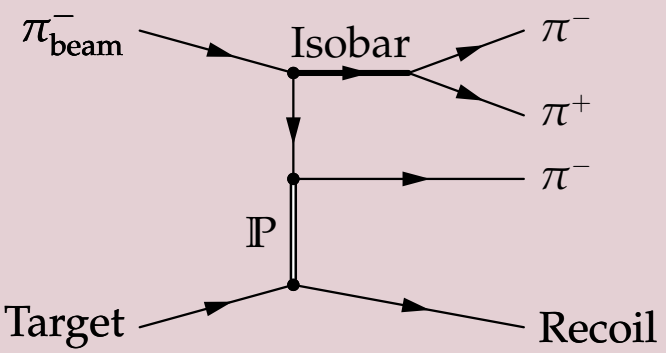

PWA of $\pi^- p \to \pi^- \eta p_{\text{slow}}$ and $\pi^- \eta' p_{\text{slow}}$

Selection of exclusive events with 3 charged tracks + 2 photons

- Kinematic range $0.1 < t' < 1.0\,(\text{GeV}/c)^2$
- η reconstructed from $\eta \to \pi^+\pi^-\pi^0$
- η' reconstructed via $\pi^+\pi^-\eta$ decay with $\eta \to \gamma\gamma$

$\gamma\gamma$ invariant mass distribution

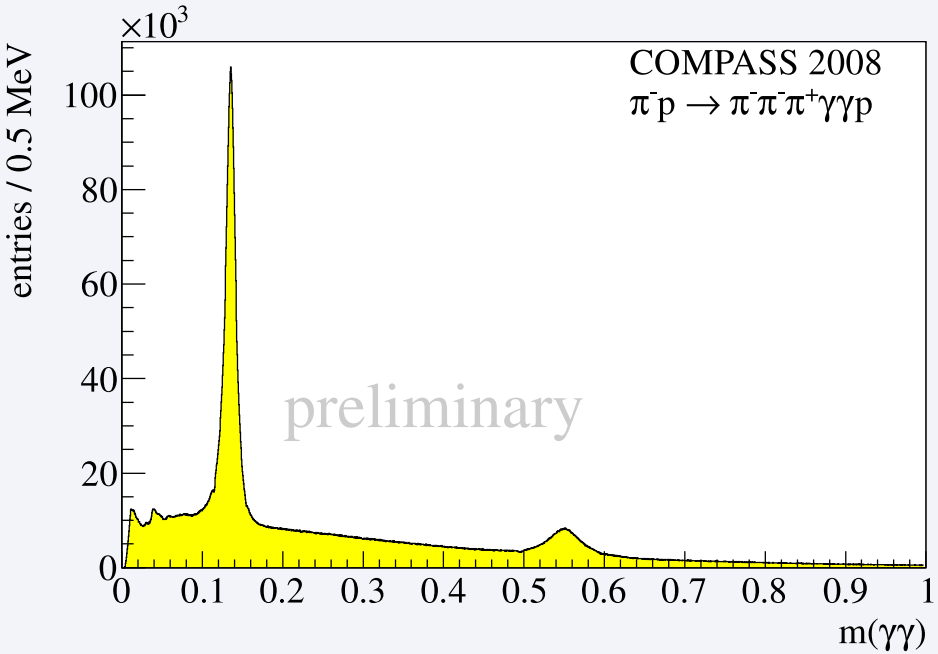

PWA of $\pi^- p \to \pi^- \eta p_{\text{slow}}$ and $\pi^- \eta' p_{\text{slow}}$

Selection of exclusive events with 3 charged tracks + 2 photons

- Kinematic range $0.1 < t' < 1.0\,(\text{GeV}/c)^2$
- η reconstructed from $\eta \to \pi^+\pi^-\pi^0$
- η' reconstructed via $\pi^+\pi^-\eta$ decay with $\eta \to \gamma\gamma$

$\gamma\gamma$ invariant mass distribution

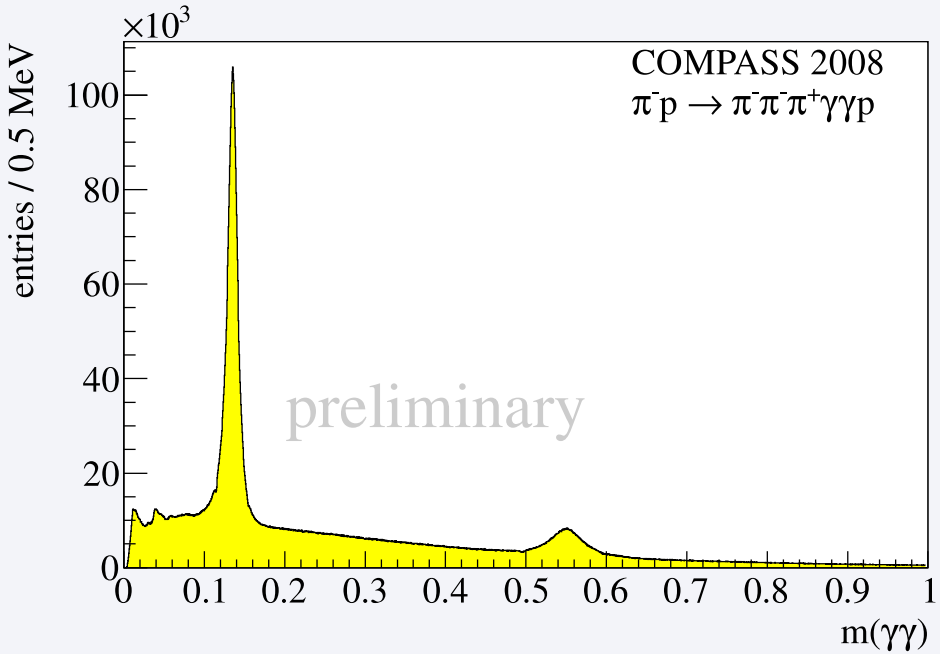

$\pi^+\pi^-\eta$ invariant mass distribution

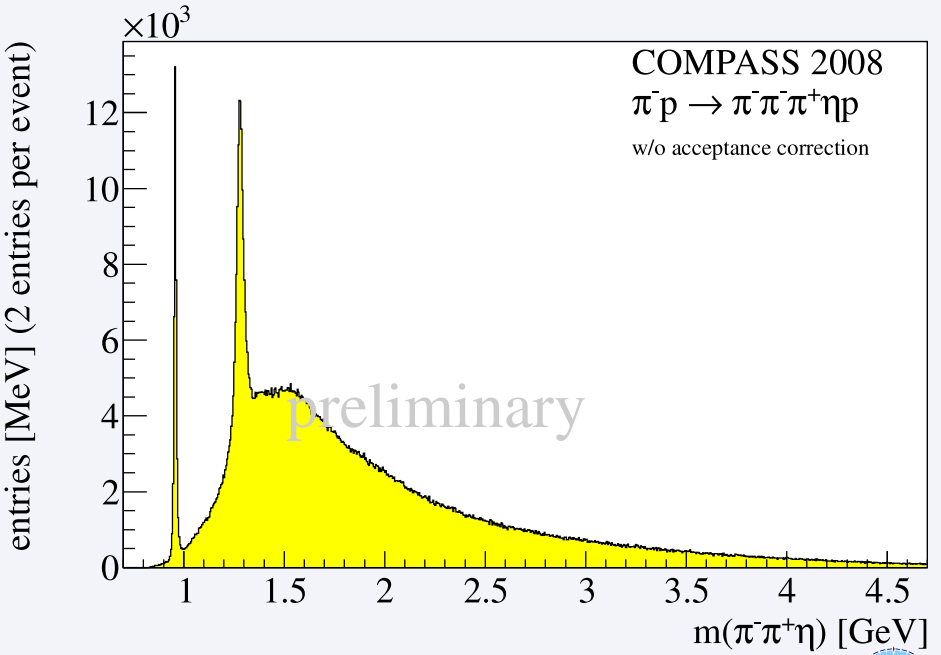

PWA of $\pi^- p \to \pi^- \eta\, p_{\text{slow}}$ and $\pi^- \eta'\, p_{\text{slow}}$

$\pi^-\eta$ invariant mass distribution

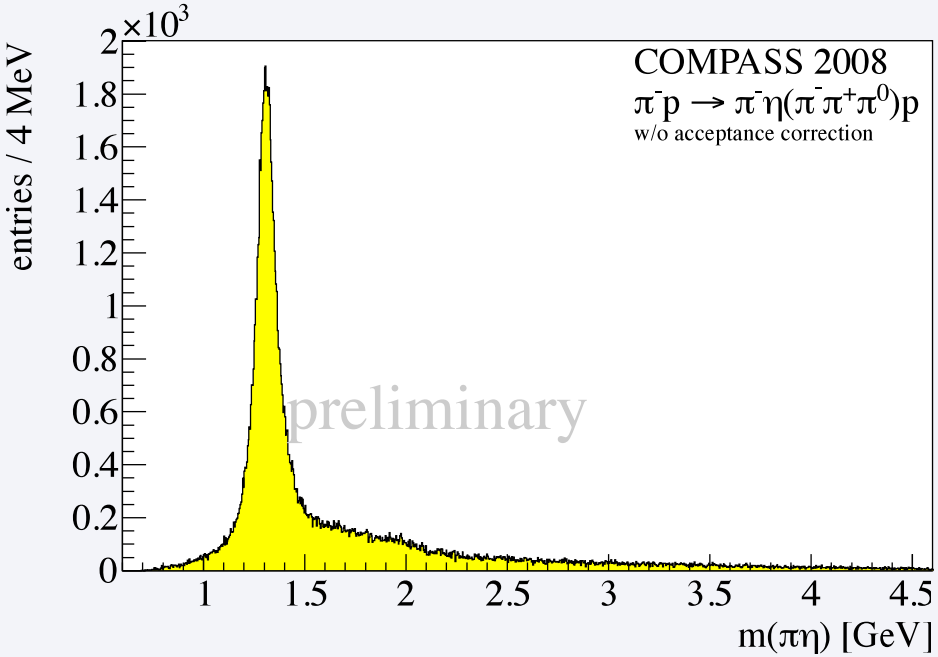

- $\pi^-\eta$: dominant $a_2(1320)$
- $\pi^-\eta'$: dominant broad structure around 1.7 GeV/c^2 and $a_2(1320)$ close to threshold
- Bulk of data described by 3 partial waves
  - $1^{-+}\,1^+$, $2^{++}\,1^+$, and $4^{++}\,1^+$

PWA of $\pi^- p \to \pi^- \eta\, p_{\text{slow}}$ and $\pi^- \eta'\, p_{\text{slow}}$

$\pi^-\eta$ invariant mass distribution

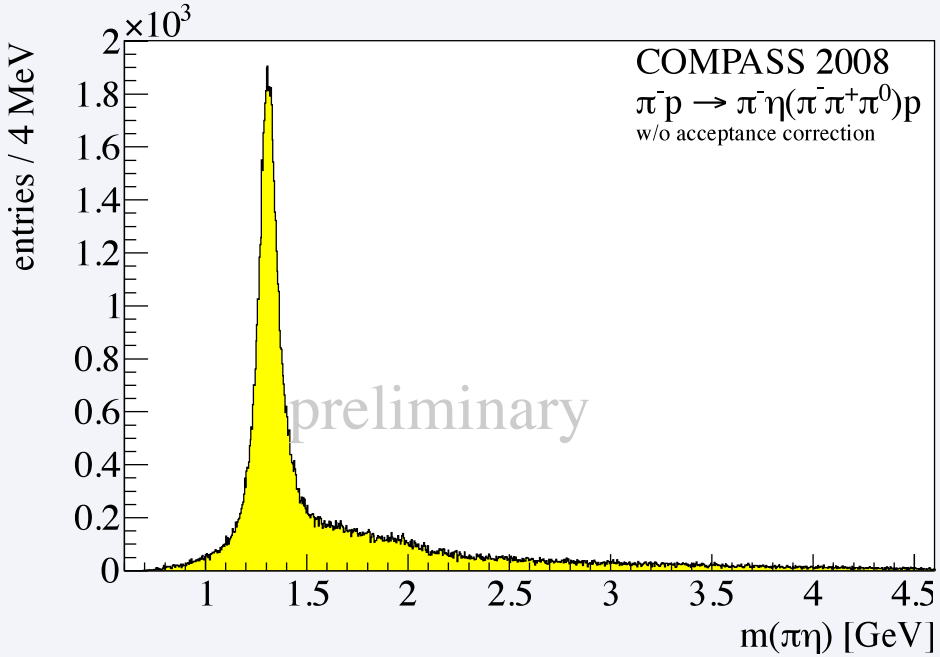

$\pi^-\eta'$ invariant mass distribution

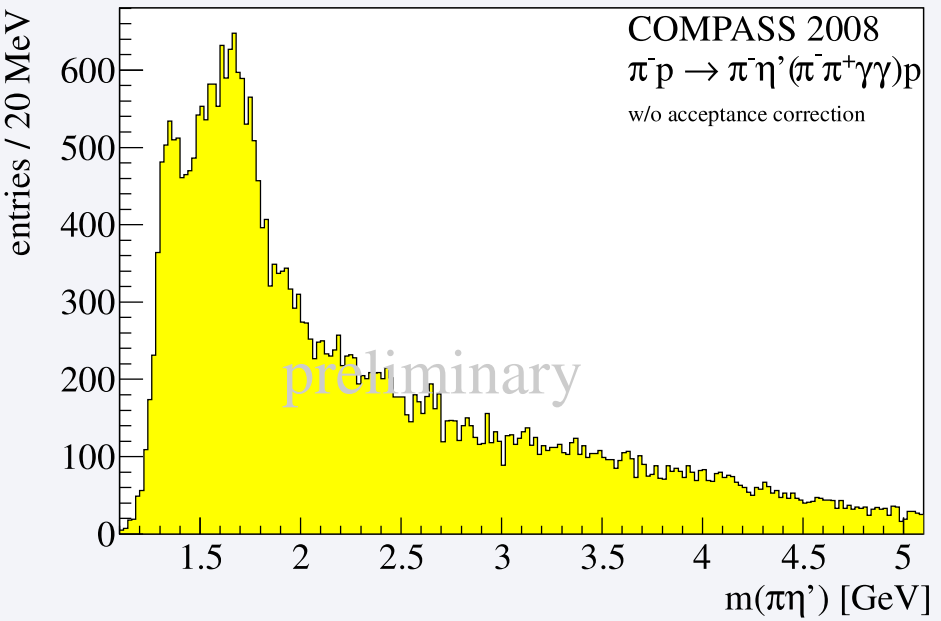

- $\pi^-\eta$: dominant $a_2(1320)$
- $\pi^-\eta'$: dominant broad structure around 1.7 GeV/c^2 and $a_2(1320)$ close to threshold
- Bulk of data described by 3 partial waves
  - $1^{-+}\,1^+$, $2^{++}\,1^+$, and $4^{++}\,1^+$

PWA of $\pi^- p \to \pi^- \eta\, p_{\text{slow}}$ and $\pi^- \eta'\, p_{\text{slow}}$

$\pi^-\eta$ invariant mass distribution

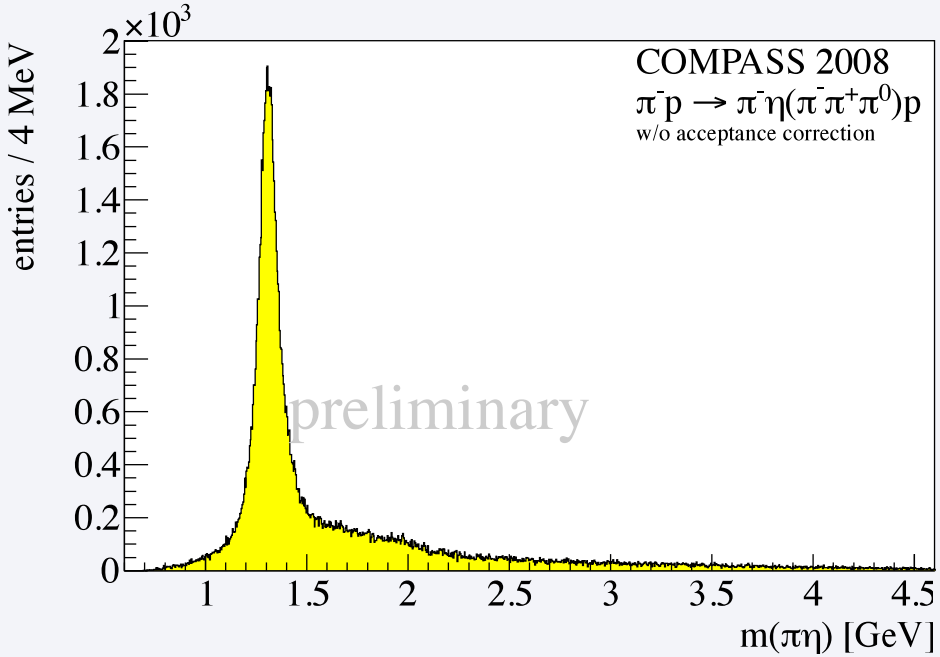

$\pi^-\eta'$ invariant mass distribution

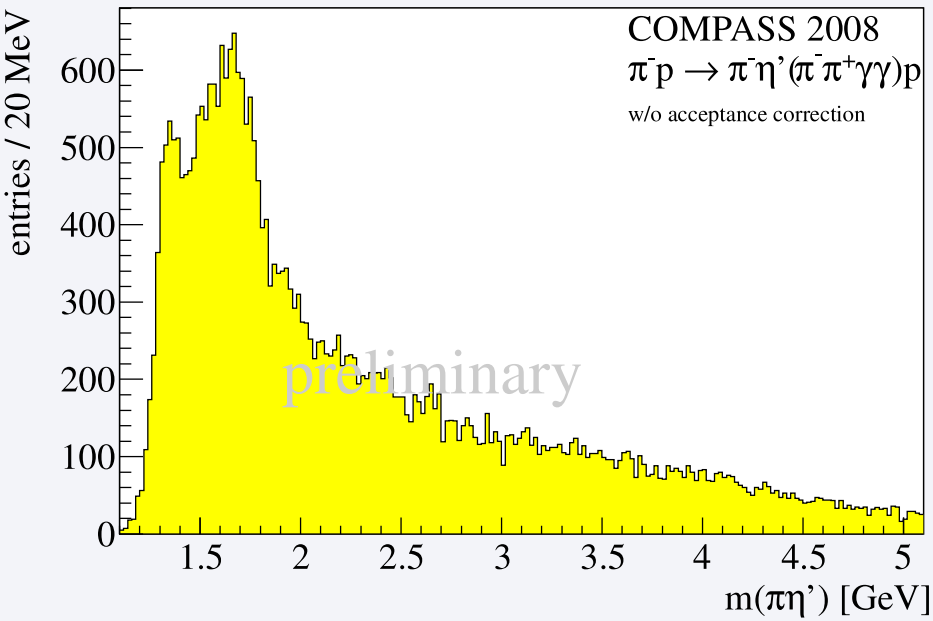

- $\pi^-\eta$: dominant $a_2(1320)$
- $\pi^-\eta'$: dominant broad structure around 1.7 GeV/c^2 and $a_2(1320)$ close to threshold
- Bulk of data described by 3 partial waves
  - $1^{-+}\,1^+$, $2^{++}\,1^+$, and $4^{++}\,1^+$

PWA of $\pi^- p \to \pi^- \eta\, p_{\text{slow}}$ and $\pi^- \eta'\, p_{\text{slow}}$

$a_2(1320)$ in $2^{++}\,1^+$ Partial Wave

$\pi^-\eta$ final state

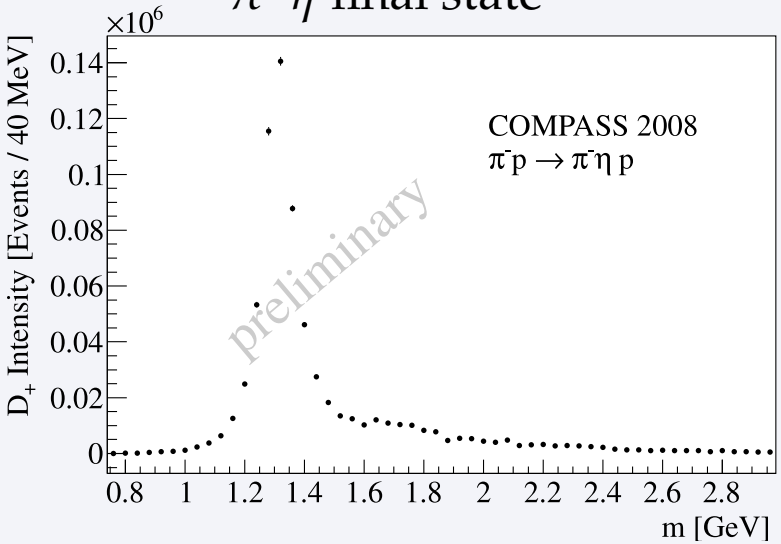

$\pi^-\eta'$ final state

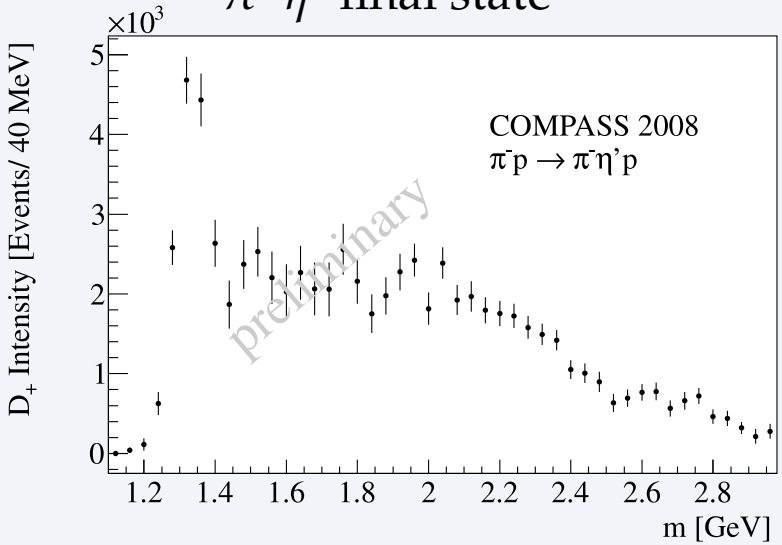

PWA of $\pi^- p \to \pi^- \eta\, p_{\text{slow}}$ and $\pi^- \eta'\, p_{\text{slow}}$

$a_2(1320)$ in $2^{++}\,1^+$ Partial Wave

$\pi^-\eta$ final state

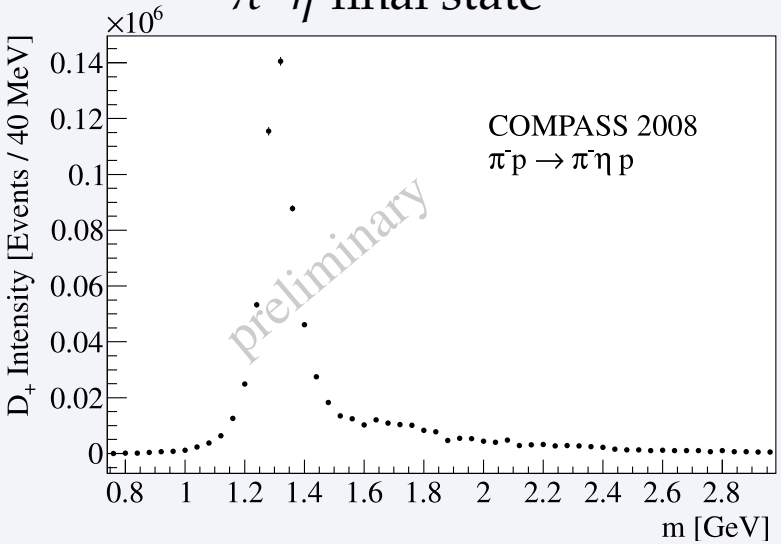

$\pi^-\eta'$ final state

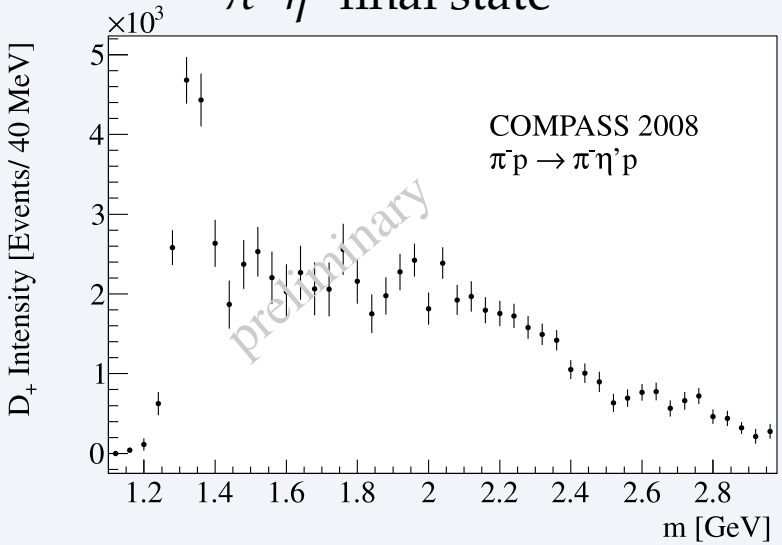

η-η' mixing together with OZI rule

- Partial-wave amplitudes for spin J related by mixing angle ϕ, phase space, and barrier factors (q = breakup momentum)

$$\frac{T_J^{\pi\eta'}(m)}{T_J^{\pi\eta}(m)} = \tan\phi \left[\frac{q^{\pi\eta'}(m)}{q^{\pi\eta}(m)}\right]^{J+1/2}$$

PWA of $\pi^- p \to \pi^- \eta\, p_{\text{slow}}$ and $\pi^- \eta'\, p_{\text{slow}}$

$a_2(1320)$ in $2^{++}\,1^+$ Partial Wave

$\pi^-\eta$ final state

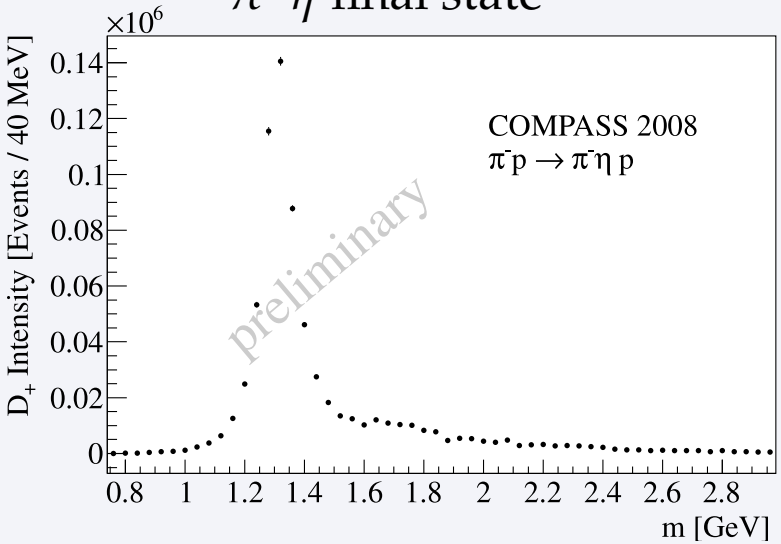

$\pi^-\eta'$ final state

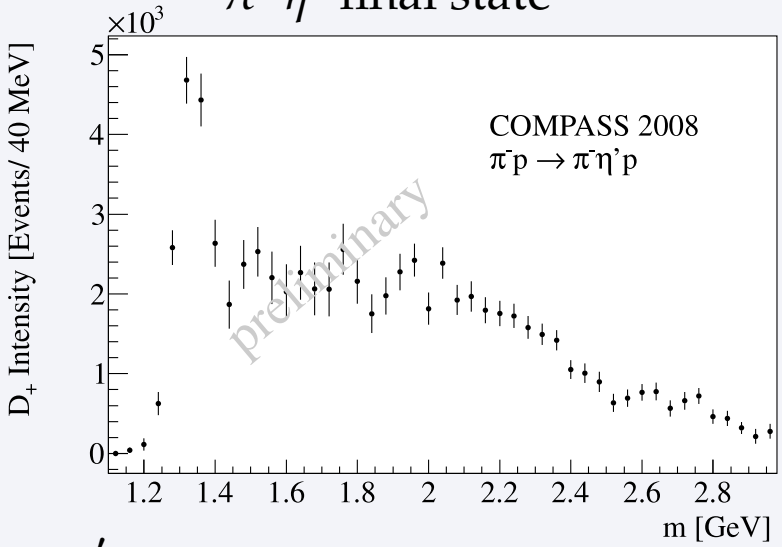

$\pi^-\eta$ scaled, $\pi^-\eta'$

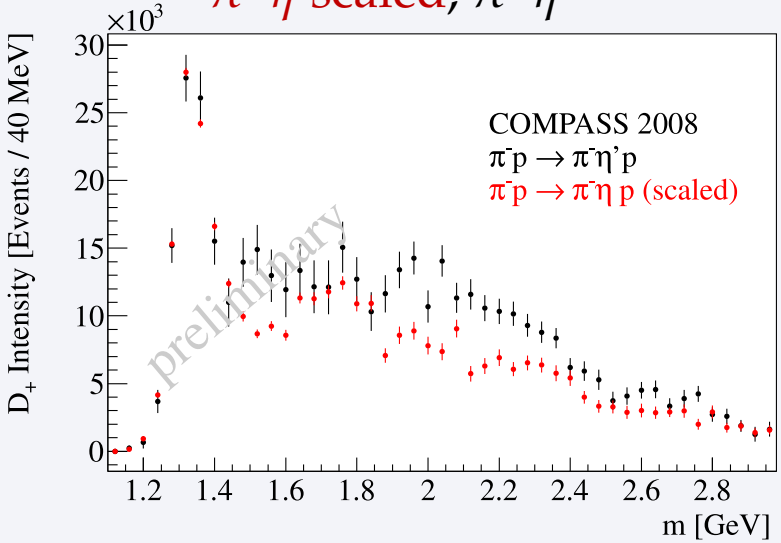

PWA of $\pi^- p \to \pi^- \eta\, p_{\text{slow}}$ and $\pi^- \eta'\, p_{\text{slow}}$

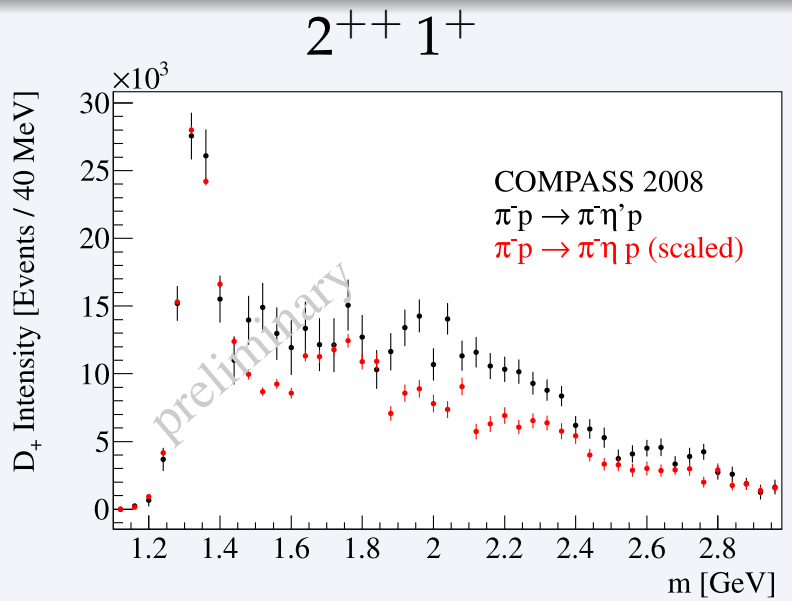

- Very similar even-spin waves
- Expected for $n\bar{n}$ resonances (OZI rule)
- Similar physical content also in non-resonant high-mass region

PWA of $\pi^- p \to \pi^- \eta\, p_{\text{slow}}$ and $\pi^- \eta'\, p_{\text{slow}}$

$2^{++}\,1^+$

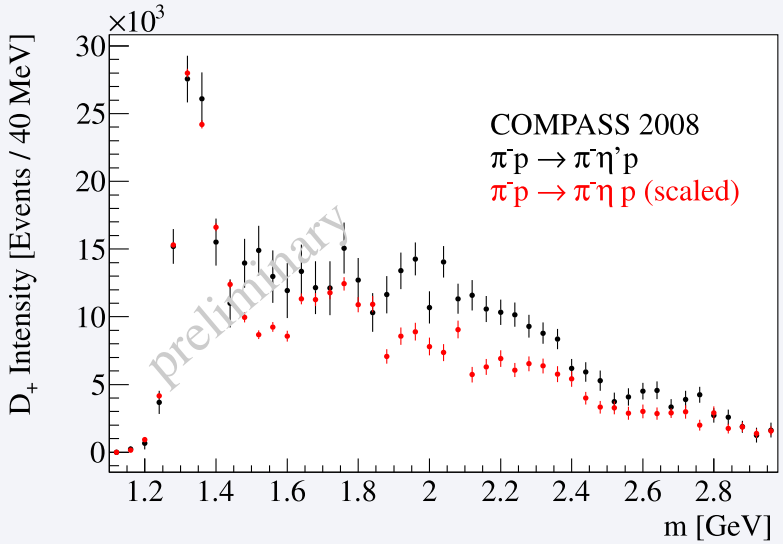

$4^{++}\,1^+$

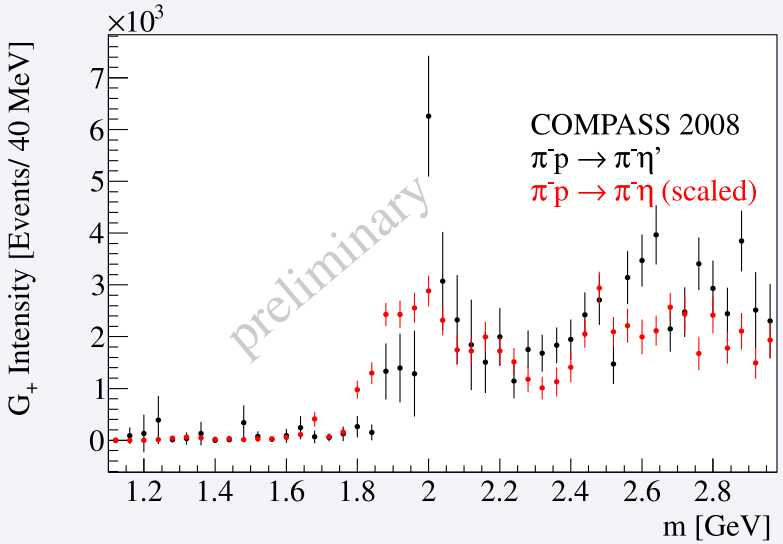

Phase: $4^{++}\,1^+ - 2^{++}\,1^+$

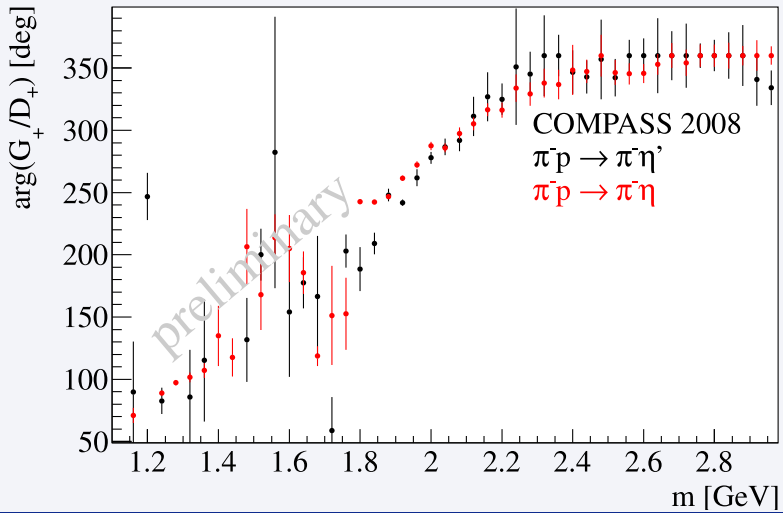

- Very similar even-spin waves
- Expected for $n\bar{n}$ resonances (OZI rule)
- Similar physical content also in non-resonant high-mass region

PWA of $\pi^- p \to \pi^- \eta\, p_{\text{slow}}$ and $\pi^- \eta'\, p_{\text{slow}}$

$2^{++}\,1^+$

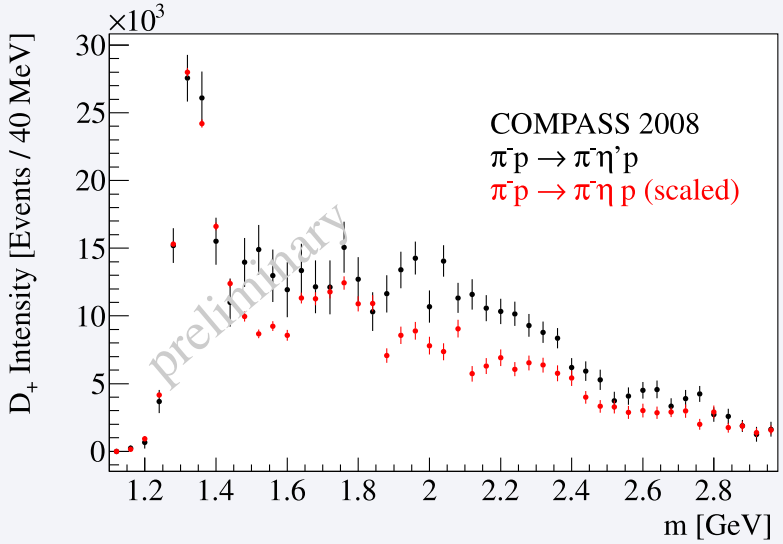

Spin-exotic $1^{-+}\,1^+$

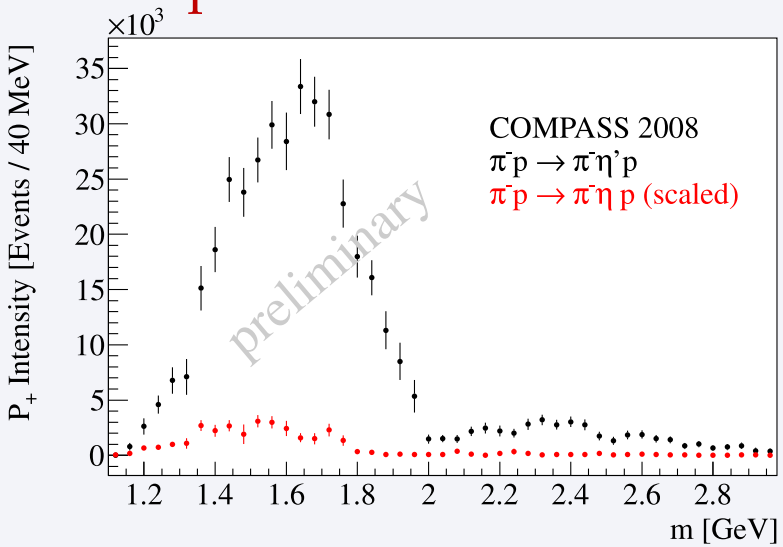

Phase: $2^{++}\,1^+ - 1^{-+}\,1^+$

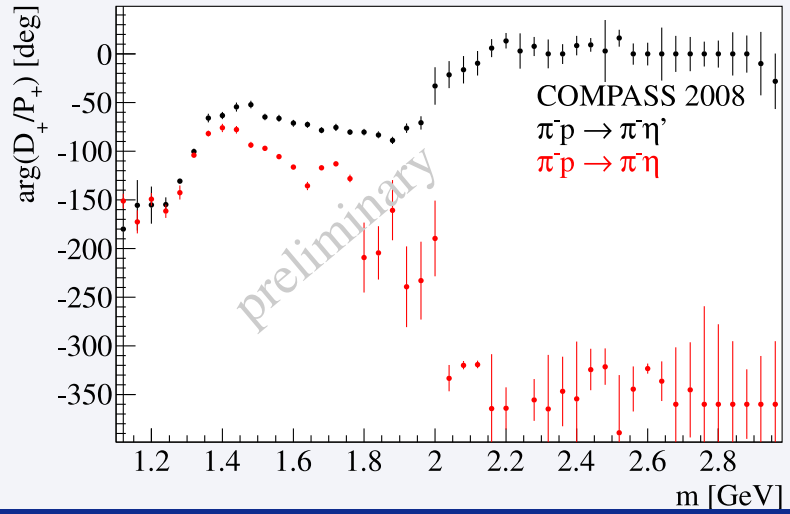

- Completely different intensity of 1^{-+} wave
- Suppression in $\pi\eta$ channel predicted for intermediate $|q\bar{q}g\rangle$ state
- Different phase motion in 1.6 GeV/c^2 region

PWA of $\pi^- p \to \pi^- \eta\, p_{\text{slow}}$ and $\pi^- \eta'\, p_{\text{slow}}$

Summary

- Found significant intensity in spin-exotic 1^{-+} wave in $\pi\eta$ and $\pi\eta'$
- 2^{++} and 4^{++} waves very similar in both channels
- 1^{-+} wave enhanced in $\pi\eta'$
- First mass-dependent fits describe data in terms of Breit-Wigner resonances and backgrounds
  - $a_2(1320)$ and $a_4(2040)$ resonance parameters consistent in both channels
  - Description of 1^{-+} wave by Breit-Wigner requires large interfering background and additional 2^{++} resonance
- Resonance interpretation of 1^{-+} wave requires
  - Better understanding of resonance structure of 2^{++} and 4^{++} waves
  - Inclusion of non-resonant contributions from double-Regge processes in high-mass region
- **Final goal:** combined analysis of both channels

PWA of $\pi^- p \to \pi^- \eta\, p_{\text{slow}}$ and $\pi^- \eta'\, p_{\text{slow}}$

Summary

- Found significant intensity in spin-exotic 1^{-+} wave in $\pi\eta$ and $\pi\eta'$
- 2^{++} and 4^{++} waves very similar in both channels
- 1^{-+} wave enhanced in $\pi\eta'$
- First mass-dependent fits describe data in terms of Breit-Wigner resonances and backgrounds
  - $a_2(1320)$ and $a_4(2040)$ resonance parameters consistent in both channels
  - Description of 1^{-+} wave by Breit-Wigner requires large interfering background and additional 2^{++} resonance
- Resonance interpretation of 1^{-+} wave requires
  - Better understanding of resonance structure of 2^{++} and 4^{++} waves
  - Inclusion of non-resonant contributions from double-Regge processes in high-mass region
- **Final goal:** combined analysis of both channels

PWA of $\pi^- p \to \pi^- \eta\, p_{\text{slow}}$ and $\pi^- \eta'\, p_{\text{slow}}$

Summary

- Found significant intensity in spin-exotic 1^{-+} wave in $\pi\eta$ and $\pi\eta'$
- 2^{++} and 4^{++} waves very similar in both channels
- 1^{-+} wave enhanced in $\pi\eta'$
- First mass-dependent fits describe data in terms of Breit-Wigner resonances and backgrounds
  - $a_2(1320)$ and $a_4(2040)$ resonance parameters consistent in both channels
  - Description of 1^{-+} wave by Breit-Wigner requires large interfering background and additional 2^{++} resonance
- Resonance interpretation of 1^{-+} wave requires
  - Better understanding of resonance structure of 2^{++} and 4^{++} waves
  - Inclusion of non-resonant contributions from double-Regge processes in high-mass region
- **Final goal:** combined analysis of both channels

PWA of $\pi^- p \to \pi^- \eta p_{\text{slow}}$ and $\pi^- \eta' p_{\text{slow}}$

Summary

- Found significant intensity in spin-exotic 1^{-+} wave in $\pi\eta$ and $\pi\eta'$

Non-resonant contributions

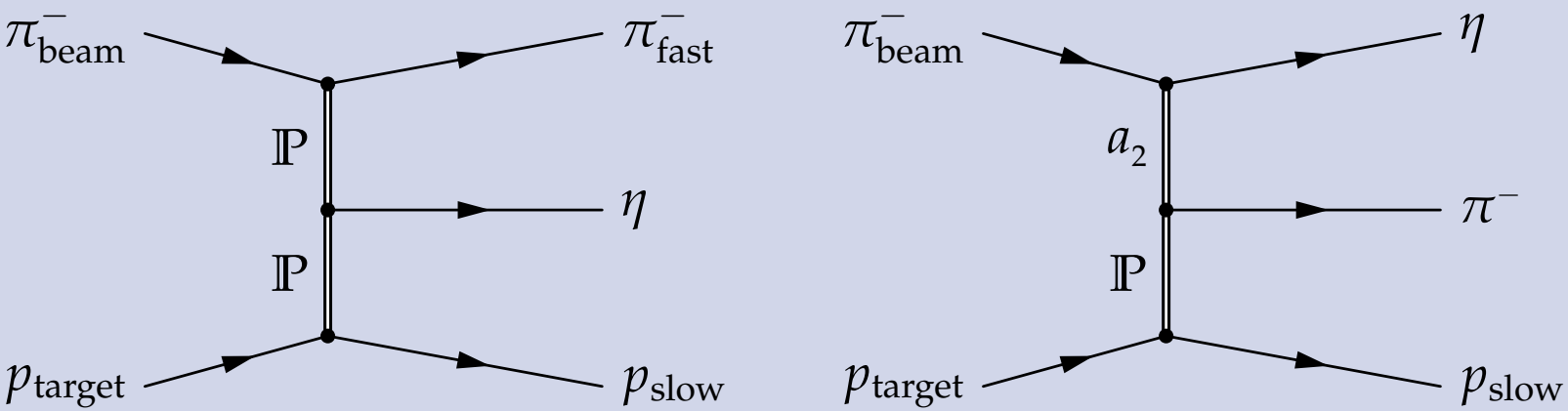

- Resonance interpretation of 1^{-+} wave requires
  - Better understanding of resonance structure of 2^{++} and 4^{++} waves
  - Inclusion of non-resonant contributions from double-Regge processes in high-mass region
- **Final goal:** combined analysis of both channels

PWA of $\pi^- p \to \pi^- \eta\, p_{\text{slow}}$ and $\pi^- \eta'\, p_{\text{slow}}$

Summary

- Found significant intensity in spin-exotic 1^{-+} wave in $\pi\eta$ and $\pi\eta'$
- 2^{++} and 4^{++} waves very similar in both channels
- 1^{-+} wave enhanced in $\pi\eta'$
- First mass-dependent fits describe data in terms of Breit-Wigner resonances and backgrounds
  - $a_2(1320)$ and $a_4(2040)$ resonance parameters consistent in both channels
  - Description of 1^{-+} wave by Breit-Wigner requires large interfering background and additional 2^{++} resonance
- Resonance interpretation of 1^{-+} wave requires
  - Better understanding of resonance structure of 2^{++} and 4^{++} waves
  - Inclusion of non-resonant contributions from double-Regge processes in high-mass region
- **Final goal:** combined analysis of both channels

PWA of π^- Pb $\to \pi^-\pi^+\pi^-\pi^+\pi^-$ Pb

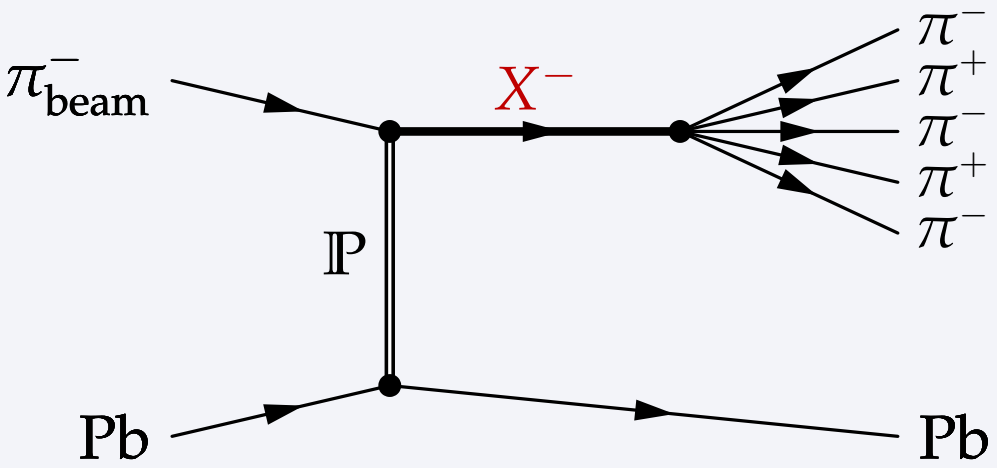

First mass-dependent PWA of this reaction

- **Light-meson frontier:** access to mesonic states in 2 GeV/c^2 region
- Little information from previous experiments

Data from pilot run

- Pb target
- Recoil not measured
- Kinematic range $t' < 5 \cdot 10^{-3}$ (GeV/c)^2

PWA of π^- Pb $\to \pi^-\pi^+\pi^-\pi^+\pi^-$ Pb

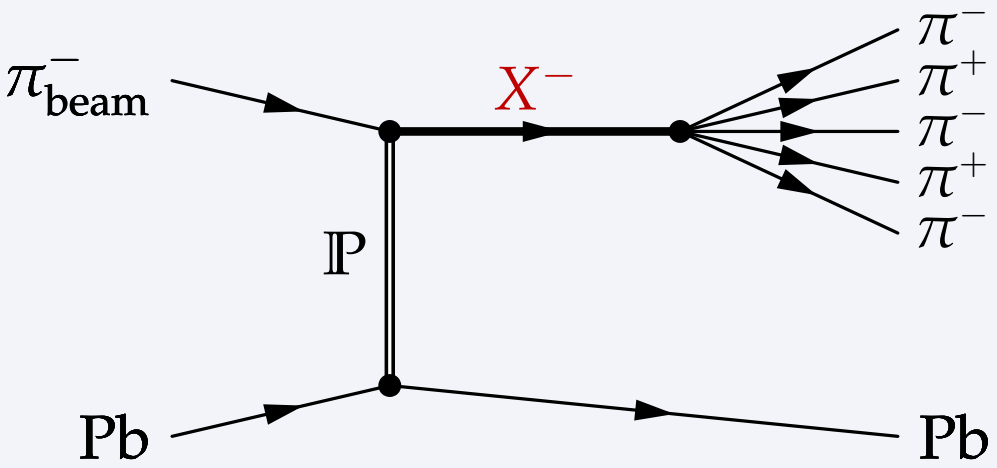

First mass-dependent PWA of this reaction

- **Light-meson frontier:** access to mesonic states in 2 GeV/c^2 region
- Little information from previous experiments

Data from pilot run

- Pb target
- Recoil not measured
- Kinematic range $t' < 5 \cdot 10^{-3}$ (GeV/c)^2

PWA of π^- Pb $\rightarrow \pi^-\pi^+\pi^-\pi^+\pi^-$ Pb

Fit model

- Complicated isobar structure
  - Large number of possible waves
  - Data exhibit no dominant waves
- Exploration of model space using evolutionary algorithm based on goodness-of-fit criterion
  - 284 waves tested
  - Also provides estimate for systematic uncertainty from fit model
- Best model: 31 waves + incoherent isotropic background
- Isobars
  - $(2\pi)^0$ isobars: $(\pi\pi)_{S-\text{wave}}$, $\rho(770)$
  - $(3\pi)^\pm$ isobars: $a_1(1260)$, $a_2(1320)$
  - $(4\pi)^0$ isobars: $f_2(1270)$, $f_1(1285)$, $f_0(1370, 1500)$, and $\rho'(1450, 1700)$
    - Only few information available for $(4\pi)^0$ isobars

PWA of π^- Pb $\rightarrow \pi^-\pi^+\pi^-\pi^+\pi^-$ Pb

Fit model

- Complicated isobar structure
  - Large number of possible waves
  - Data exhibit no dominant waves
- Exploration of model space using evolutionary algorithm based on goodness-of-fit criterion
  - 284 waves tested
  - Also provides estimate for systematic uncertainty from fit model
- Best model: 31 waves + incoherent isotropic background
- Isobars
  - $(2\pi)^0$ isobars: $(\pi\pi)_{S-\text{wave}}$, $\rho(770)$
  - $(3\pi)^\pm$ isobars: $a_1(1260)$, $a_2(1320)$
  - $(4\pi)^0$ isobars: $f_2(1270)$, $f_1(1285)$, $f_0(1370, 1500)$, and $\rho'(1450, 1700)$
    - Only few information available for $(4\pi)^0$ isobars

PWA of π^- Pb $\rightarrow \pi^-\pi^+\pi^-\pi^+\pi^-$ Pb

Fit model

- Complicated isobar structure
  - Large number of possible waves
  - Data exhibit no dominant waves
- Exploration of model space using evolutionary algorithm based on goodness-of-fit criterion
  - 284 waves tested
  - Also provides estimate for systematic uncertainty from fit model
- Best model: 31 waves + incoherent isotropic background
- Isobars
  - $(2\pi)^0$ isobars: $(\pi\pi)_{S-\text{wave}}$, $\rho(770)$
  - $(3\pi)^\pm$ isobars: $a_1(1260)$, $a_2(1320)$
  - $(4\pi)^0$ isobars: $f_2(1270)$, $f_1(1285)$, $f_0(1370, 1500)$, and $\rho'(1450, 1700)$
    - Only few information available for $(4\pi)^0$ isobars

PWA of π^- Pb $\rightarrow \pi^-\pi^+\pi^-\pi^+\pi^-$ Pb

Fit model

- Complicated isobar structure
  - Large number of possible waves
  - Data exhibit no dominant waves
- Exploration of model space using evolutionary algorithm based on goodness-of-fit criterion
  - 284 waves tested
  - Also provides estimate for systematic uncertainty from fit model
- Best model: 31 waves + incoherent isotropic background
- Isobars
  - $(2\pi)^0$ isobars: $(\pi\pi)_{S-\text{wave}}$, $\rho(770)$
  - $(3\pi)^\pm$ isobars: $a_1(1260)$, $a_2(1320)$
  - $(4\pi)^0$ isobars: $f_2(1270)$, $f_1(1285)$, $f_0(1370, 1500)$, and $\rho'(1450, 1700)$
    - Only few information available for $(4\pi)^0$ isobars

PWA of π^- Pb $\rightarrow \pi^-\pi^+\pi^-\pi^+\pi^-$ Pb

$0^{-+}\pi^- f_0(1500)\ S$

$0^{-+}\rho a_1(1260)\ S$

$1^{++}\pi^- f_0(1370)\ P$

$1^{++}\pi^- f_1(1285)\ P$

$1^{++}\rho\pi(1300)\ S$

$1^{++}(\pi\pi)_S a_1\ D$

$2^{-+}\pi^- f_2(1270)\ S$

$2^{-+}\rho a_1(1260)\ S$

$2^{-+}\rho a_2(1320)\ S$

$2^{-+}\rho a_1(1260)\ D$

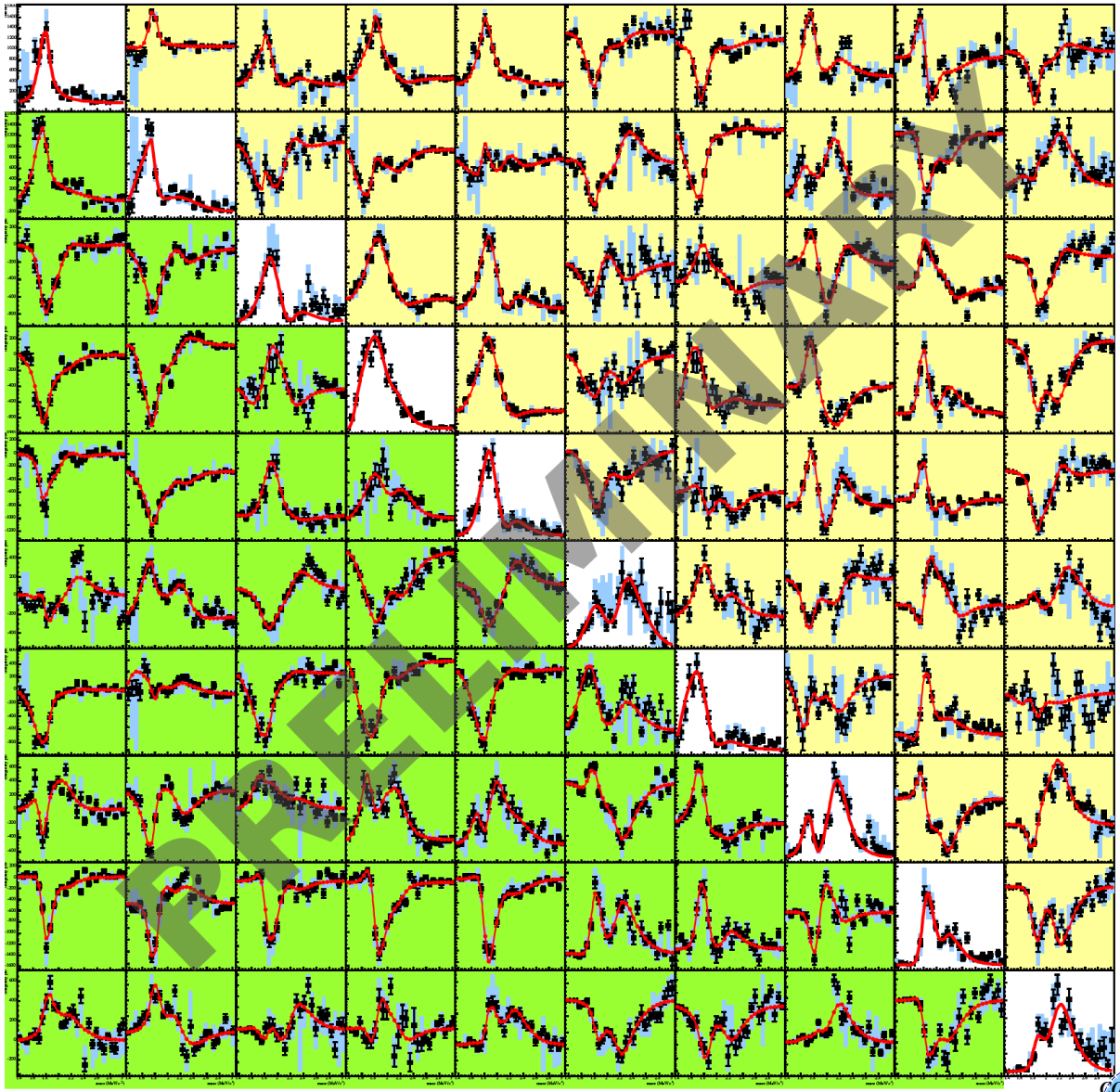

PWA of π^- Pb $\rightarrow \pi^-\pi^+\pi^-\pi^+\pi^-$ Pb

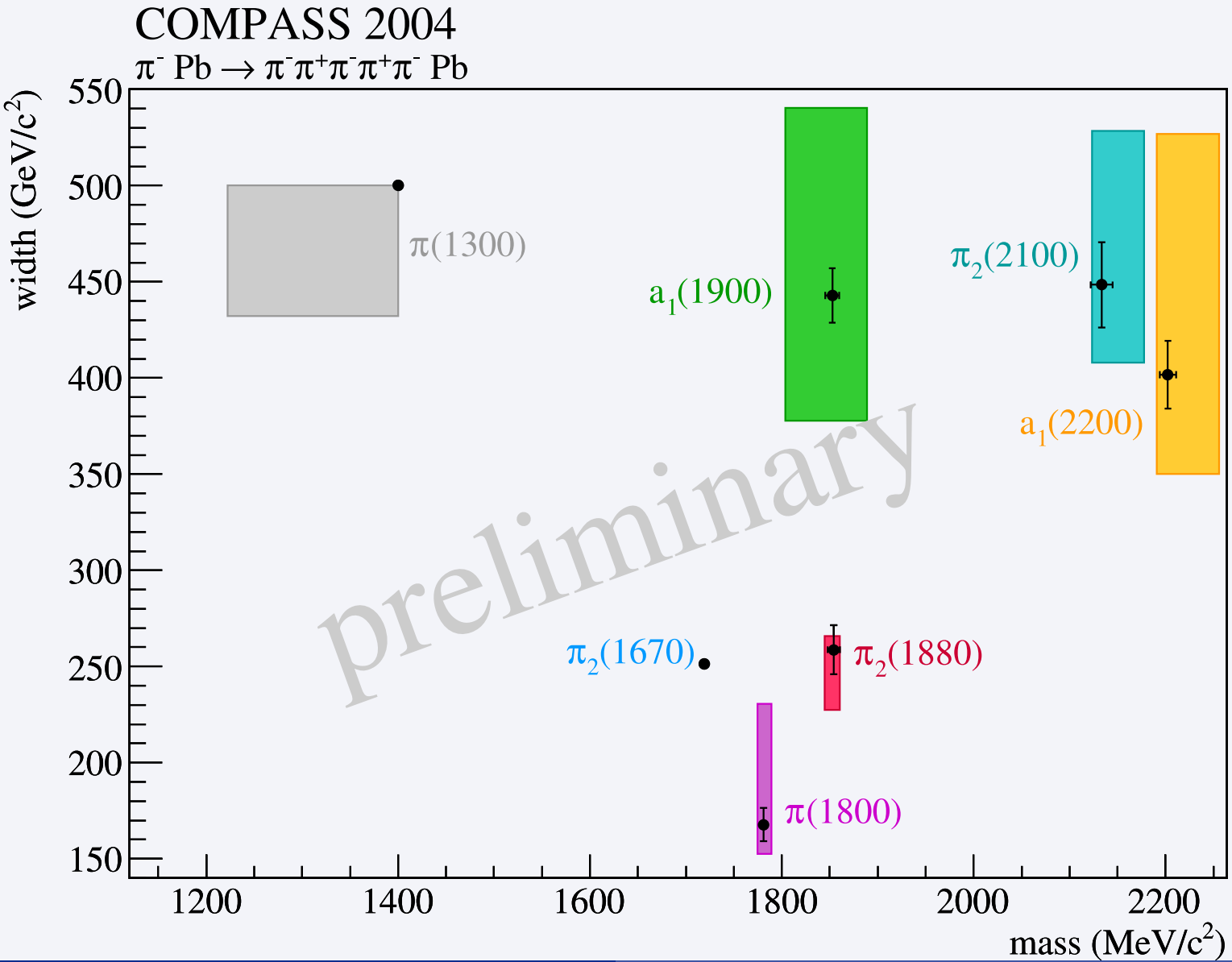

PWA of π^- Pb $\rightarrow \pi^-\pi^+\pi^-\pi^+\pi^-$ Pb

Proof of Principle: First mass-dependent five-body PWA

- Spin-density sub-matrix of 10 waves described using 7 resonances + background terms
- Rather simplistic fit model
  - Parameterization by sum of relativistic constant-width Breit-Wigners
  - Mixing and coupled-channel effects neglected
  - Multi-peripheral processes (Deck-effect) not taken into account
- Good description of data

Work in progress

- Much more data on tape
  - Proton target, kinematic range $0.1 < t' < 1\,(\mathrm{GeV}/c)^2$
- Improvement of fit models
  - Analysis of $(4\pi)^0$ subsystem

PWA of π^- Pb $\rightarrow \pi^-\pi^+\pi^-\pi^+\pi^-$ Pb

Proof of Principle: First mass-dependent five-body PWA

- Spin-density sub-matrix of 10 waves described using 7 resonances + background terms
- Rather simplistic fit model
  - Parameterization by sum of relativistic constant-width Breit-Wigners
  - Mixing and coupled-channel effects neglected
  - Multi-peripheral processes (Deck-effect) not taken into account
- Good description of data

Work in progress

- Much more data on tape
  - Proton target, kinematic range $0.1 < t' < 1\,(\mathrm{GeV}/c)^2$
- Improvement of fit models
  - Analysis of $(4\pi)^0$ subsystem

Outline

PWA of $p\,p \to p_{\text{fast}}\,\pi^+\pi^-\,p_{\text{slow}}$

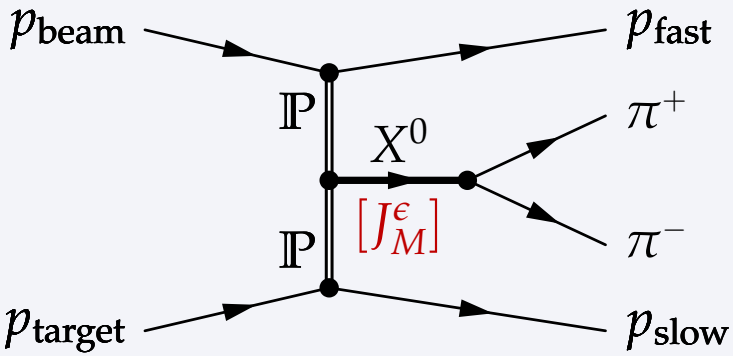

Search for **glueballs**

- Mesonic state with no valence quarks
- Lattice QCD simulations predict lightest glueballs to be scalars
  - Strong mixing with conventional scalar mesons expected
  - Difficult to disentangle
- Pomeron-Pomeron fusion well-suited to study scalar mesons
  - Mesons produced at central rapidities

PWA of $p\,p \to p_{\text{fast}}\,\pi^+\pi^-\,p_{\text{slow}}$

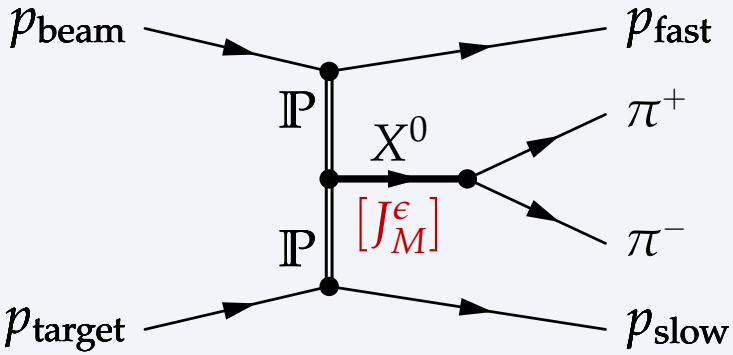

Suppression of diffractive background with $m(p_{\text{fast}}\pi^{\pm}) > 1.5$ GeV/c^2

$p_{\text{fast}}\pi^+$ invariant mass

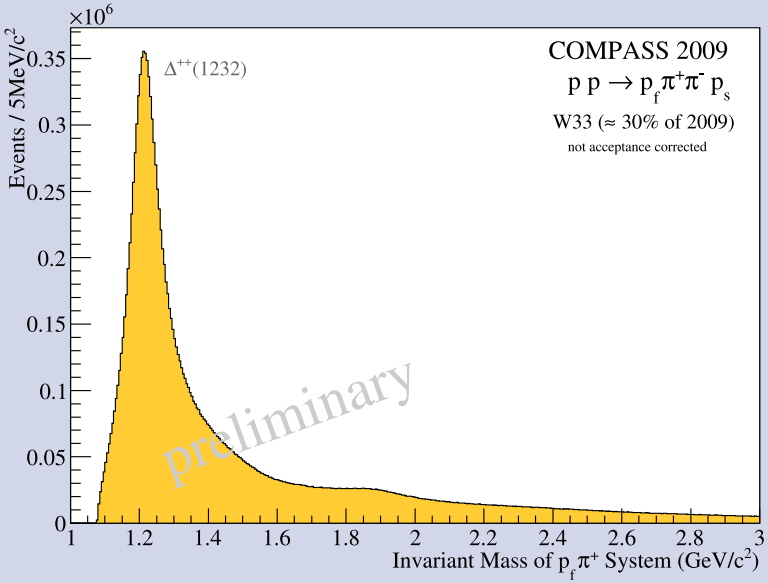

$p_{\text{fast}}\pi^-$ invariant mass

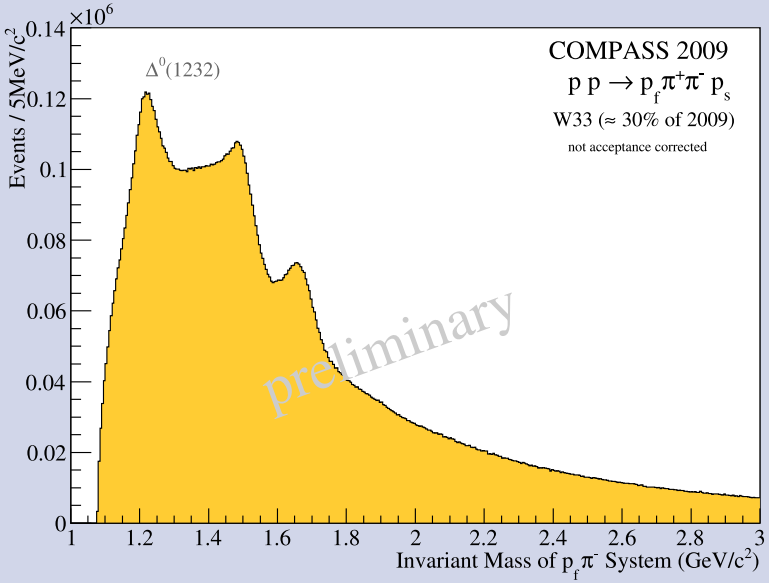

PWA of $p\,p \to p_{\text{fast}}\,\pi^+\pi^-\,p_{\text{slow}}$

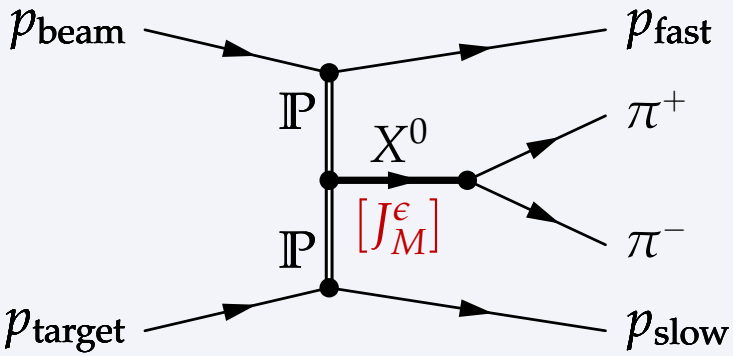

Selected central events

x_F distribution

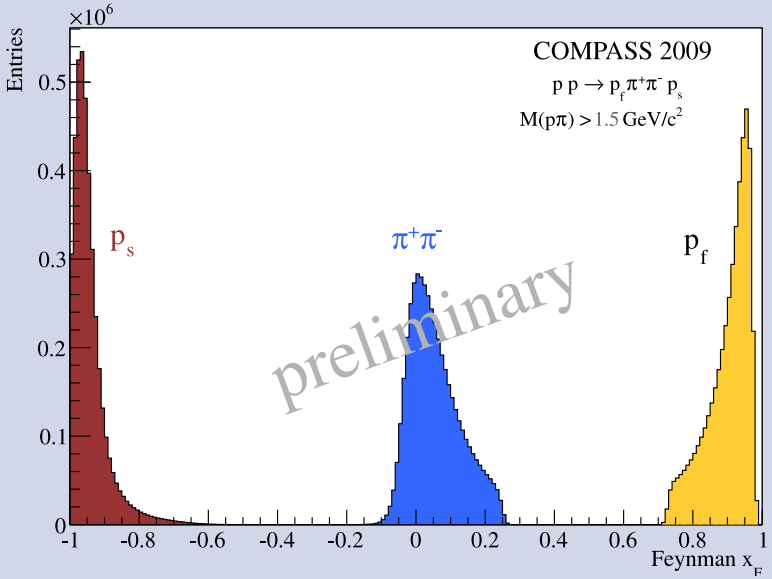

$\pi^+\pi^-$ invariant mass

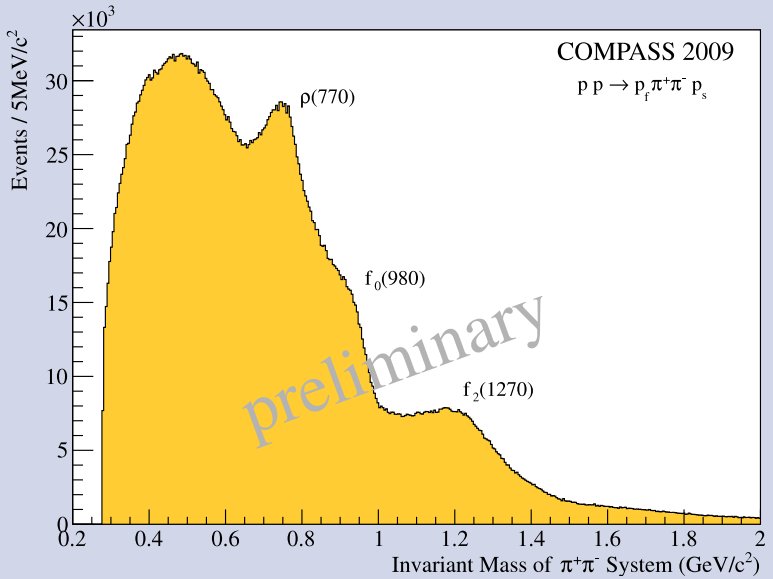

PWA of $p\,p \to p_{\text{fast}}\,\pi^+\pi^-\,p_{\text{slow}}$

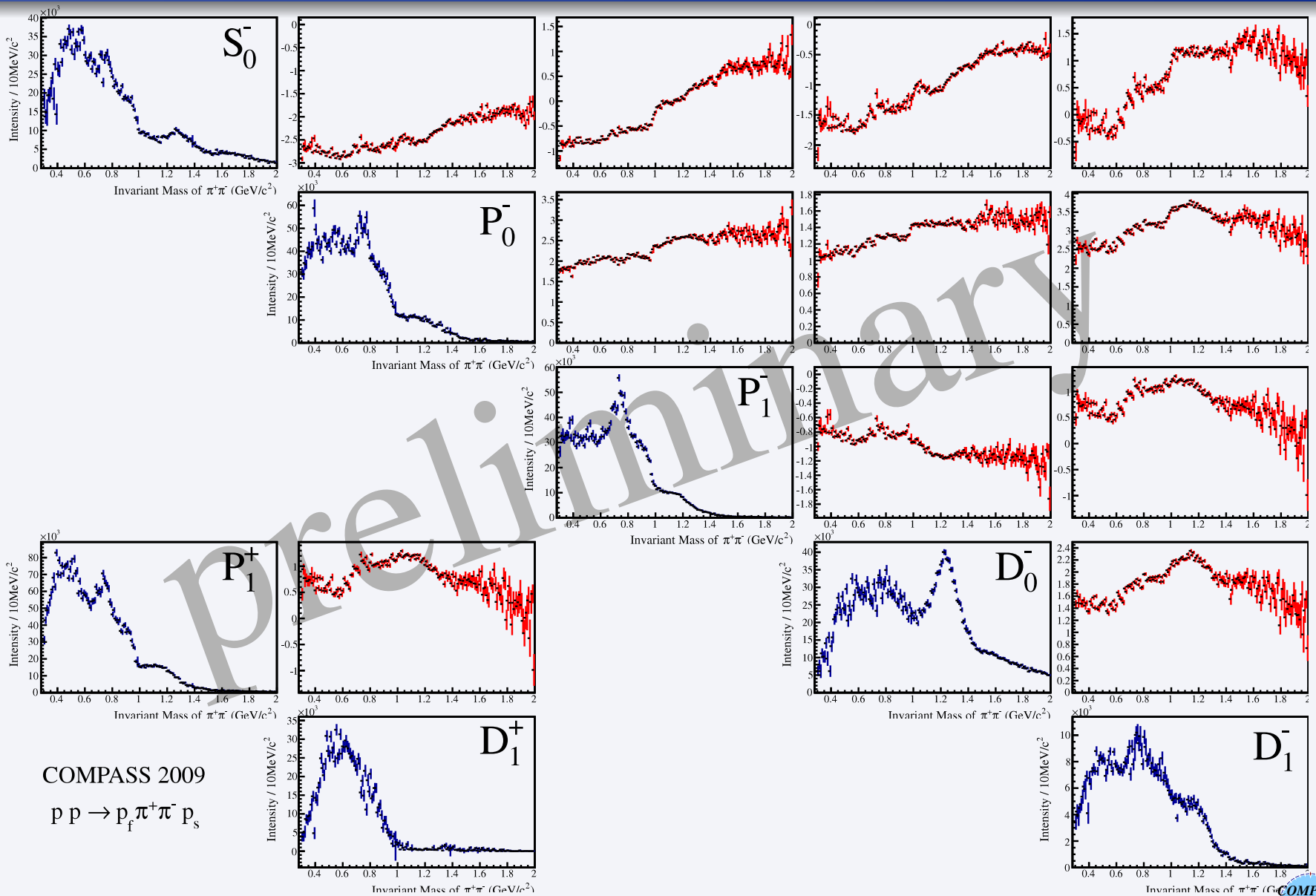

PWA of $p\,p \to p_{\text{fast}}\,\pi^+\pi^-\,p_{\text{slow}}$

Work in progress

- Analysis similar to WA102 experiment
  - Comparable results
- Simplistic fit model
  - Angular information of the two proton scattering planes not taken into account
- 8 different mathematically ambiguous solutions
  - Additional constraints needed to select physical solution

Next steps

- Fit of mass dependence
- Analysis of K^+K^- final state
- Data for $K^0_S K^0_S$, $\pi^0\pi^0$, and $\eta\eta$ final states on tape

PWA of $p\,p \to p_{\text{fast}}\,\pi^+\pi^-\,p_{\text{slow}}$

Work in progress

- Analysis similar to WA102 experiment
  - Comparable results
- Simplistic fit model
  - Angular information of the two proton scattering planes not taken into account
- 8 different mathematically ambiguous solutions
  - Additional constraints needed to select physical solution

Next steps

- Fit of mass dependence
- Analysis of K^+K^- final state
- Data for $K^0_S K^0_S$, $\pi^0\pi^0$, and $\eta\eta$ final states on tape

Conclusions and Outlook

- **COMPASS has large data sets for many final states**
  - Diffractive π^-, K^-, and p dissociation on various targets
  - Central production with π^- and p beam
  - $\pi^-\gamma$ and $K^-\gamma$ Primakoff reaction
- Main focus on J^{PC}-exotic mesons and glueballs
  - *Pilot run:* significant $J^{PC} = 1^{-+}$ signal consistent with $\pi_1(1600)$ seen in $\pi^-\pi^+\pi^-$ data on Pb target PRL **104** (2010) 241803
  - Detailed study of $\pi^-\pi^+\pi^-$ final state on p target
  - Significant 1^{-+} signal also in $\eta\pi^-$ and $\eta'\pi^-$
  - First mass-dependent $\pi^-\pi^+\pi^-\pi^+\pi^-$ PWA in diffractive production
  - Search for scalar glueballs in central production of $\pi^+\pi^-$ and K^+K^-
  - Further channels under analyses
    - K^- diffraction into $K^-\pi^+\pi^-$
    - π^- diffraction into $\pi^-\eta\eta$, $(\pi\pi K\bar{K})^-$, ...

COMPASS is a unique apparatus to study light-quark hadron spectroscopy and chiral dynamics

Conclusions and Outlook

- **COMPASS has large data sets for many final states**
  - Diffractive π^-, K^-, and p dissociation on various targets
  - Central production with π^- and p beam
  - $\pi^-\gamma$ and $K^-\gamma$ Primakoff reaction
- Main focus on J^{PC}-exotic mesons and glueballs
  - *Pilot run:* significant $J^{PC} = 1^{-+}$ signal consistent with $\pi_1(1600)$ seen in $\pi^-\pi^+\pi^-$ data on Pb target PRL **104** (2010) 241803
  - Detailed study of $\pi^-\pi^+\pi^-$ final state on p target
  - Significant 1^{-+} signal also in $\eta\pi^-$ and $\eta'\pi^-$
  - First mass-dependent $\pi^-\pi^+\pi^-\pi^+\pi^-$ PWA in diffractive production
  - Search for scalar glueballs in central production of $\pi^+\pi^-$ and K^+K^-
  - Further channels under analyses
    - K^- diffraction into $K^-\pi^+\pi^-$
    - π^- diffraction into $\pi^-\eta\eta$, $(\pi\pi K\bar{K})^-$, ...

COMPASS is a unique apparatus to study light-quark hadron spectroscopy and chiral dynamics

Conclusions and Outlook

- **COMPASS has large data sets for many final states**
  - Diffractive π^-, K^-, and p dissociation on various targets
  - Central production with π^- and p beam
  - $\pi^-\gamma$ and $K^-\gamma$ Primakoff reaction
- Main focus on J^{PC}-exotic mesons and glueballs
  - *Pilot run:* significant $J^{PC} = 1^{-+}$ signal consistent with $\pi_1(1600)$ seen in $\pi^-\pi^+\pi^-$ data on Pb target PRL **104** (2010) 241803
  - Detailed study of $\pi^-\pi^+\pi^-$ final state on p target
  - Significant 1^{-+} signal also in $\eta\pi^-$ and $\eta'\pi^-$
  - First mass-dependent $\pi^-\pi^+\pi^-\pi^+\pi^-$ PWA in diffractive production
  - Search for scalar glueballs in central production of $\pi^+\pi^-$ and K^+K^-
  - Further channels under analyses
    - K^- diffraction into $K^-\pi^+\pi^-$
    - π^- diffraction into $\pi^-\eta\eta$, $(\pi\pi K\bar{K})^-$, ...

COMPASS is a unique apparatus to study light-quark hadron spectroscopy and chiral dynamics

Conclusions and Outlook

- **COMPASS has large data sets for many final states**
  - Diffractive π^-, K^-, and p dissociation on various targets
  - Central production with π^- and p beam
  - $\pi^-\gamma$ and $K^-\gamma$ Primakoff reaction
- Main focus on J^{PC}-exotic mesons and glueballs
  - *Pilot run:* significant $J^{PC} = 1^{-+}$ signal consistent with $\pi_1(1600)$ seen in $\pi^-\pi^+\pi^-$ data on Pb target PRL **104** (2010) 241803
  - Detailed study of $\pi^-\pi^+\pi^-$ final state on p target
  - Significant 1^{-+} signal also in $\eta\pi^-$ and $\eta'\pi^-$
  - First mass-dependent $\pi^-\pi^+\pi^-\pi^+\pi^-$ PWA in diffractive production
  - Search for scalar glueballs in central production of $\pi^+\pi^-$ and K^+K^-
  - Further channels under analyses
    - K^- diffraction into $K^-\pi^+\pi^-$
    - π^- diffraction into $\pi^-\eta\eta$, $(\pi\pi K\bar{K})^-$, ...

COMPASS is a unique apparatus to study light-quark hadron spectroscopy and chiral dynamics

COMPASS II Timeline

Proposal *CERN-SPSC-2010-014*

2012 Primakoff Reaction $\pi, K + \gamma$

- π, K polarizability
- Chiral anomaly
- Spectroscopy

2014 Drell-Yan

- π beam on polarized target
- TMDs
- Sign of Sivers PDF

2015-16 Deeply Virtual Compton Scattering

- μ beam on (unpolarized) ℓH target
- Generalized PDFs

COMPASS II Timeline

Proposal *CERN-SPSC-2010-014*

2012 Primakoff Reaction $\pi, K + \gamma$

- π, K polarizability
- Chiral anomaly
- Spectroscopy

2014 Drell-Yan

- π beam on polarized target
- TMDs
- Sign of Sivers PDF

2015-16 Deeply Virtual Compton Scattering

- μ beam on (unpolarized) ℓH target
- Generalized PDFs

COMPASS II Timeline

Proposal *CERN-SPSC-2010-014*

2012 Primakoff Reaction $\pi, K + \gamma$

- π, K polarizability
- Chiral anomaly
- Spectroscopy

2014 Drell-Yan

- π beam on polarized target
- TMDs
- Sign of Sivers PDF

2015-16 Deeply Virtual Compton Scattering

- μ beam on (unpolarized) ℓH target
- Generalized PDFs

Outline

Meson Production in Diffractive Dissociation

Reaction similar to diffraction of light by black disk

- Relevant kinematic variable is squared four-momentum transfer $t = (p_{\text{beam}} - p_X)^2 < 0$; more practical $t' \equiv |t| - |t|_{\text{min}} > 0$
- **"Intermediate-t'"** region: diffraction pattern of Pb nucleus
- **"High-t'"** region: scattering on individual nucleons in nucleus

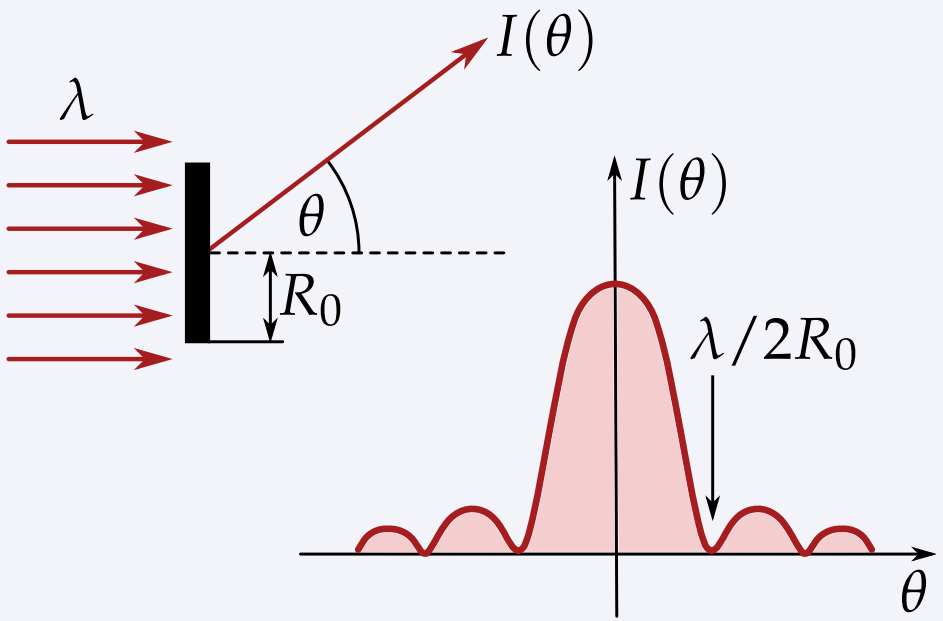

Meson Production in Diffractive Dissociation

Reaction similar to diffraction of light by black disk

- Relevant kinematic variable is squared four-momentum transfer $t = (p_{\text{beam}} - p_X)^2 < 0$; more practical $t' \equiv |t| - |t|_{\text{min}} > 0$
- **"Intermediate-t'"** region: diffraction pattern of Pb nucleus
- "High-t'" region: scattering on individual nucleons in nucleus

$t' \in [0, 0.1]\ (\text{GeV}/c)^2$

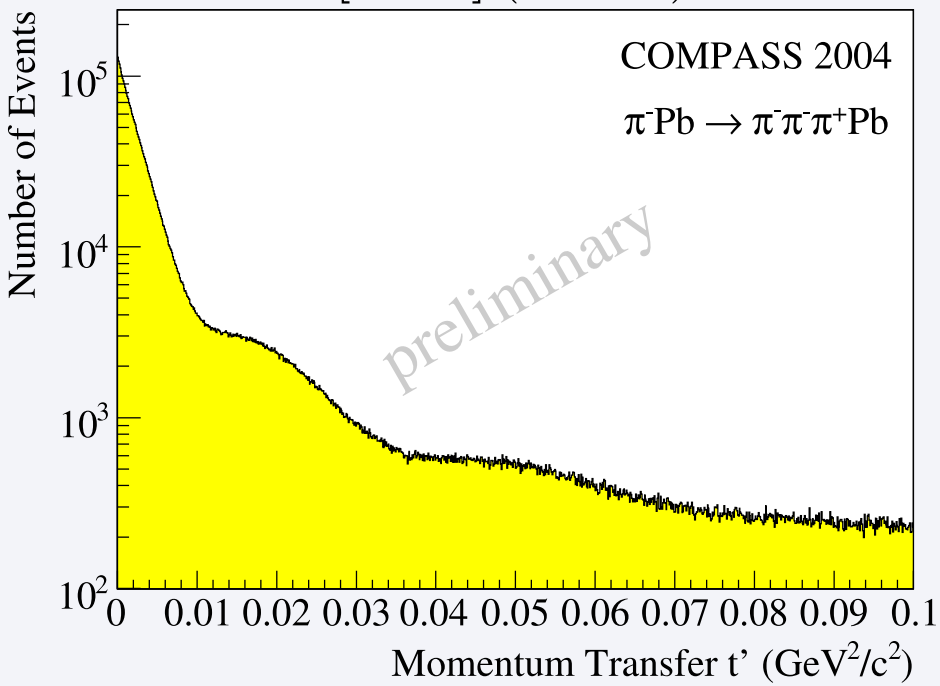

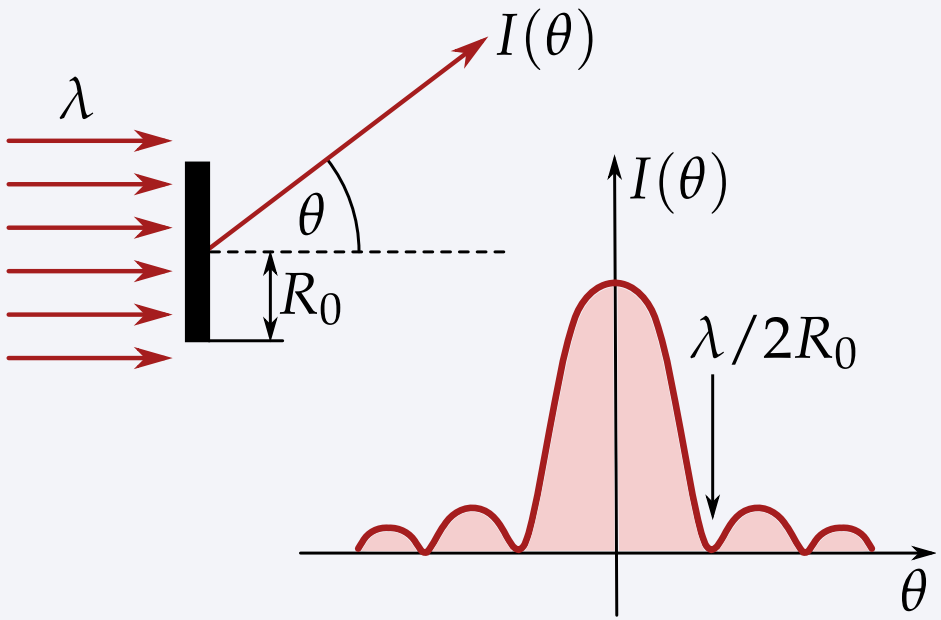

Meson Production in Diffractive Dissociation

Reaction similar to diffraction of light by black disk

- Relevant kinematic variable is squared four-momentum transfer $t = (p_{\text{beam}} - p_X)^2 < 0$; more practical $t' \equiv |t| - |t|_{\text{min}} > 0$
- **"Intermediate-t'"** region: diffraction pattern of Pb nucleus
- **"High-t'"** region: scattering on individual nucleons in nucleus

$t' \in [0, 0.1]\ (\text{GeV}/c)^2$

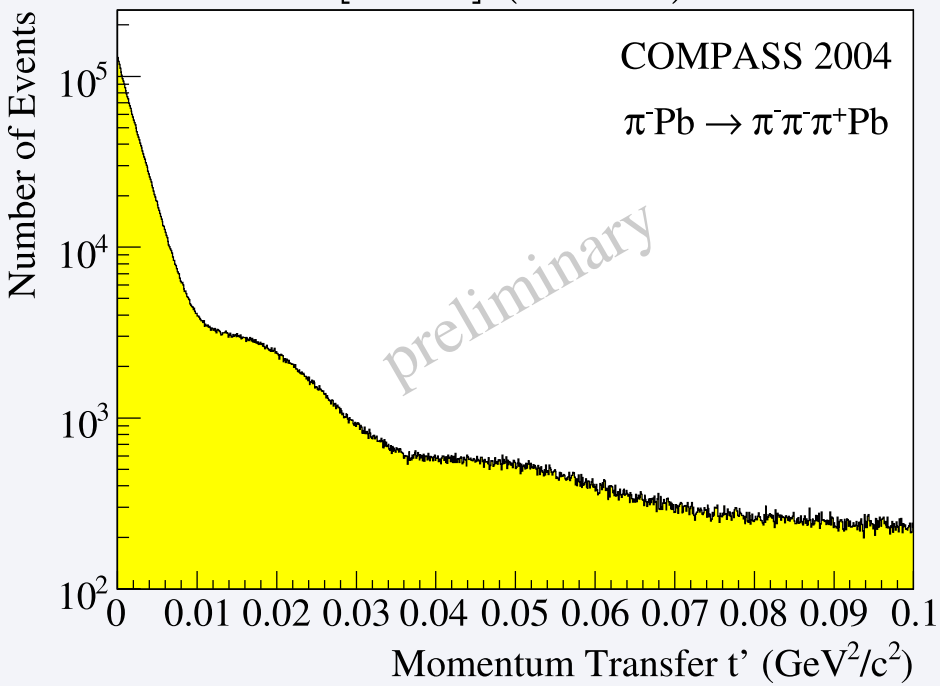

$t' \in [0.1, 1]\ (\text{GeV}/c)^2$

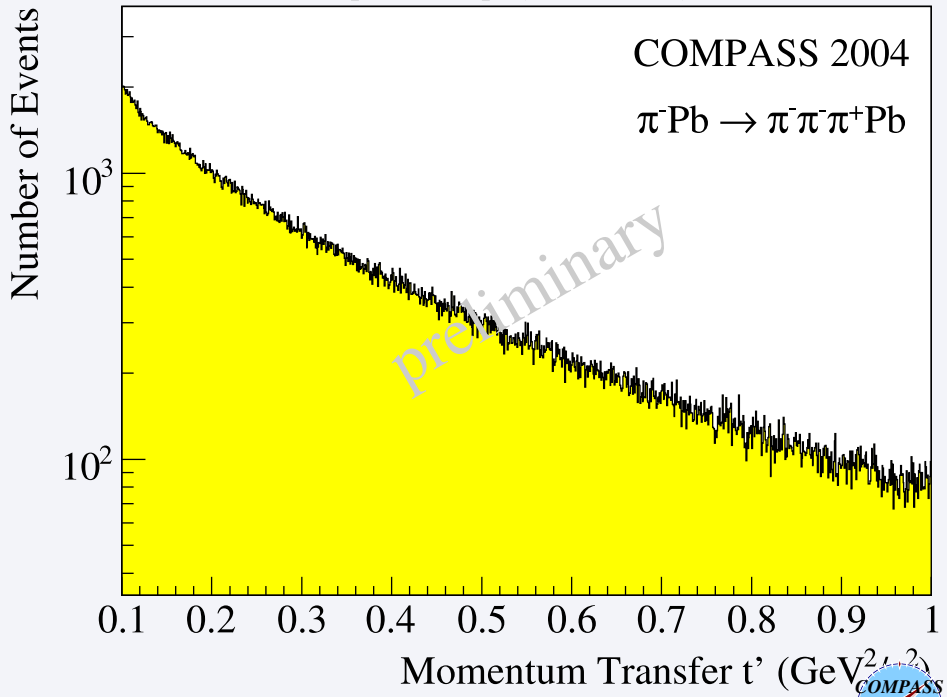

Gottfried-Jackson Coordinate System

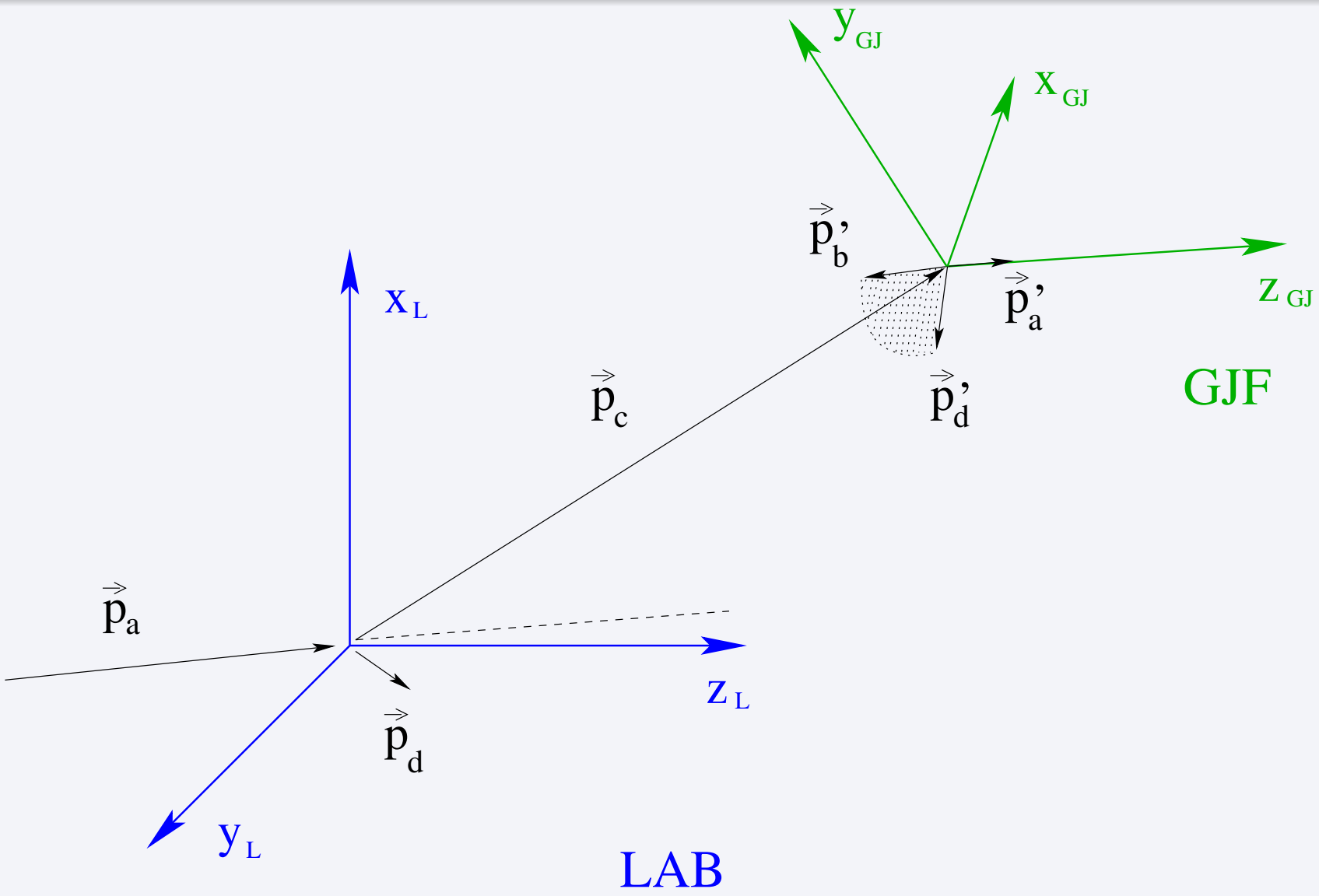

Canonical vs. Helicity Coordinate System

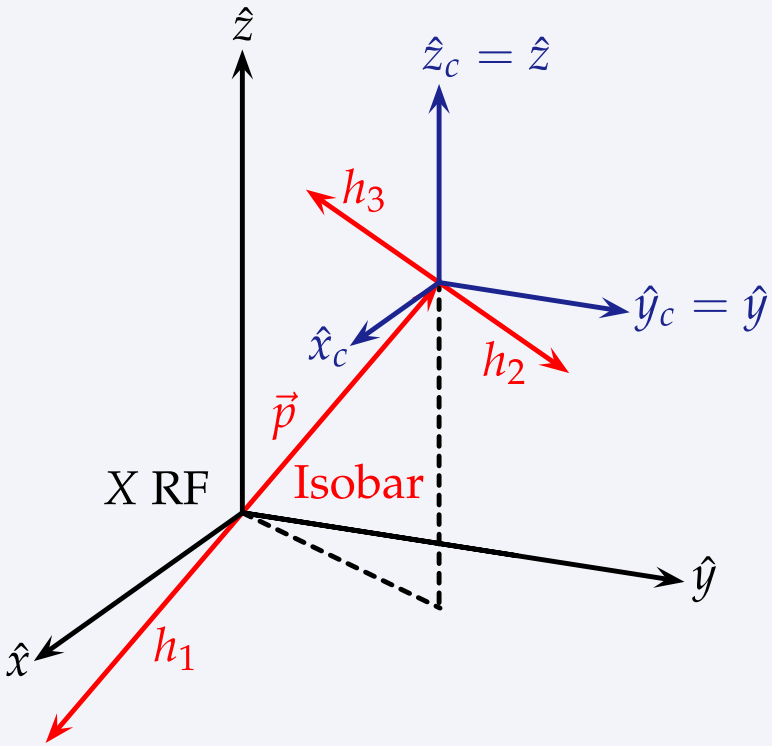

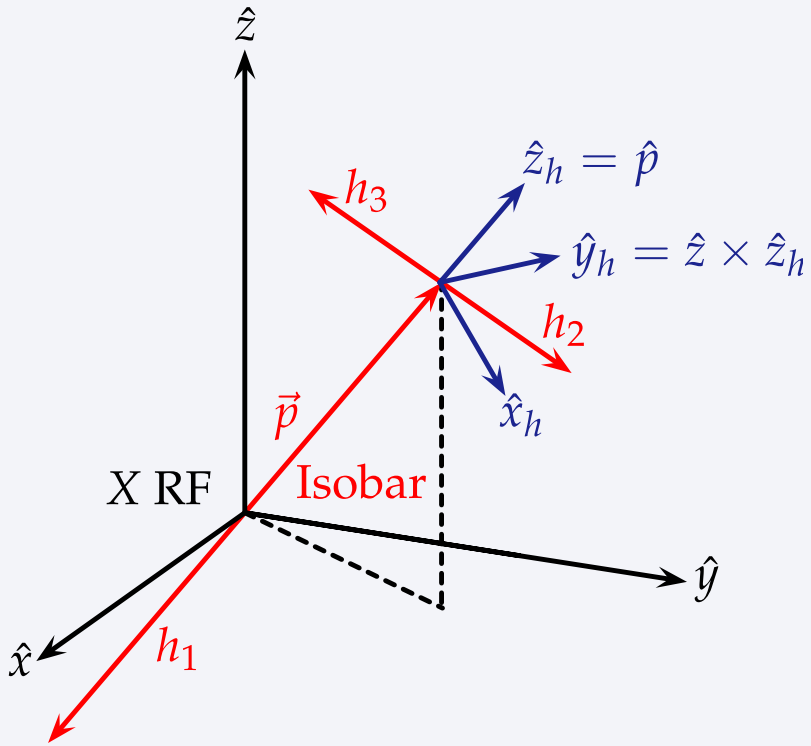

Partial-Wave Analysis Formalism

Cross section parameterization in mass-independent PWA

$$\sigma(\tau; m_X) = \sum_{\epsilon=\pm 1} \sum_{r=1}^{N_r} \left| \sum_{i}^{\text{waves}} T^{\epsilon}_{ir}(m_X)\, A^{\epsilon}_{i}(\tau) \right|^2$$

- ϵ, i: quantum numbers of partial wave ($J^{PC} M^{\epsilon}[\text{isobar}] L$)
- T^{ϵ}_{ir}: complex production amplitudes; fit parameters
- A^{ϵ}_{i}: complex decay amplitudes
- τ: phase space coordinates

Spin-density matrix

$$\rho^{\epsilon}_{ij} = \sum_{r=1}^{N_r} T^{\epsilon}_{ir}\, T^{\epsilon *}_{jr} \qquad \sigma(\tau; m_X) = \sum_{\epsilon=\pm 1} \sum_{i,j}^{\text{waves}} \rho^{\epsilon}_{ij}(m_X)\, A^{\epsilon}_{i}(\tau)\, A^{\epsilon *}_{j}(\tau)$$

- Diagonal elements ρ_{ii}: intensities
- Off-diagonal elements $\rho_{ii},\ i \neq j$: interference terms

Partial-Wave Analysis Formalism

Two-body decay amplitude in helicity formalism

- Decay $X(w, J, \lambda) \to 1(J_1, \lambda_1)\ [L, S]\ 2(J_2, \lambda_2)$

$$A_X^{\text{hel}} = \sqrt{2L+1} \sum_{\lambda_1, \lambda_2} (J_1\, \lambda_1\ J_2\, -\lambda_2 | S\, \delta)\ (L\, 0\ S\, \delta | J\, \delta)$$
$$D^{J*}_{\lambda\delta}(\theta, \phi, 0)\ F_L(q)\ \Delta(w)\ A_1\ A_2$$

- $\delta = \lambda_1 - \lambda_2$
- $D^{J*}_{\lambda\delta}(\theta, \phi, 0)$ — Wigner D-function describes rotational properties of helicity states
- θ, ϕ — polar angles of decay daughter 1 in X rest frame (GJ or helicity frame)
- $F_L(q)$ — Blatt-Weisskopf barrier factor
- $\Delta(w)$ — amplitude that describes resonance shape of X
- $A_{1,2}$ — decay amplitudes of (unstable) daughter particles 1 and 2

Partial-Wave Analysis Formalism

Two-body decay amplitude in canonical formalism

- Decay $X(w, J, M) \to 1(J_1, M_1)\ [L, S]\ 2(J_2, M_2)$

$$A_X^{\text{can}} = \sqrt{2J+1} \sum_{M_1, M_2} (J_1\, M_1\ J_2\, M_2 | S\, M_S) \sum_{M_L} (L\, M_L\ S\, M_S | J\, M)$$
$$\sqrt{\frac{4\pi}{2L+1}} Y_{M_L}^L(\theta, \phi)\, F_L(q)\, \Delta(w)\, A_1\, A_2$$

- $Y_{M_L}^L(\theta, \phi)$ — Spherical harmonic describes rotational property of $|L\, M_L\rangle$ state
- θ, ϕ — polar angles of decay daughter 1 in X rest frame (reached by simple boost, no rotations)
- $F_L(q)$ — Blatt-Weisskopf barrier factor
- $\Delta(w)$ — amplitude that describes resonance shape of X
- $A_{1,2}$ — decay amplitudes of (unstable) daughter particles 1 and 2

Partial-Wave Analysis Formalism

Extended maximum-likelihood method

- Likelihood $\mathcal{L}$ to observe N events distributed according to $\sigma(\tau; m_X)$ and acceptance $\mathrm{Acc}(\tau; m_X)$

$$\mathcal{L} = \underbrace{\left[\frac{\overline{N}^N}{N!} e^{-\overline{N}}\right]}_{\text{Poisson likelihood}} \prod_{n=1}^{N} \underbrace{\left[\frac{\sigma(\tau_n; m_X)}{\int \mathrm{d}\tau\, \sigma(\tau; m_X)\, \mathrm{Acc}(\tau; m_X)}\right]}_{\text{Likelihood of event } n}$$

$$\text{with} \qquad \overline{N} \propto \int \mathrm{d}\tau\, \sigma(\tau; m_X)\, \mathrm{Acc}(\tau; m_X)$$

$$\mathcal{L} \propto \left[\frac{\overline{N}^N}{N!} e^{-\overline{N}}\right] \left[\frac{1}{\overline{N}^N} \prod_{n=1}^{N} \sigma(\tau_n; m_X)\right]$$

$$\mathcal{L} \propto e^{-\int \mathrm{d}\tau\, \sigma(\tau; m_X)\, \mathrm{Acc}(\tau; m_X)} \prod_{n=1}^{N} \sigma(\tau_n; m_X)$$

Partial-Wave Analysis Formalism

Extended maximum-likelihood method (cont.)

- Insert parameterization of cross section for $\sigma(\tau_n; m_X)$

$$\mathcal{L} \propto e^{-\int \mathrm{d}\tau\, \sigma(\tau;m_X)\,\mathrm{Acc}(\tau;m_X)} \prod_{n=1}^{N} \sum_{r=1}^{N_r} \left| \sum_{\text{waves}} T_{r,\text{wave}}(m_X)\, A_{\text{wave}}(\tau_n; m_X) \right|^2$$

- Make expression less unwieldy by taking logarithm

$$\ln \mathcal{L} = \sum_{n=1}^{N} \ln \left[\sum_{r=1}^{N_r} \left| \sum_{\text{waves}} T_{r,\text{wave}}(m_X)\, A_{\text{wave}}(\tau_n; m_X) \right|^2 \right] - \underbrace{\int \mathrm{d}\tau\, \sigma(\tau; m_X)\,\mathrm{Acc}(\tau; m_X)}_{\text{Normalization integral}}$$

- Normalization integral estimated using phase space Monte Carlo

$\pi^-\pi^+\pi^-$ Final State

Acceptance (p Target)

$\pi^-\pi^+\pi^-$ mass

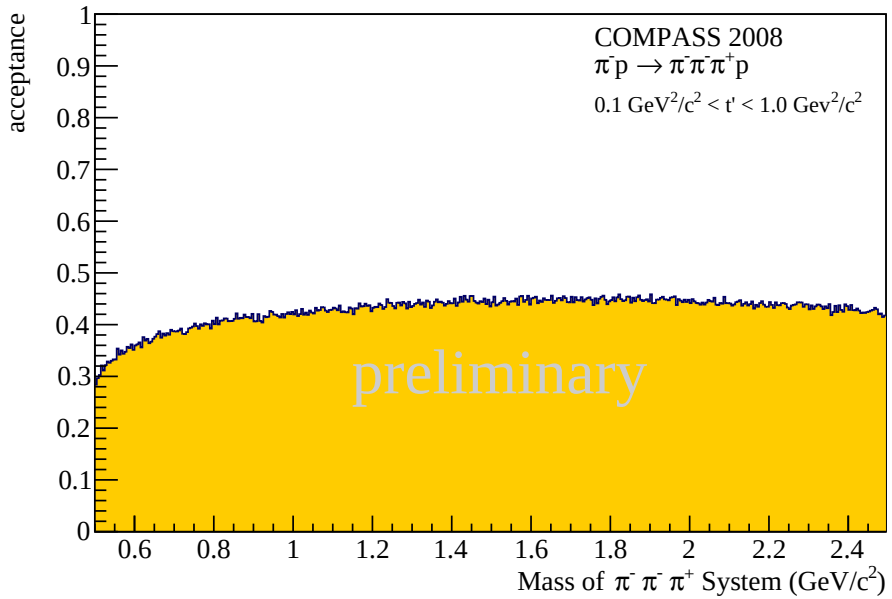

$\pi^+\pi^-$ mass

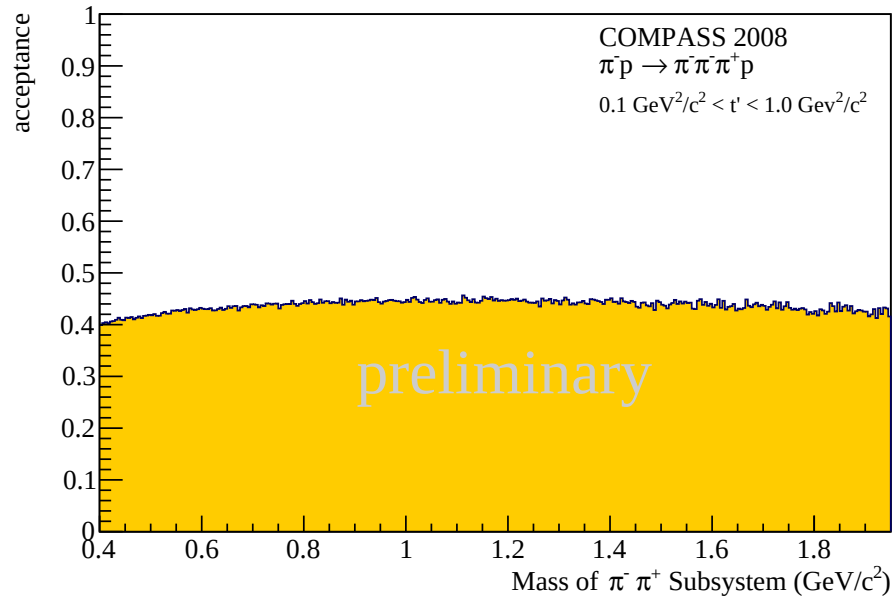

$\pi^-\pi^+\pi^-$ Final State

Acceptance (p Target)

Gottfried-Jackson frame: $\cos\theta_{GJ}$

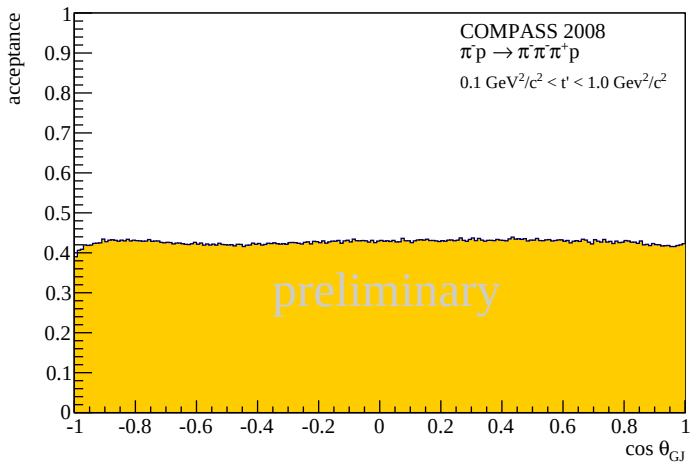

Gottfried-Jackson frame: φ_{TY}

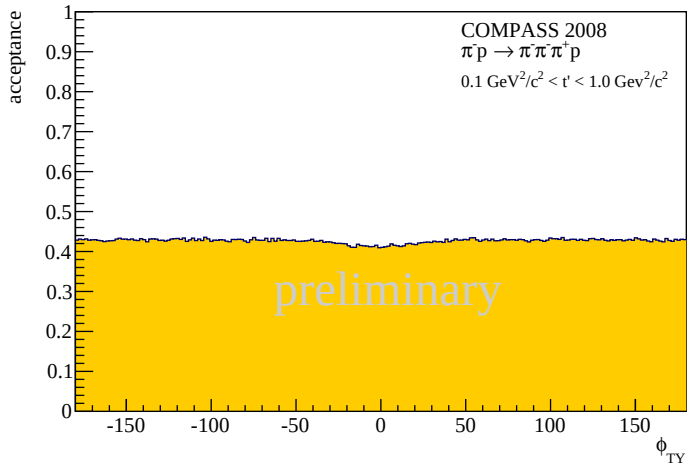

Helicity frame: $\cos\theta_{HF}$

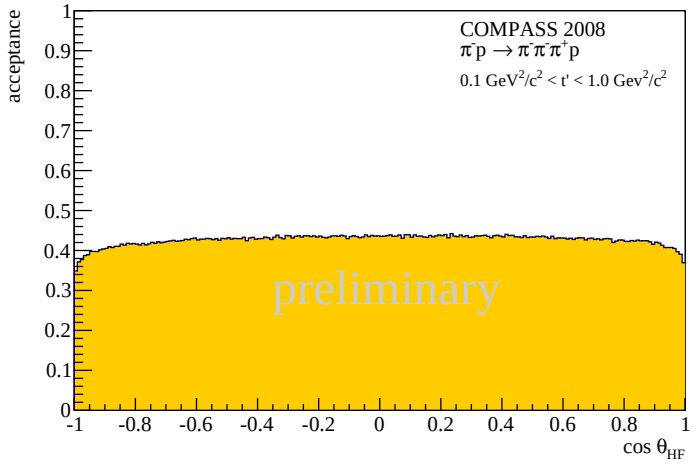

Helicity frame: φ_{HF}

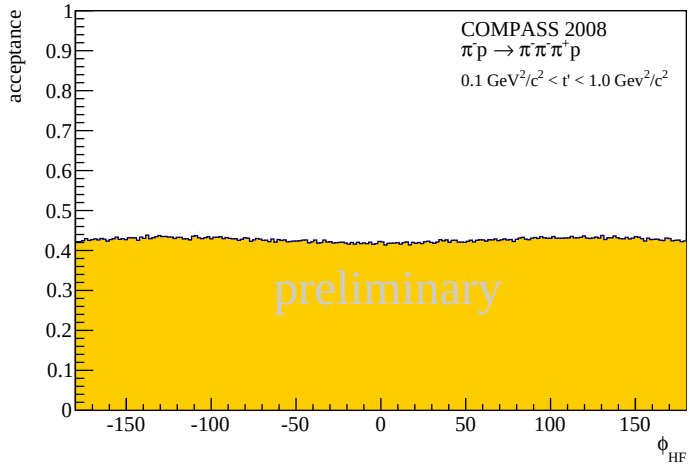

$\eta'\pi^-$ Final State

$\cos\theta_{GJ}$ vs. $\eta'\pi^-$ Invariant Mass

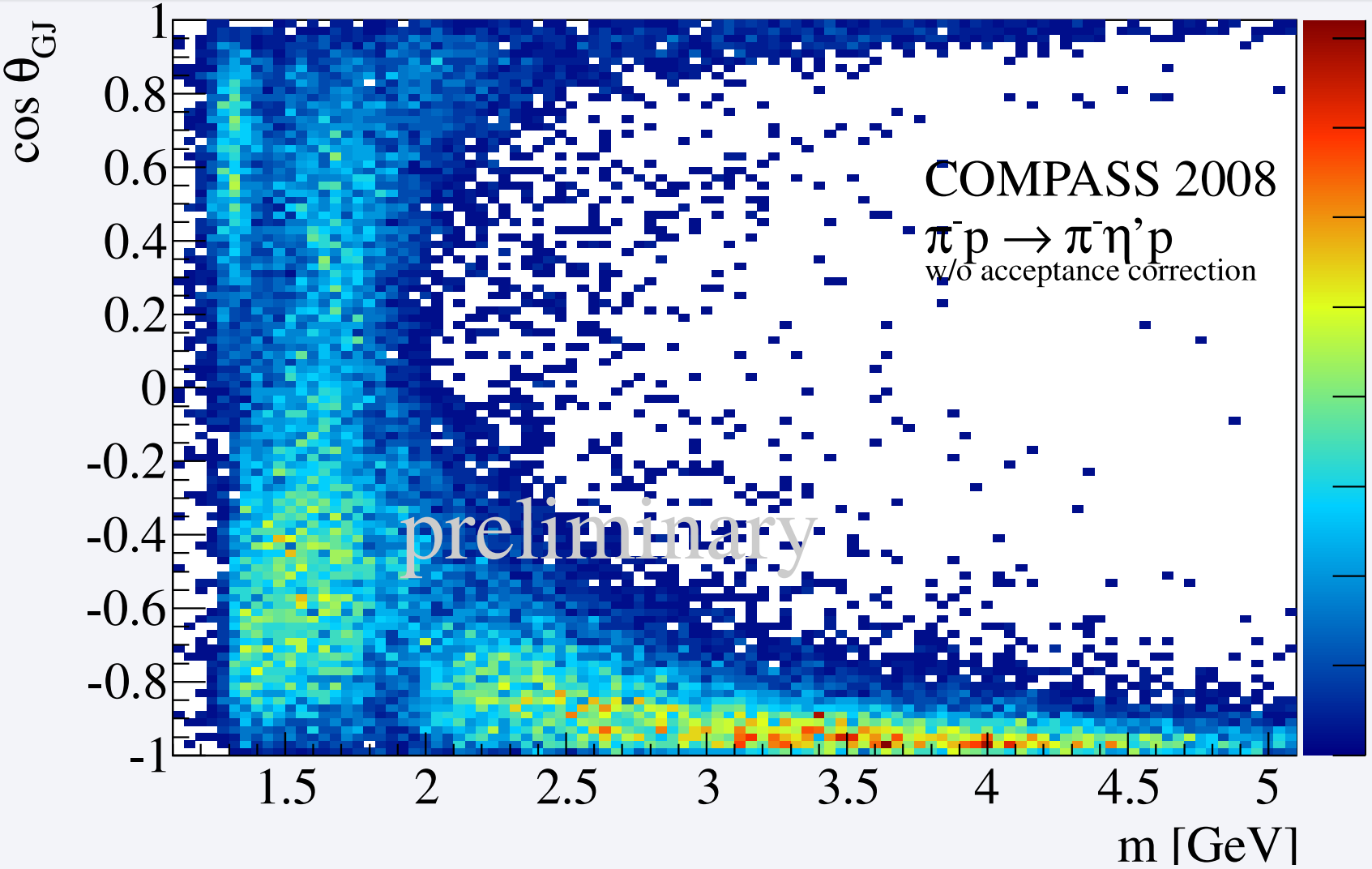

Introduction

Chiral Perturbation Theory (χPT) in a nutshell

- QCD Lagrangian chiral symmetric in limit $m_{u,d,s} \to 0$
- Leads to degeneracy of $J^P = 0^-$ and 0^+ states
  - Not observed
- Chiral symmetry of QCD spontaneously broken
  - 8 massless $J^P = 0^-$ Goldstone bosons
- Small u, d, and s masses
  - Explicit breaking of chiral symmetry $\Longrightarrow$ treated perturbatively
  - 8 light $J^P = 0^-$ pseudo-Goldstone bosons: π, K, and η
- Low-energy effective field theory with same symmetries as QCD
  - C, P, T, Lorentz invariance, and chiral symmetry
- Hadrons as fundamental degrees of freedom
- Inner d.o.f. "condensed" into low-energy constants
- Series expansion in $p_{\text{hadron}} \lesssim 1$ GeV/c
- Model-independent approach to describe interaction of mesons

Introduction

Chiral Perturbation Theory (χPT) in a nutshell

- QCD Lagrangian chiral symmetric in limit $m_{u,d,s} \to 0$
- Leads to degeneracy of $J^P = 0^-$ and 0^+ states
  - Not observed
- Chiral symmetry of QCD spontaneously broken
  - 8 massless $J^P = 0^-$ Goldstone bosons
- Small u, d, and s masses
  - Explicit breaking of chiral symmetry $\implies$ treated perturbatively
  - 8 light $J^P = 0^-$ pseudo-Goldstone bosons: π, K, and η
- Low-energy effective field theory with same symmetries as QCD
  - C, P, T, Lorentz invariance, and chiral symmetry
- Hadrons as fundamental degrees of freedom
- Inner d.o.f. "condensed" into low-energy constants
- Series expansion in $p_{\text{hadron}} \lesssim 1$ GeV/c
- Model-independent approach to describe interaction of mesons

Introduction

Chiral Perturbation Theory (χPT) in a nutshell

- QCD Lagrangian chiral symmetric in limit $m_{u,d,s} \to 0$
- Leads to degeneracy of $J^P = 0^-$ and 0^+ states
  - Not observed
- Chiral symmetry of QCD spontaneously broken
  - 8 massless $J^P = 0^-$ Goldstone bosons
- Small u, d, and s masses
  - Explicit breaking of chiral symmetry $\implies$ treated perturbatively
  - 8 light $J^P = 0^-$ pseudo-Goldstone bosons: π, K, and η
- Low-energy effective field theory with same symmetries as QCD
  - C, P, T, Lorentz invariance, and chiral symmetry
- Hadrons as fundamental degrees of freedom
- Inner d.o.f. "condensed" into low-energy constants
- Series expansion in $p_{\text{hadron}} \lesssim 1$ GeV/c
- Model-independent approach to describe interaction of mesons

Chiral dynamics in $\pi\gamma \to \pi^-\pi^+\pi^-$

Pb target: Production mechanism depends on t' region

- $t' \in [0.1, 1]\ (\mathrm{GeV}/c)^2$: scattering on individual nucleons in nucleus
- For $t' \lesssim 0.01\ (\mathrm{GeV}/c)^2$: coherent scattering on Pb nucleus
- For $t' \lesssim 10^{-3}\ (\mathrm{GeV}/c)^2$ additional contribution from reactions in Coulomb field of nucleus

$t' \in [0.1, 1]\ (\mathrm{GeV}/c)^2$

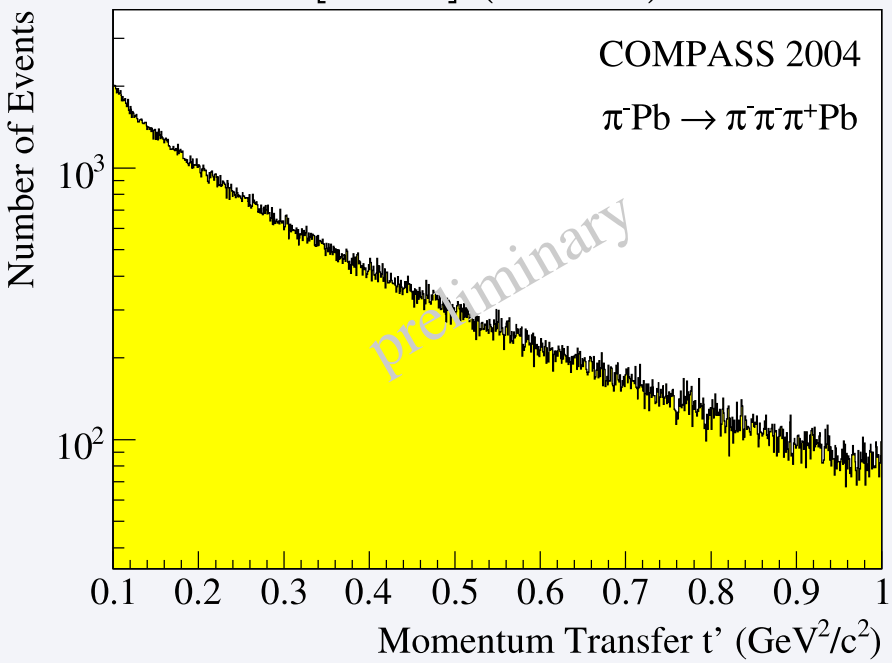

Chiral dynamics in $\pi\gamma \to \pi^-\pi^+\pi^-$

Pb target: Production mechanism depends on t' region

- $t' \in [0.1, 1]\ (\mathrm{GeV}/c)^2$: scattering on individual nucleons in nucleus
- For $t' \lesssim 0.01\ (\mathrm{GeV}/c)^2$: coherent scattering on Pb nucleus
- For $t' \lesssim 10^{-3}\ (\mathrm{GeV}/c)^2$ additional contribution from reactions in Coulomb field of nucleus

$t' \in [0.1, 1]\ (\mathrm{GeV}/c)^2$

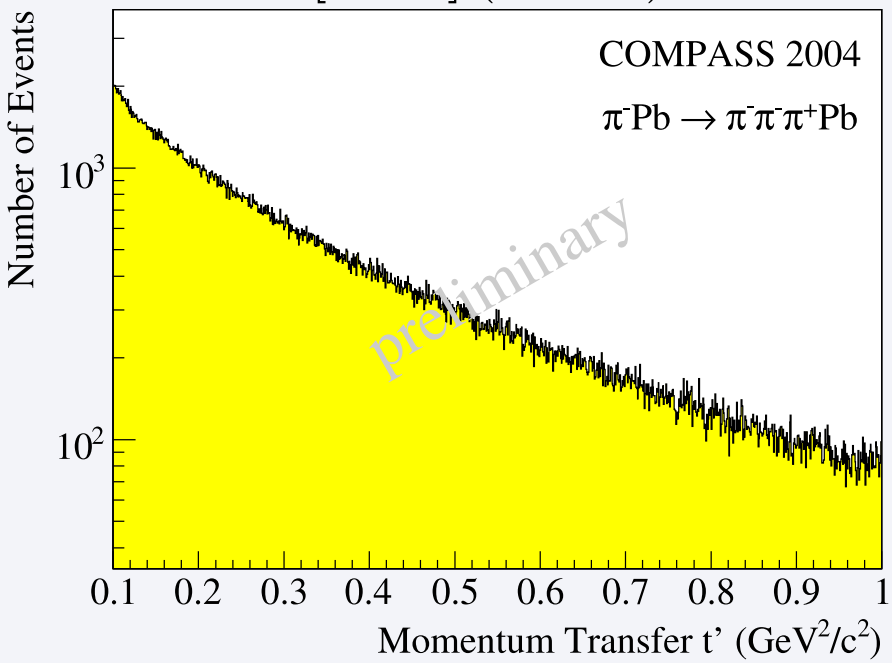

$t' < 0.1\ (\mathrm{GeV}/c)^2$

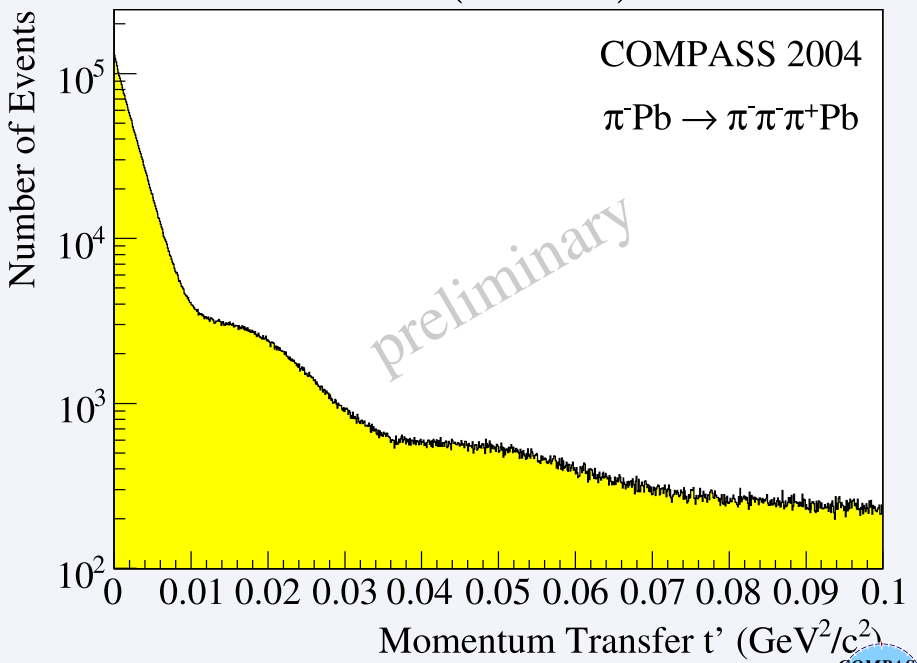

Chiral dynamics in $\pi\gamma \to \pi^-\pi^+\pi^-$

Pb target: Production mechanism depends on t' region

- $t' \in [0.1, 1]\ (\mathrm{GeV}/c)^2$: scattering on individual nucleons in nucleus
- For $t' \lesssim 0.01\ (\mathrm{GeV}/c)^2$: coherent scattering on Pb nucleus
- For $t' \lesssim 10^{-3}\ (\mathrm{GeV}/c)^2$ additional contribution from reactions in Coulomb field of nucleus

$t' < 0.01\ (\mathrm{GeV}/c)^2$

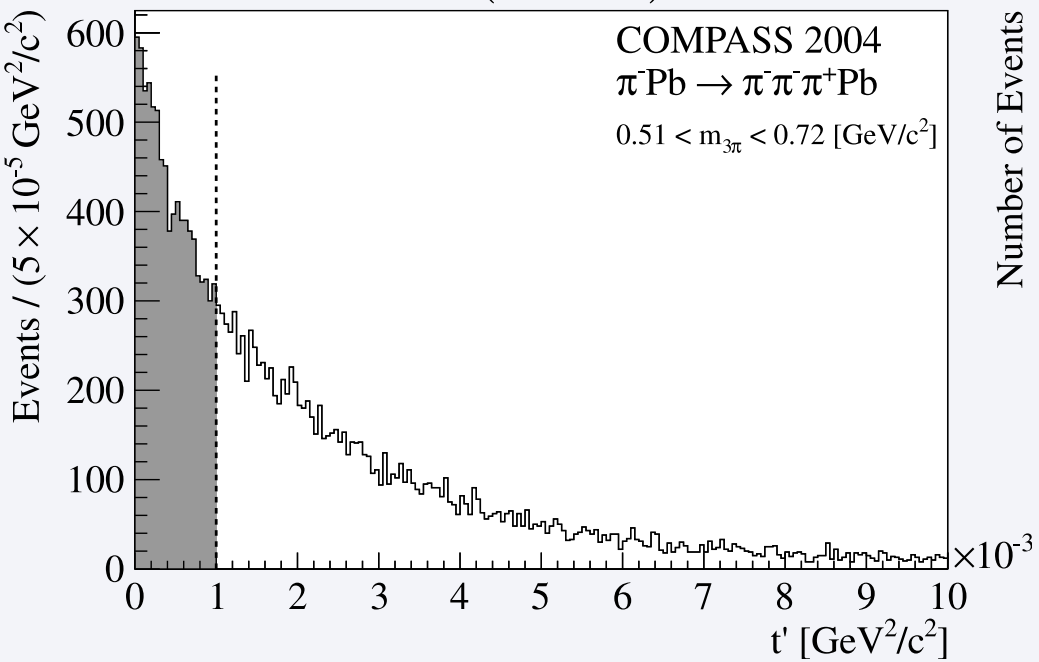

$t' < 0.1\ (\mathrm{GeV}/c)^2$

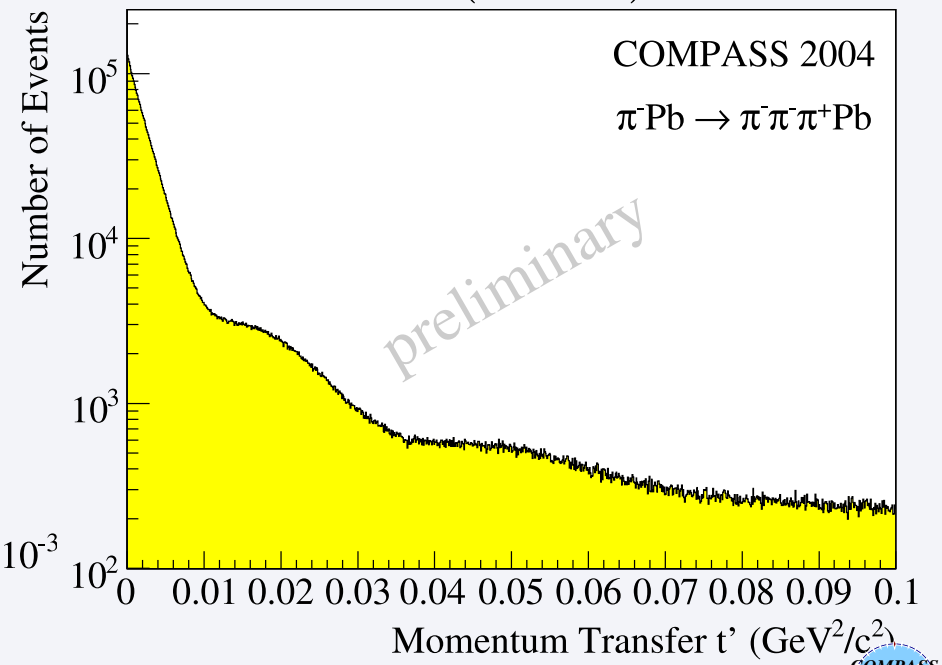

Chiral dynamics in $\pi\gamma \to \pi^-\pi^+\pi^-$

Test of χPT

- Parameter-free prediction from χPT for $\pi^-\gamma \to \pi^-\pi^+\pi^-$ with $m_{3\pi} < 700$ MeV/c^2

Kaiser, Friedrich, EPJ A36 (2008) 181

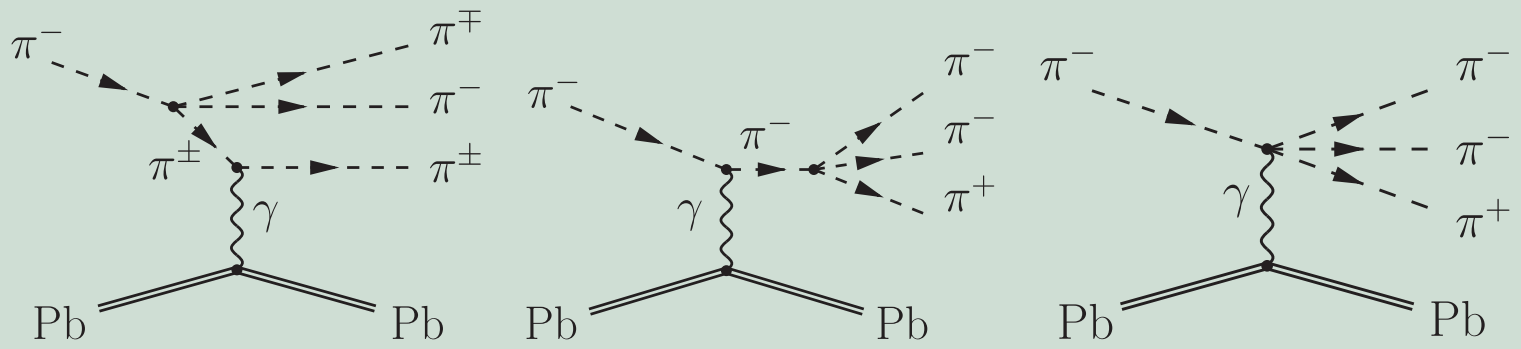

- Interactions in Coulomb field separable from strong background in region $t' < 10^{-3}$ (GeV/c)^2
- PWA method used to extract strength of χPT amplitude as function of $m_{3\pi}$
- Absolute cross section from beam flux measurement
  - Using $K^- \to \pi^-\pi^+\pi^-$ decay of beam K^- (2.4 %)

Chiral dynamics in $\pi\gamma \to \pi^-\pi^+\pi^-$

Test of χPT

- Parameter-free prediction from χPT for $\pi^-\gamma \to \pi^-\pi^+\pi^-$ with $m_{3\pi} < 700$ MeV/c^2

Kaiser, Friedrich, EPJ A36 (2008) 181

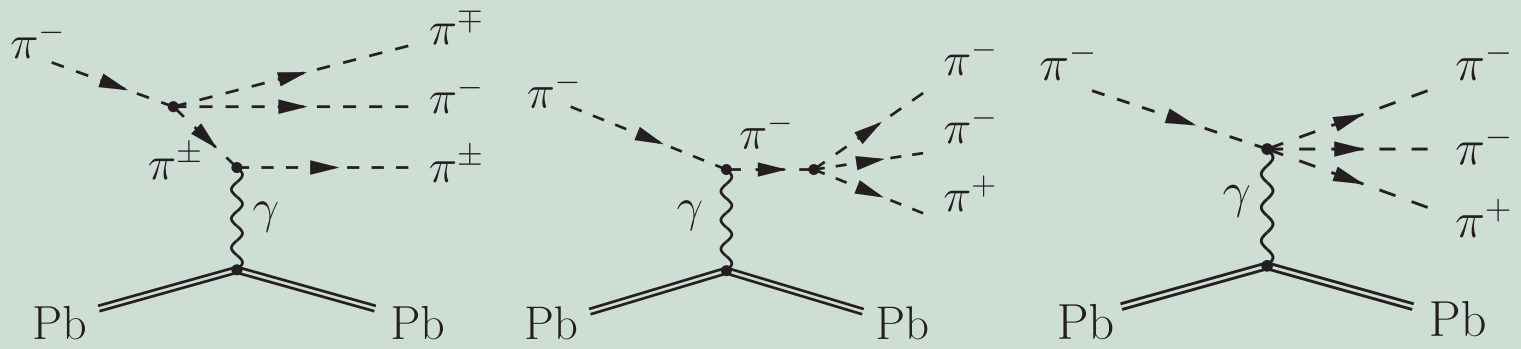

- Interactions in Coulomb field separable from strong background in region $t' < 10^{-3}$ (GeV/c)^2
- PWA method used to extract strength of χPT amplitude as function of $m_{3\pi}$
- Absolute cross section from beam flux measurement
  - Using $K^- \to \pi^-\pi^+\pi^-$ decay of beam K^- (2.4 %)

First Measurement of $\pi^-\gamma \to \pi^-\pi^+\pi^-$ Cross Section

PRL 108 (2012) 192001

Data confirm leading-order χPT calculation

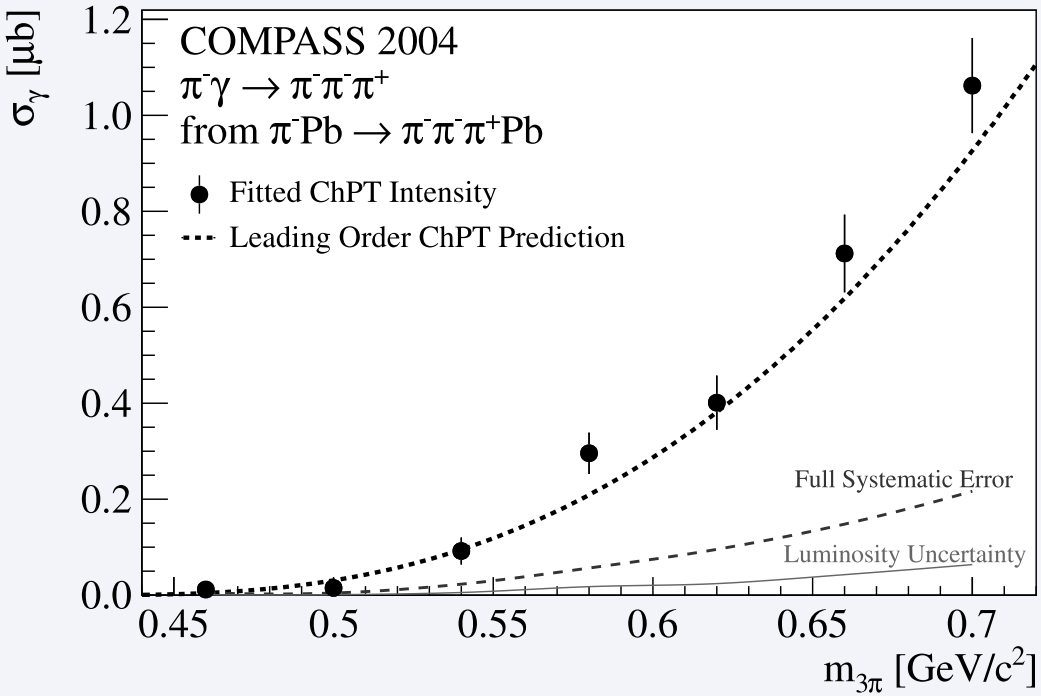

Work in progress: analysis of $\pi^-\pi^0\pi^0$ final state

- More sensitive to loop contributions

PWA of π^- Pb $\rightarrow \pi^-\pi^+\pi^-$ Pb at low t' (Pilot Run)

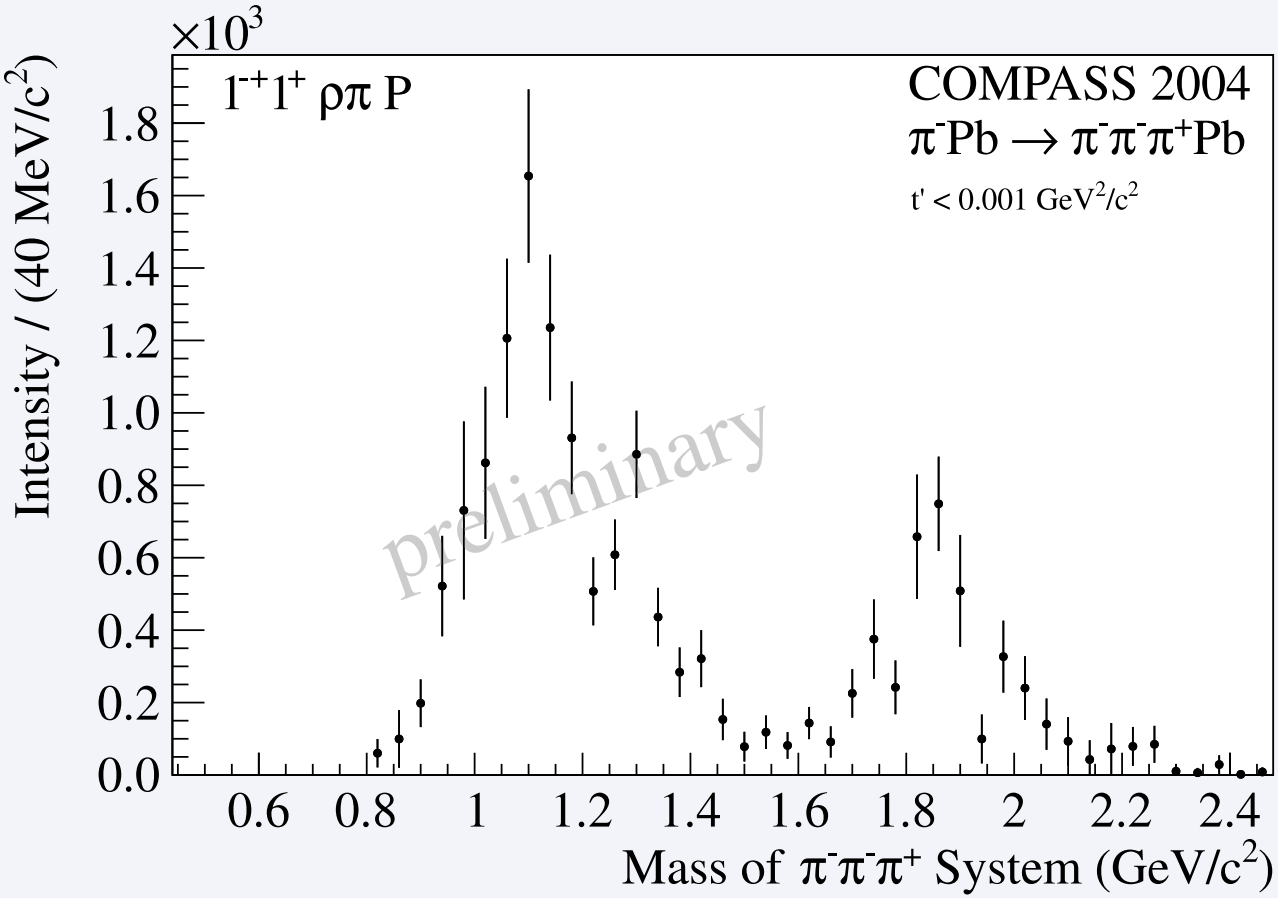

Photoproduction

No evidence for spin-exotic $\pi_1(1600)$

Charged-Pion Polarizability

Electromagnetic structure of bound state

- Charge
- Charge radius
- **Dipole polarizability**

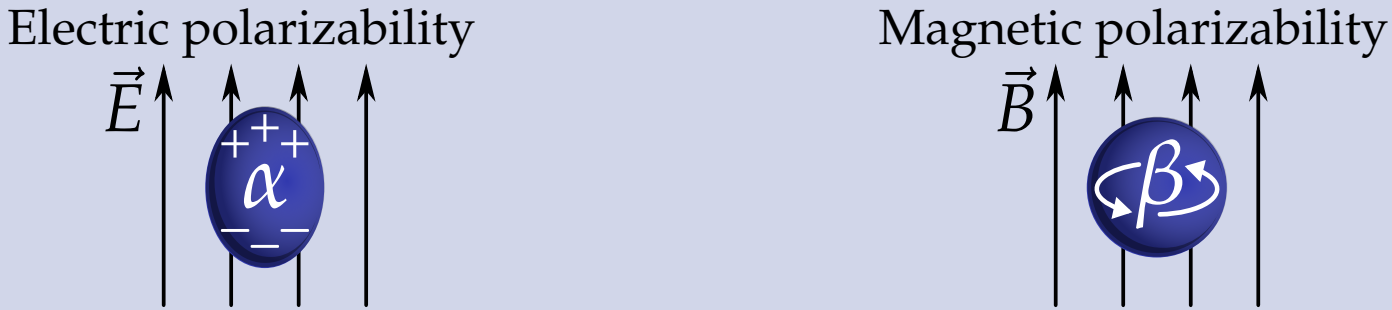

- Higher terms (quadrupole polarizability, ...)

Prediction from χPT two-loop calculation

Gasser, Ivanov, Sainio, NPB 745 (2006) 84

- Electric polarizability $\alpha_\pi^{\chi\mathrm{PT}} = (2.93 \pm 0.5) \cdot 10^{-4}\,\mathrm{fm}^3$
- Magnetic polarizability $\beta_\pi^{\chi\mathrm{PT}} = (-2.77 \pm 0.5) \cdot 10^{-4}\,\mathrm{fm}^3$
- Approximation: $\alpha_\pi + \beta_\pi = 0$
- Compare: proton polarizability $\alpha_p = 12 \cdot 10^{-4}\,\mathrm{fm}^3$

Charged-Pion Polarizability

How to measure pion-photon scattering?

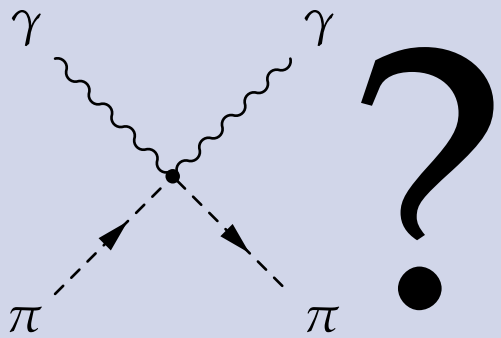

Embed processes:

Photon-photon fusion

Radiative pion photoproduction

Primakoff-Compton process

Charged-Pion Polarizability

How to measure pion-photon scattering?

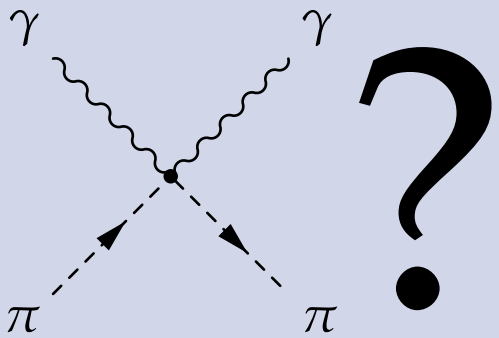

Embed processes:

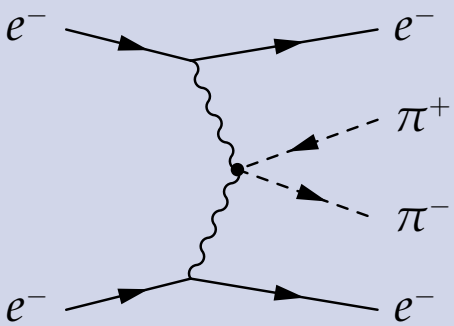

Photon-photon fusion

Radiative pion photoproduction

Primakoff-Compton process

Charged-Pion Polarizability

How to measure pion-photon scattering?

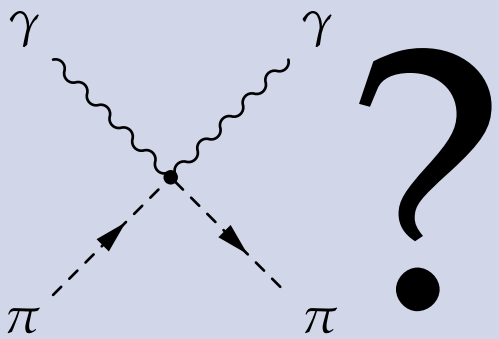

Embed processes:

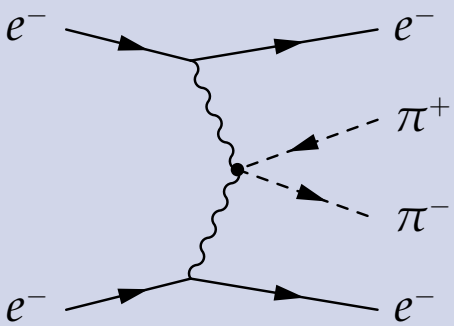

Photon-photon fusion

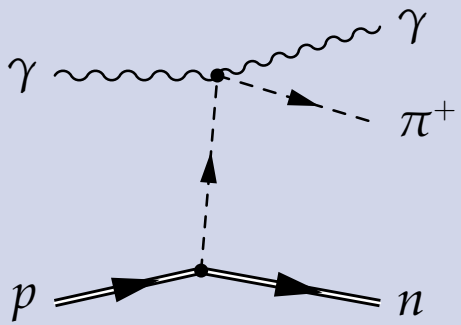

Radiative pion photoproduction

Primakoff-Compton process

Charged-Pion Polarizability

How to measure pion-photon scattering?

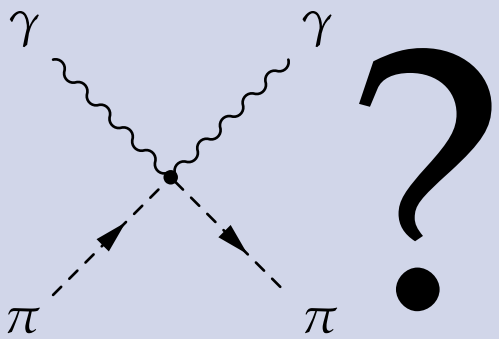

Embed processes:

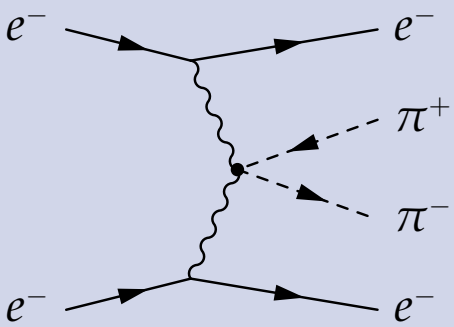

Photon-photon fusion

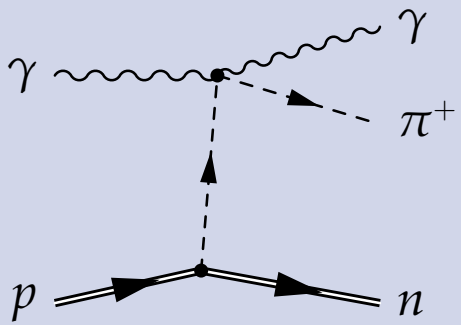

Radiative pion photoproduction

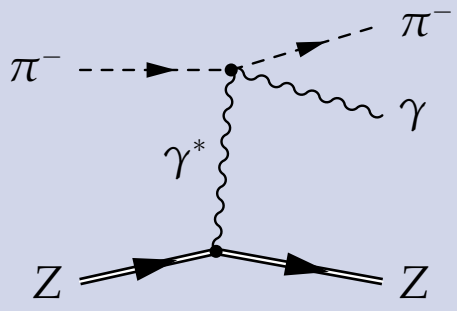

Primakoff-Compton process

Previous Measurements of Charged-Pion Polarizability

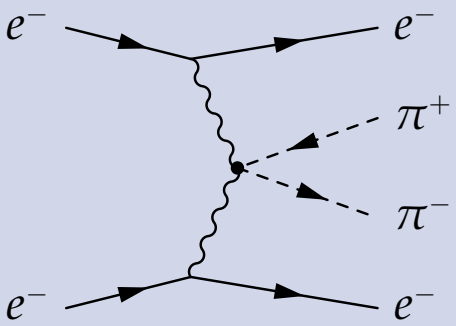

Photon-photon fusion

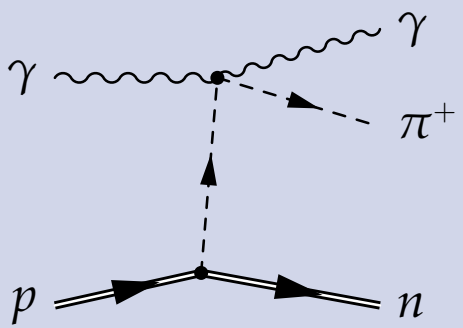

Radiative pion photoproduction

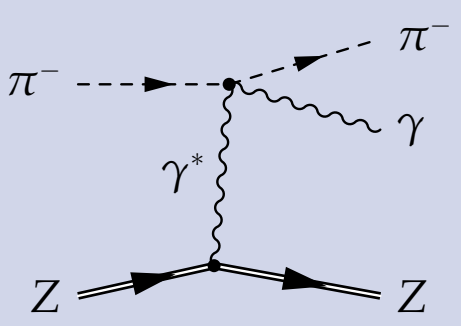

Primakoff-Compton process

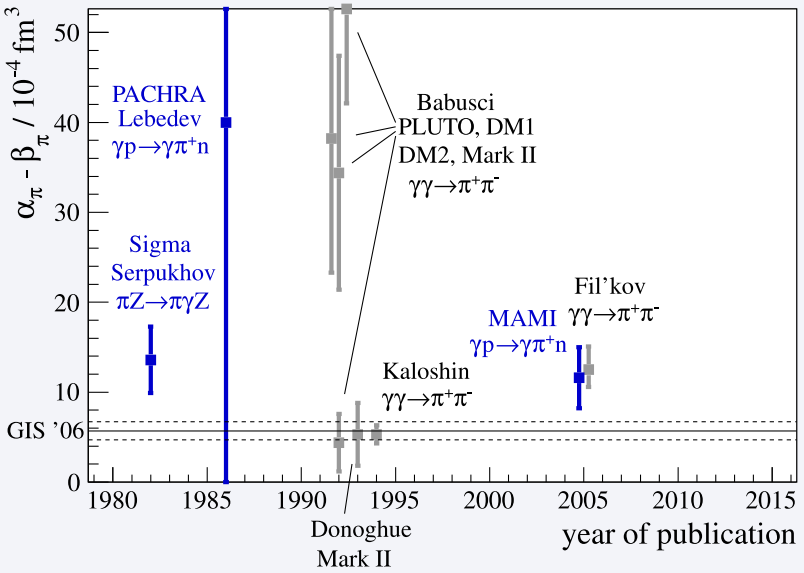

Previous Measurements of Charged-Pion Polarizability

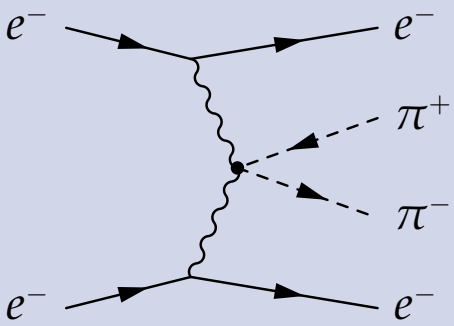

Photon-photon fusion

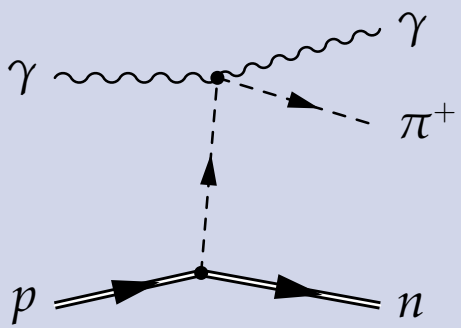

Radiative pion photoproduction

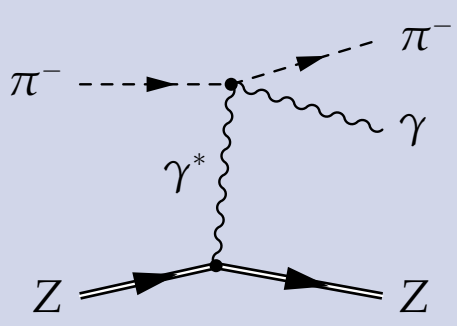

Primakoff-Compton process

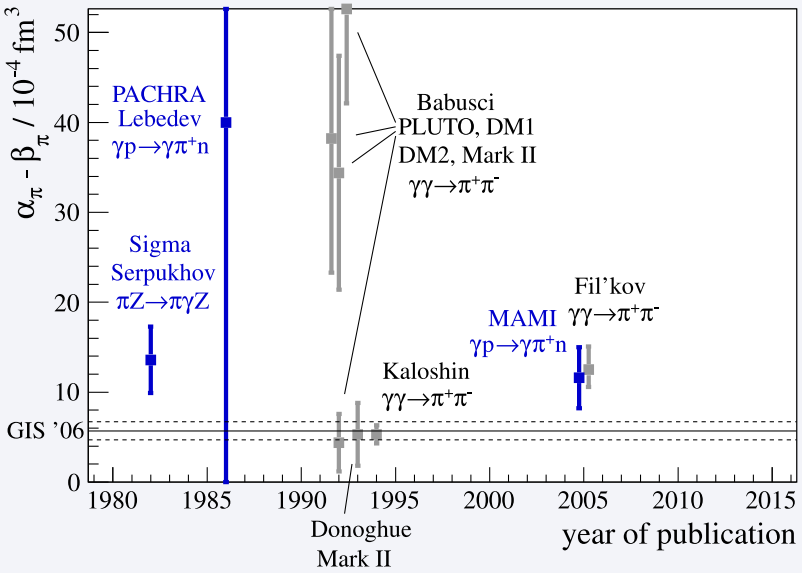

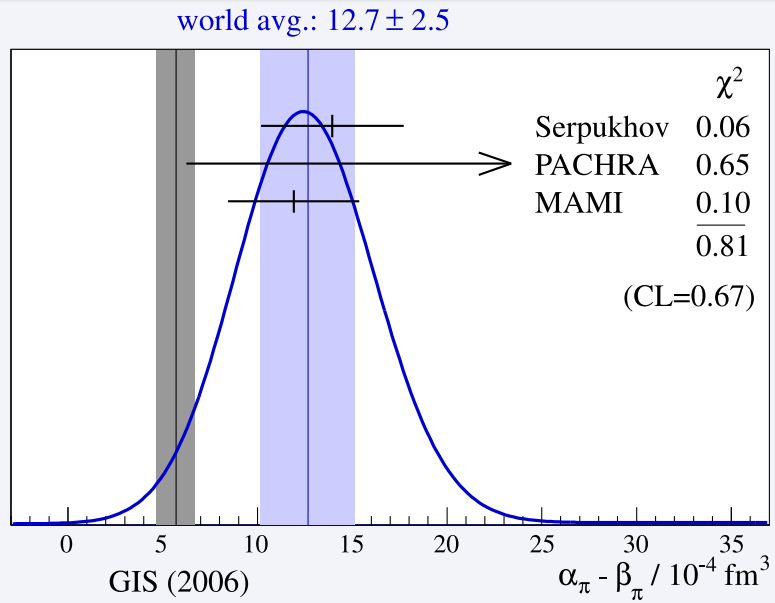

Charged-Pion Polarizability at COMPASS

Primakoff-Compton process

- Coulomb field of Ni nucleus
  - Typical field strength at $5R_{\text{nucl}}$ distance: $E = \mathcal{O}(300\ \text{kV/fm})$
  - Charge separation $\mathcal{O}(10^{-5}\ \text{fm} \cdot e)$
- Emission of Bremsstrahlung
  - Scattering off equivalent photons (Weizsäcker-Williams)
  - Pion Compton scattering
- Polarizability lowers Compton cross section
- Identify exclusive reactions at lowest momentum transfer $< 1.5 \cdot 10^{-3}\ (\text{GeV}/c)^2$

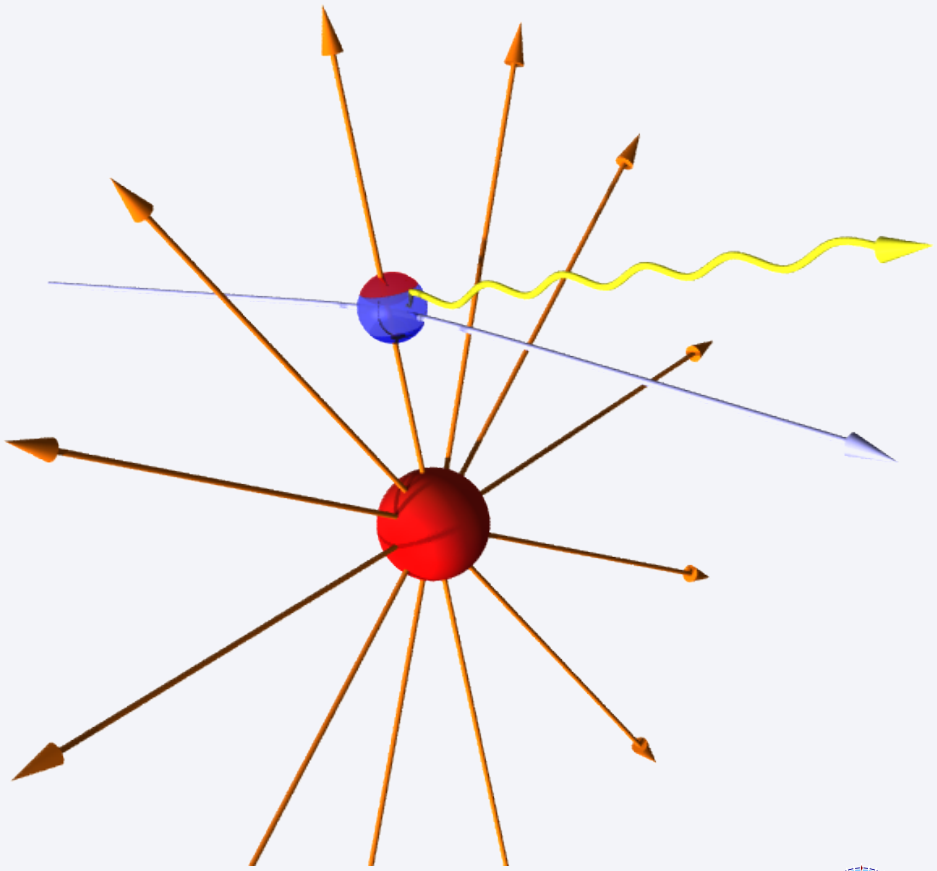

Charged-Pion Polarizability at COMPASS

Primakoff-Compton process

- Coulomb field of Ni nucleus
  - Typical field strength at $5R_{\text{nucl}}$ distance: $E = \mathcal{O}(300\ \text{kV/fm})$
  - Charge separation $\mathcal{O}(10^{-5}\ \text{fm} \cdot e)$
- Emission of Bremsstrahlung
  - Scattering off equivalent photons (Weizsäcker-Williams)
  - Pion Compton scattering
- Polarizability lowers Compton cross section
- Identify exclusive reactions at lowest momentum transfer $< 1.5 \cdot 10^{-3}\ (\text{GeV}/c)^2$

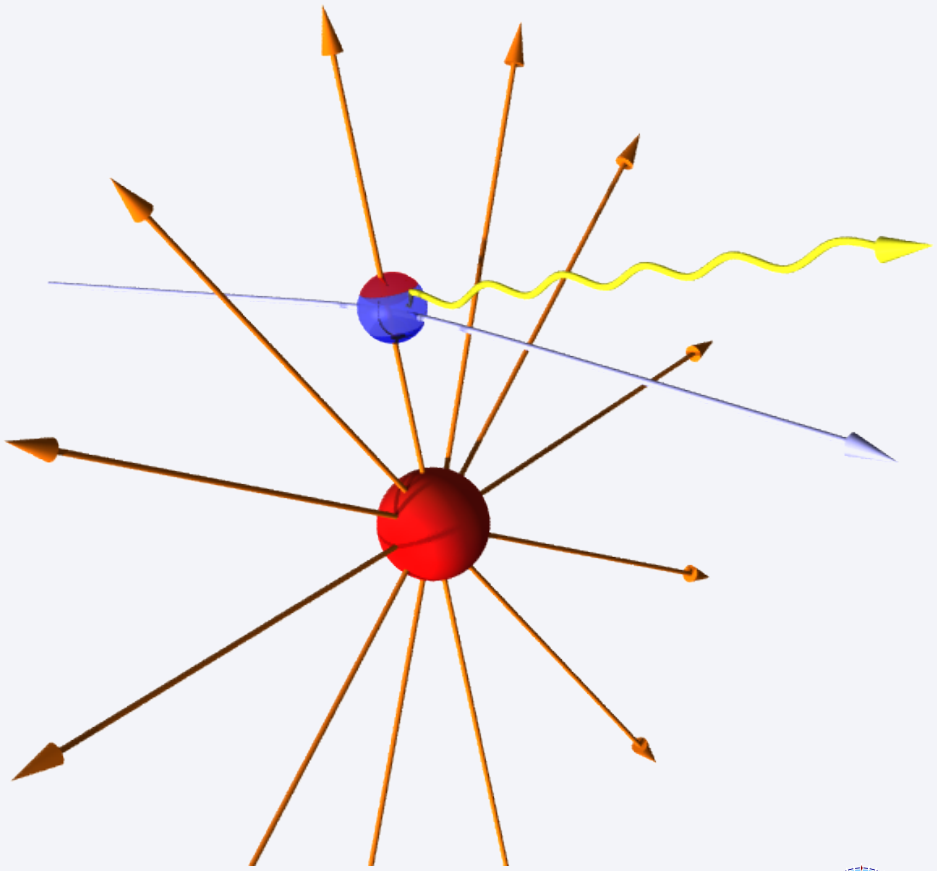

Charged-Pion Polarizability at COMPASS

Primakoff-Compton process

- Coulomb field of Ni nucleus
  - Typical field strength at $5R_{\text{nucl}}$ distance: $E = \mathcal{O}(300\ \text{kV/fm})$
  - Charge separation $\mathcal{O}(10^{-5}\ \text{fm} \cdot e)$
- Emission of Bremsstrahlung
  - Scattering off equivalent photons (Weizsäcker-Williams)
  - Pion Compton scattering
- Polarizability lowers Compton cross section
- Identify exclusive reactions at lowest momentum transfer $< 1.5 \cdot 10^{-3}\ (\text{GeV}/c)^2$

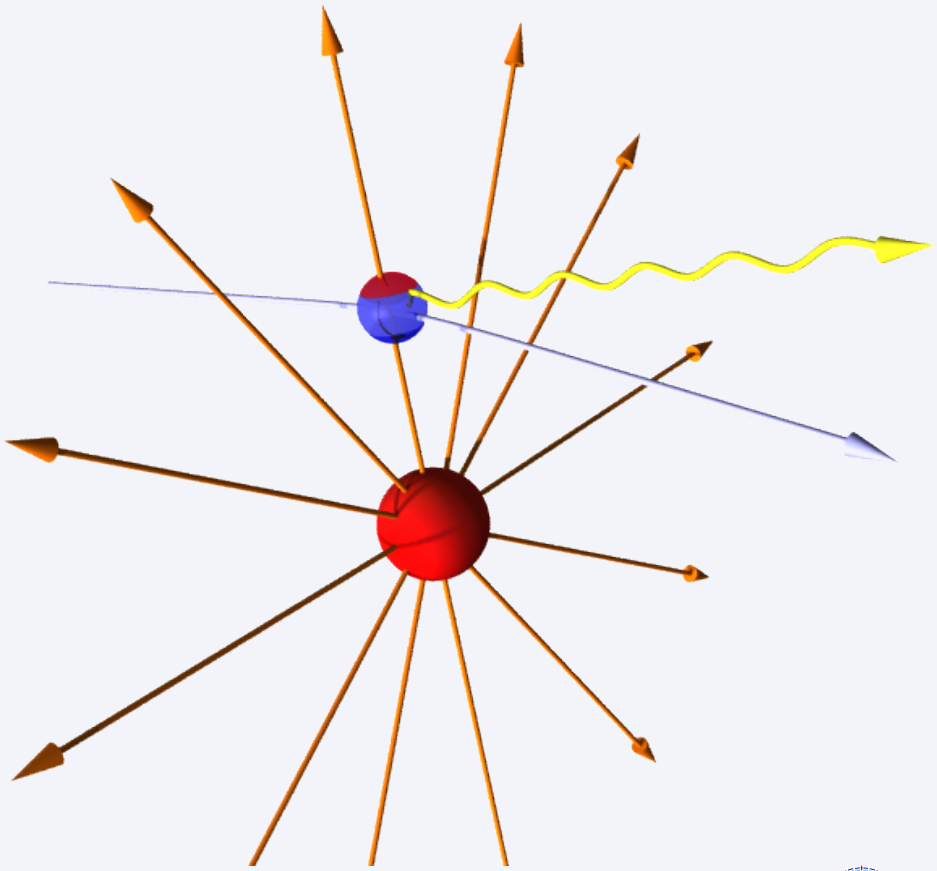

Method of Charged-Pion Polarizability Extraction

Primakoff-Compton cross section

- Decomposition into Born-term for point-like particle and term that depends on polarizability

$$\frac{\mathrm{d}\sigma_{\pi\gamma}}{\mathrm{d}E_\gamma} = \frac{\mathrm{d}\sigma_{\mathrm{Born}}}{\mathrm{d}E_\gamma} + \frac{\mathrm{d}\sigma_{\mathrm{pol}}}{\mathrm{d}E_\gamma}$$

- Cross section ratio as function of $x_\gamma \equiv E_\gamma / E_{\mathrm{beam}}$

$$R(x_\gamma) \equiv \frac{\mathrm{d}\sigma_{\pi\gamma} \,/\, \mathrm{d}x_\gamma}{\mathrm{d}\sigma_{\mathrm{Born}} \,/\, \mathrm{d}x_\gamma} \approx 1 + \frac{3}{2}\,\frac{m_\pi^3}{\alpha_{\mathrm{em}}}\,\frac{x_\gamma^2}{1-x_\gamma}\,\alpha_\pi$$

- Combine extraction of polarizability with acceptance correction

$$R(x_\gamma) = \frac{1}{c}\,\frac{N_{\mathrm{meas}}(x_\gamma)}{N_{\mathrm{sim}}^{\mathrm{Born}}(x_\gamma)}$$

  - $N_{\mathrm{meas}}(x_\gamma)$ number of measured events in x_γ bin
  - $N_{\mathrm{sim}}^{\mathrm{Born}}(x_\gamma)$ number of simulated events in detector acceptance assuming point-like particle
  - Nuisance parameter c fixed by $R(x_\gamma = 0) = 1$

Control Measurement with Muon Beam

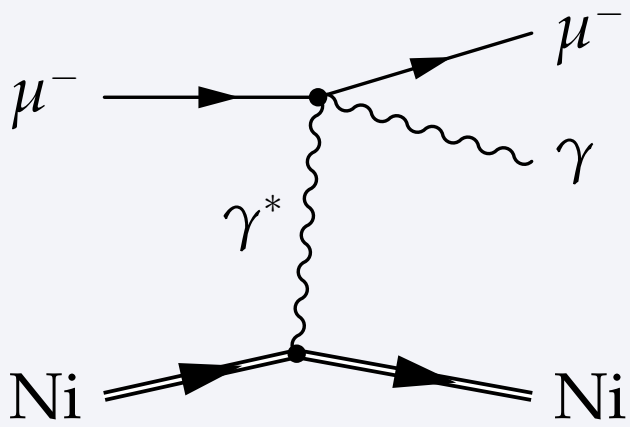

$$\alpha_\mu^{\text{false}} = (0.64 \pm 0.52_{\text{stat}}) \cdot 10^{-4}\,\text{fm}^3$$

- Compatible with zero

$N_{\text{meas}}(x_\gamma)$, $N_{\text{sim}}^{\text{Born}}(x_\gamma)$

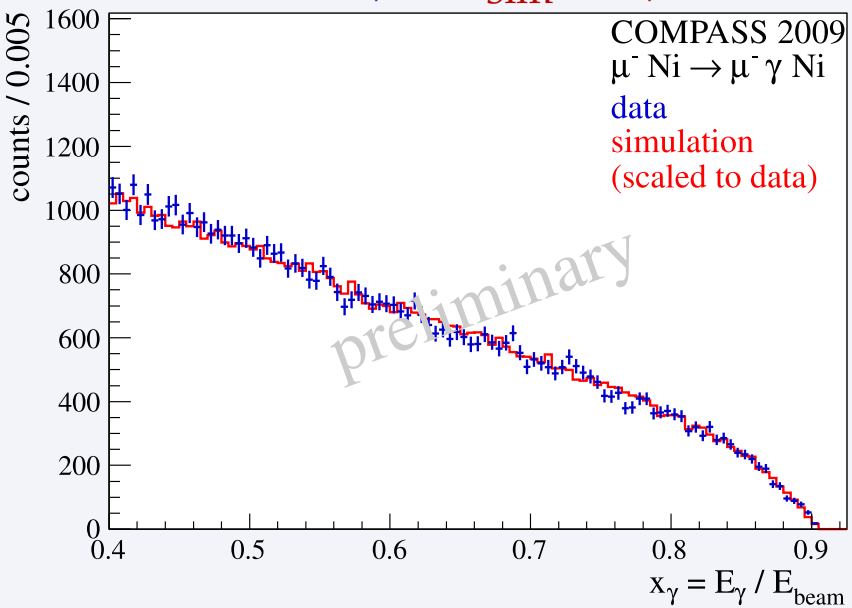

Cross section ratio $R(x_\gamma)$

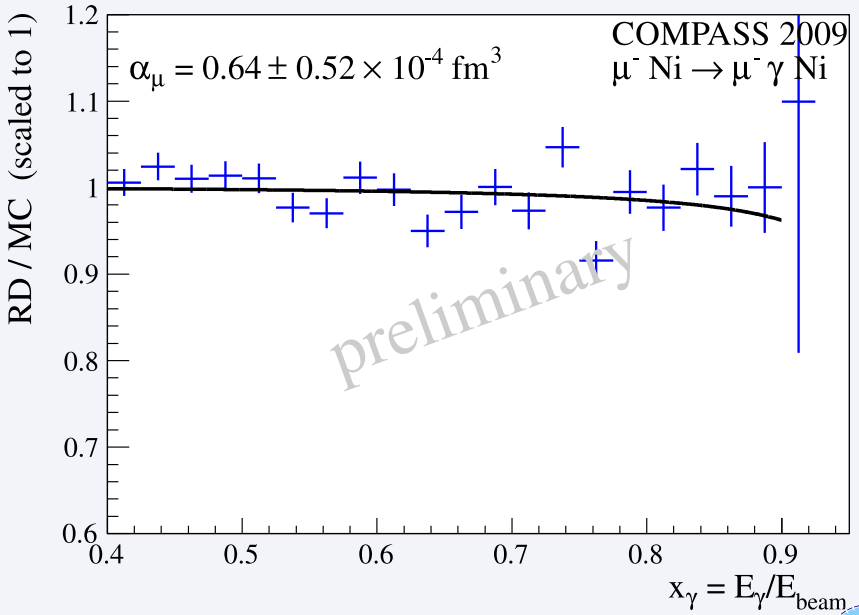

Identifying the $\pi^-\gamma \to \pi^-\gamma$ Reaction

Exclusivity

- $\Delta E \equiv E_{\mu,\pi} + E_\gamma - E_{\text{beam}}$
- 30 000 exclusive events around $\Delta E = 0$ (cf. Serpukhov $\approx 7\,000$)
- Resolution $\sigma_{\Delta E} \approx 2.6\,\text{GeV}$
- $\pi^-\gamma$ data: non-exclusive background at negative ΔE

$\mu^-\gamma$ control data

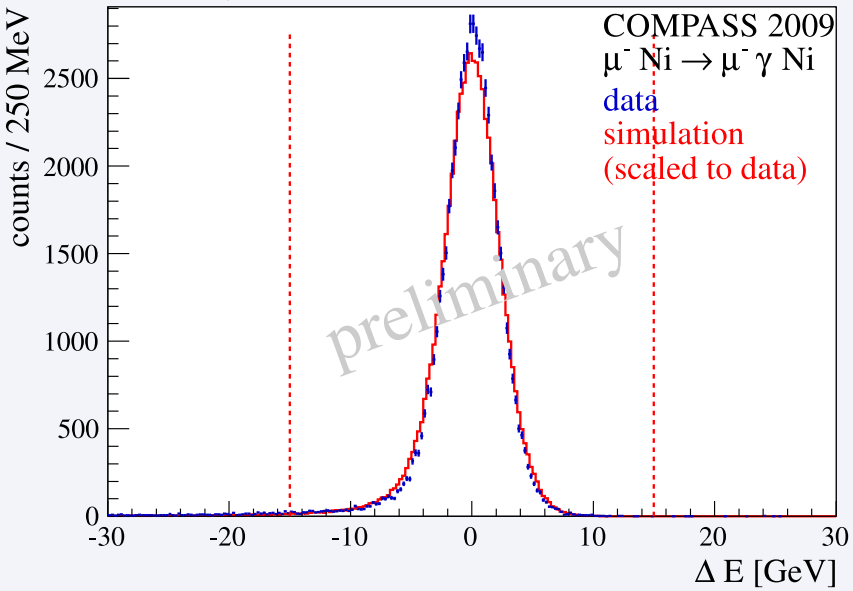

$\pi^-\gamma$ data

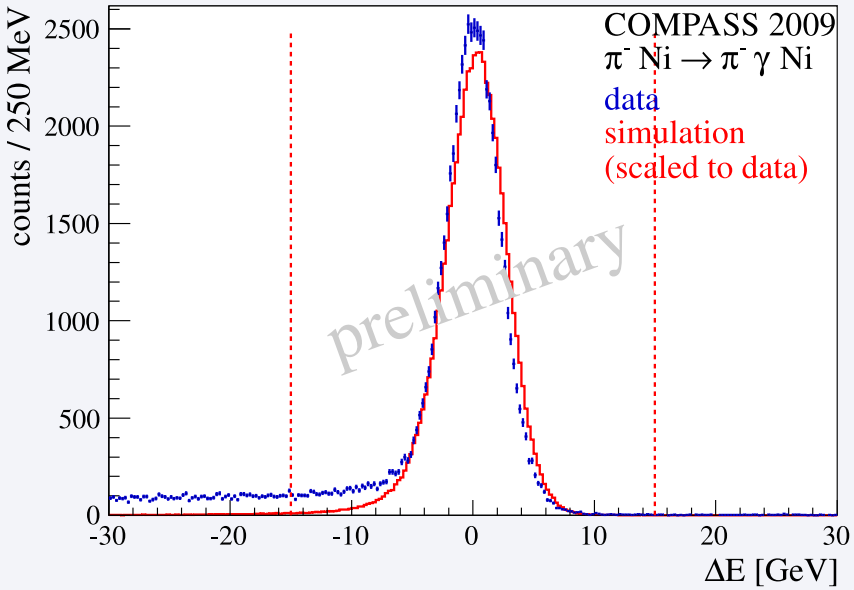

Identifying the $\pi^-\gamma \to \pi^-\gamma$ Reaction

Primakoff Peak

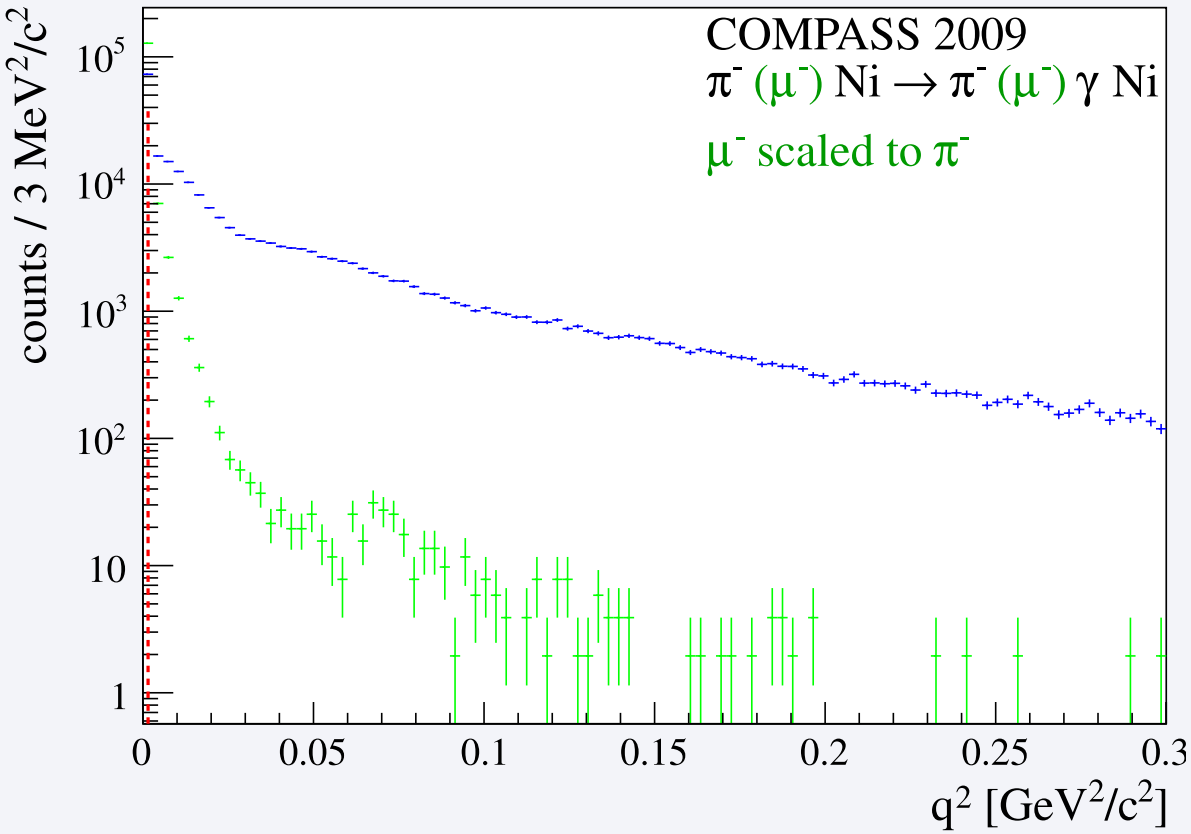

- Photon-exchange peak in first bin

Identifying the $\pi^-\gamma \to \pi^-\gamma$ Reaction

Primakoff Peak

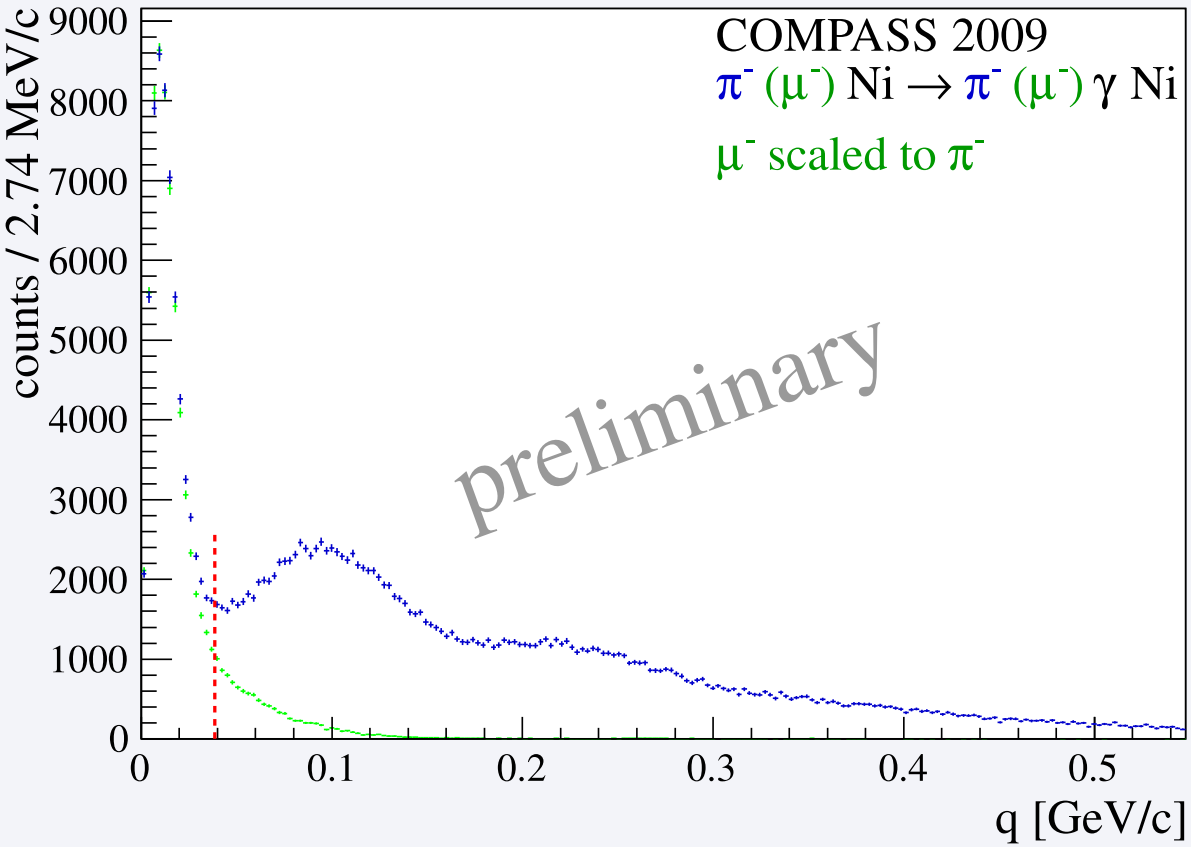

- Peak at $Q_T \approx 12$ MeV/c (cf. beam: 190 GeV/c)
  - Requires few-µrad angular resolution
- First diffractive minimum on Ni nucleus at $Q \approx 190$ MeV/c

Charged-Pion Polarizability at COMPASS

After background subtraction

$N_{\text{meas}}(x_\gamma)$, $N_{\text{sim}}^{\text{Born}}(x_\gamma)$

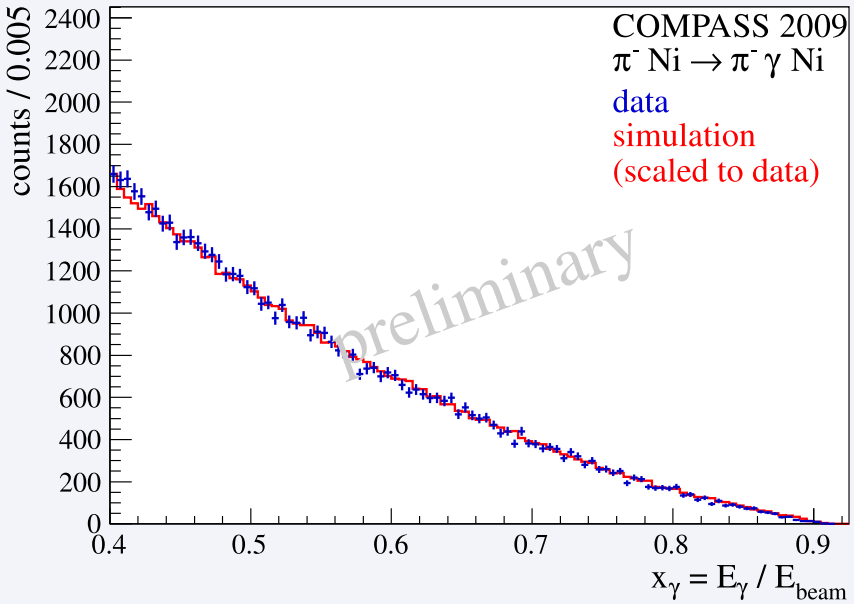

Cross section ratio $R(x_\gamma)$

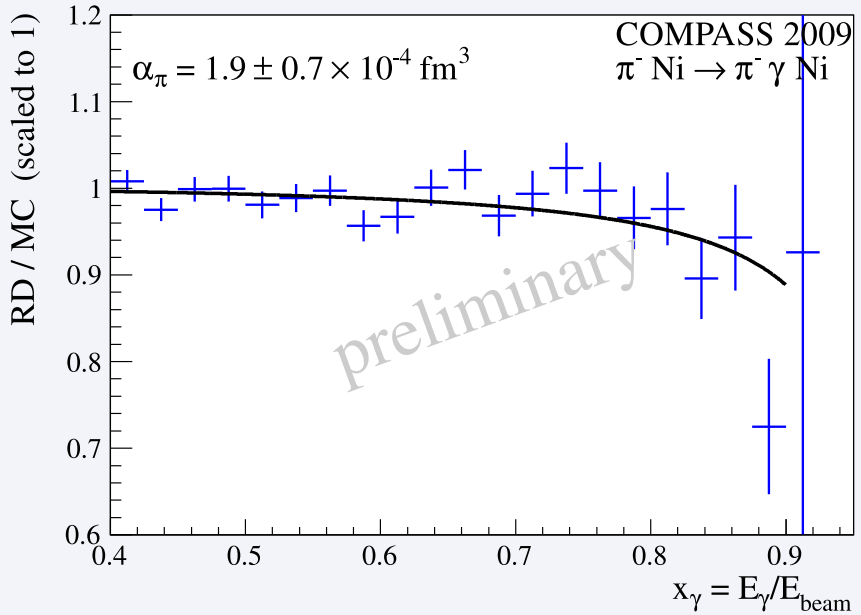

Preliminary result

$$\alpha_\pi = (1.9 \pm 0.7_{\text{stat}} \pm 0.8_{\text{sys}}) \cdot 10^{-4}\ \text{fm}^3$$

- Determined under assumption $\alpha_\pi + \beta_\pi = 0$
- Systematic uncertainty from sources common to pions and muons $\approx 0.6 \cdot 10^{-4}\,\text{fm}^3$

Charged-Pion Polarizability at COMPASS

After background subtraction

Background fraction

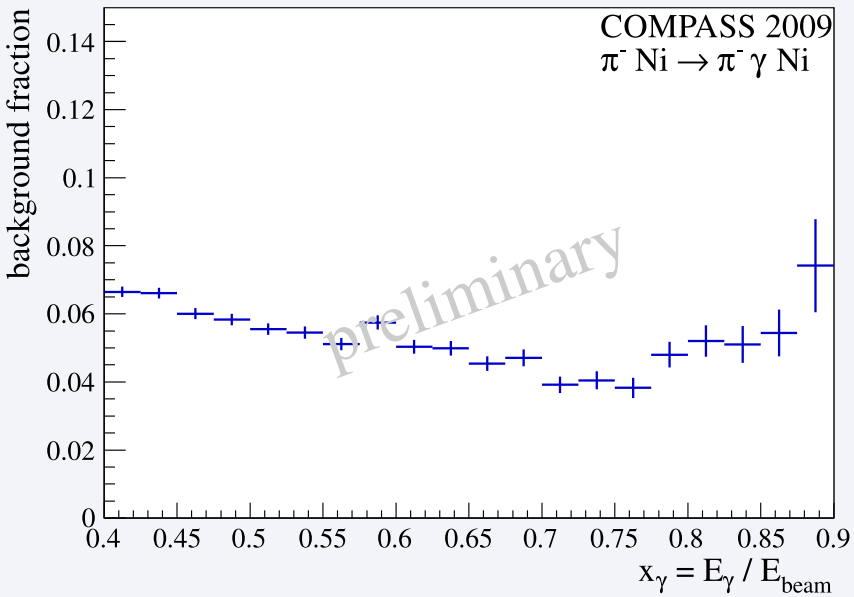

Cross section ratio $R(x_\gamma)$

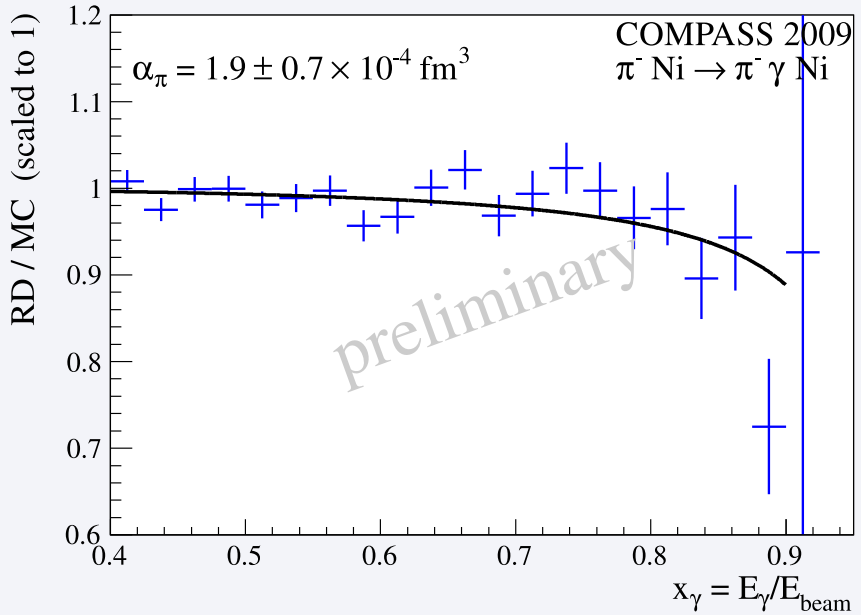

Preliminary result

$$\alpha_\pi = (1.9 \pm 0.7_{\text{stat}} \pm 0.8_{\text{sys}}) \cdot 10^{-4}\ \text{fm}^3$$

- Determined under assumption $\alpha_\pi + \beta_\pi = 0$
- Systematic uncertainty from sources common to pions and muons $\approx 0.6 \cdot 10^{-4}\,\text{fm}^3$

Charged-Pion Polarizability at COMPASS

After background subtraction

Background fraction

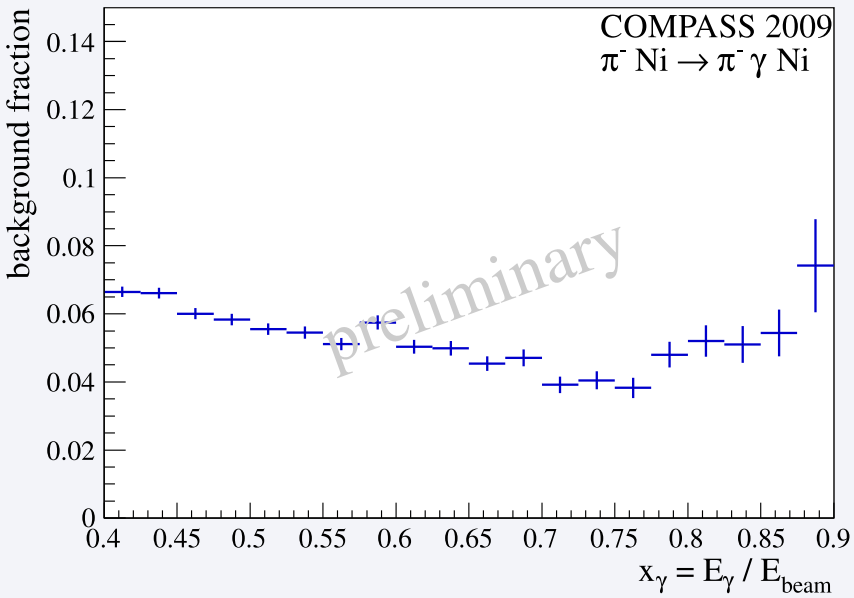

Cross section ratio $R(x_\gamma)$

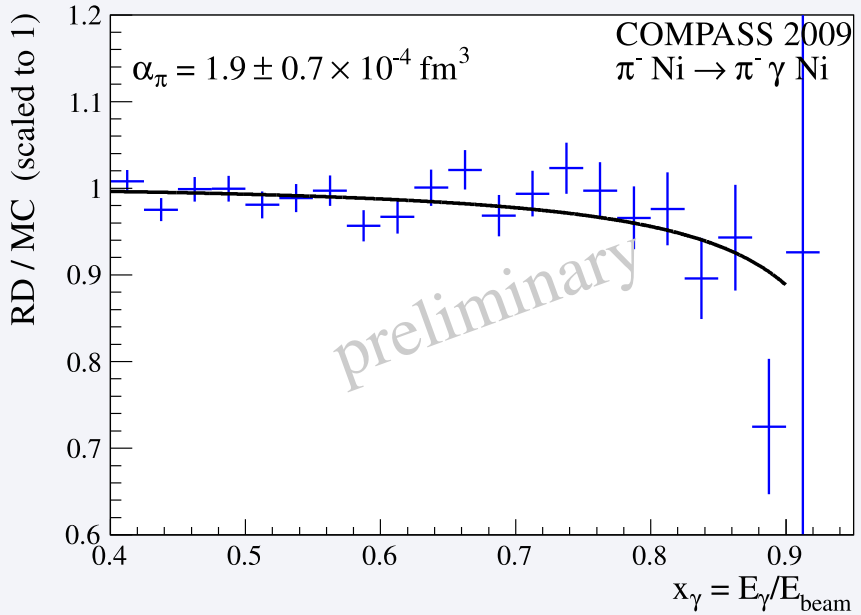

Preliminary result

$$\alpha_\pi = (1.9 \pm 0.7_{\text{stat}} \pm 0.8_{\text{sys}}) \cdot 10^{-4}\ \text{fm}^3$$

- Determined under assumption $\alpha_\pi + \beta_\pi = 0$
- Systematic uncertainty from sources common to pions and muons $\approx 0.6 \cdot 10^{-4}\,\text{fm}^3$

Charged-Pion Polarizability at COMPASS

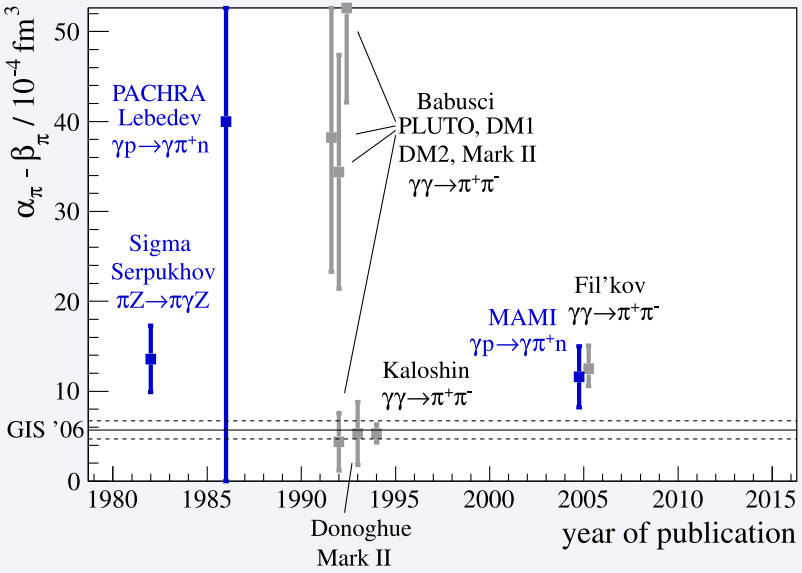

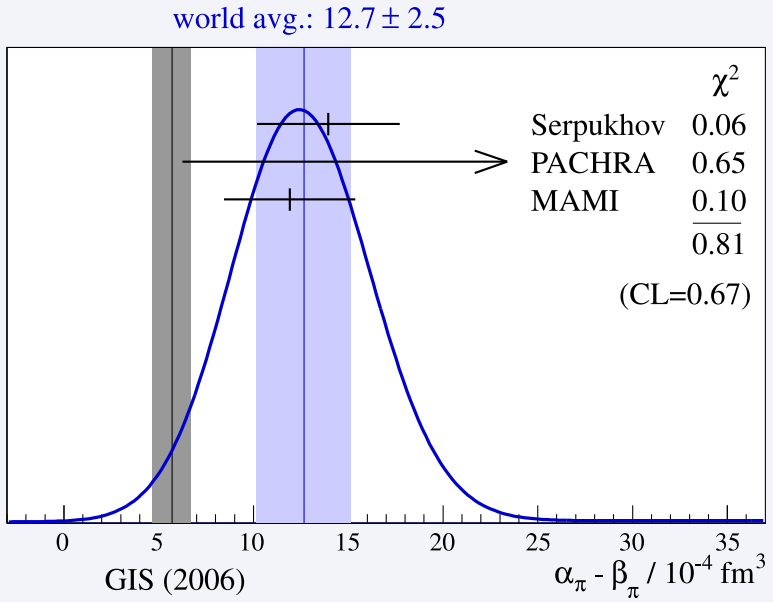

Preliminary result

$$\alpha_\pi = (1.9 \pm 0.7_{\text{stat}} \pm 0.8_{\text{sys}}) \cdot 10^{-4} \text{ fm}^3$$

- Most precise measurement to date
- Resolves tension between experimental average and χPT prediction
- In tension with earlier measurements

Charged-Pion Polarizability at COMPASS

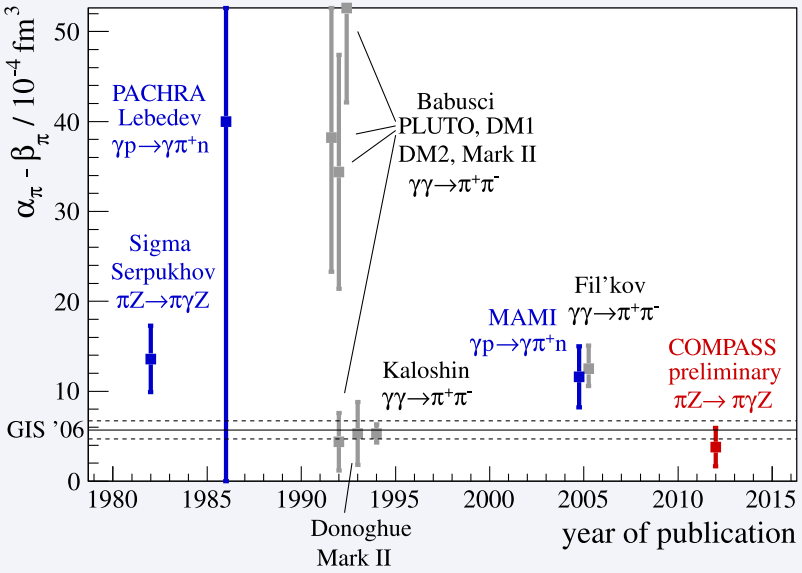

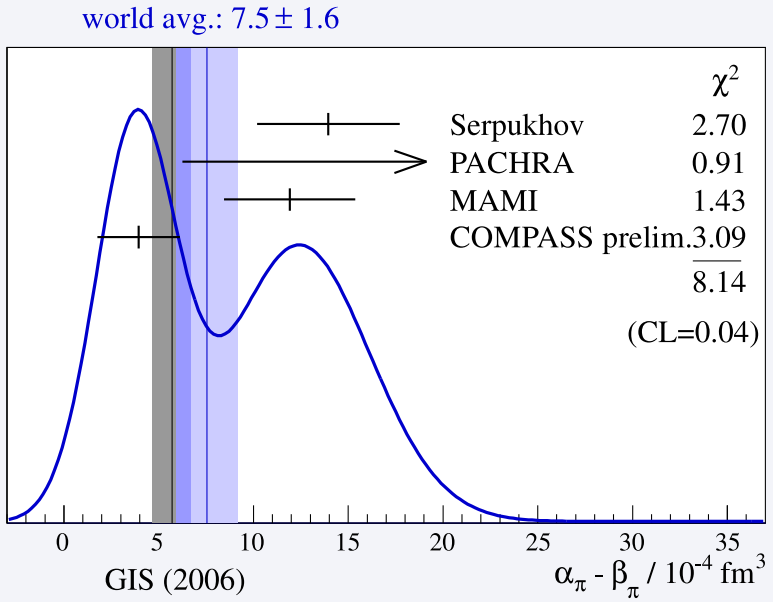

Preliminary result

$$\alpha_\pi = (1.9 \pm 0.7_{\text{stat}} \pm 0.8_{\text{sys}}) \cdot 10^{-4} \text{ fm}^3$$

- Most precise measurement to date
- Resolves tension between experimental average and χPT prediction
- In tension with earlier measurements

Future Measurement: Polarized Drell-Yan (2014)

$\pi p^{\Uparrow} \to \mu^+\mu^- X$

- Intense 190 GeV/c π^- beam on transversely polarized p target
- u-quark dominance
  - $\bar{u}$ from π^- annihilates with u from nucleon
- Hadron absorber

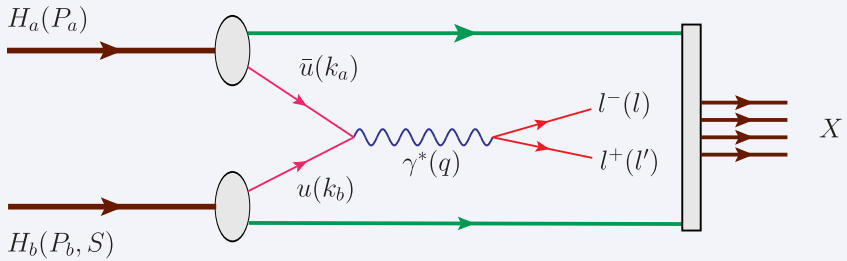

Azimuthal cross section asymmetries

- Access $k_\perp$-dependent PDFs: Sivers, Boer-Mulders
- Test of factorization by comparing to SIDIS
  - DY: convolution of two TMDs
  - SIDIS: convolution of TMD and fragmentation function

Future Measurement: Polarized Drell-Yan (2014)

$\pi p^{\Uparrow} \rightarrow \mu^+\mu^- X$

- Intense 190 GeV/c π^- beam on transversely polarized p target
- u-quark dominance
  - $\bar{u}$ from π^- annihilates with u from nucleon
- Hadron absorber

Azimuthal cross section asymmetries

- Access $k_\perp$-dependent PDFs: Sivers, Boer-Mulders
- Test of factorization by comparing to SIDIS
  - DY: convolution of two TMDs
  - SIDIS: convolution of TMD and fragmentation function

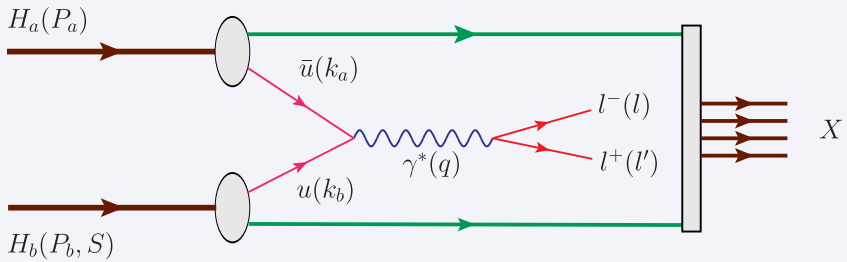

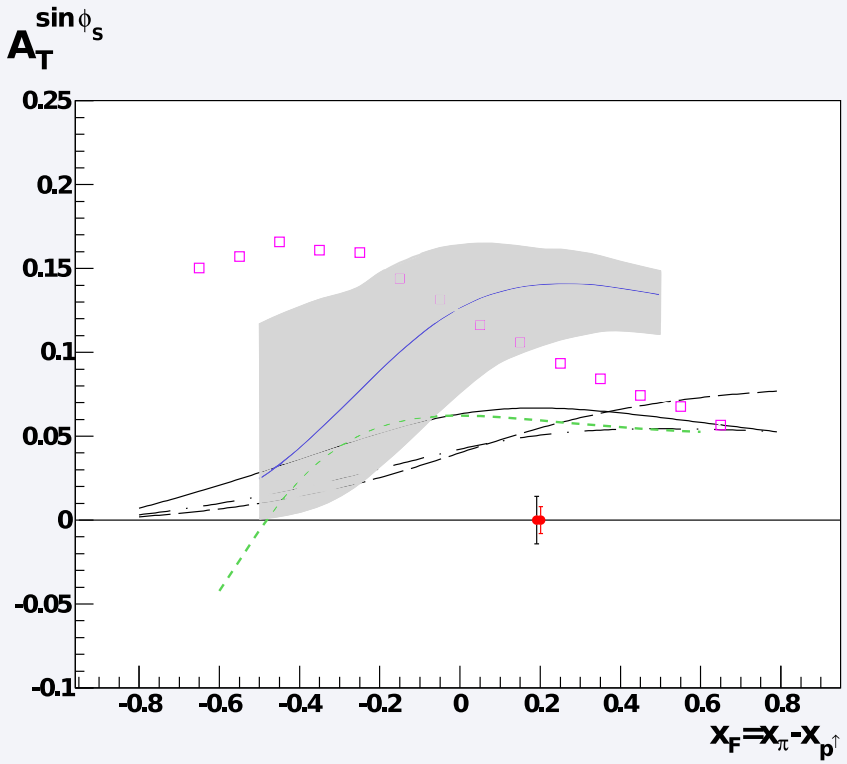

Future Meas.: Generalized Parton Distributions (2015-16)

Access via DVCS and HEMP

- *Goal:* 3D image of partonic structure of nucleon
- $\mu^{+\leftarrow}$ and $\mu^{-\rightarrow}$ beams on unpolarized ℓH_2 target
  - Measure beam-charge/spin cross section sum
    $$\frac{d\sigma_{DVCS}}{d|t|} \propto e^{-B|t|}; \quad B(x_{Bj}) \propto \langle r_\perp^2(x_{Bj}) \rangle$$
  - Transverse imaging of the nucleon
  - Contraint GPDs via azimuthal dependence of beam-charge/spin sum and difference

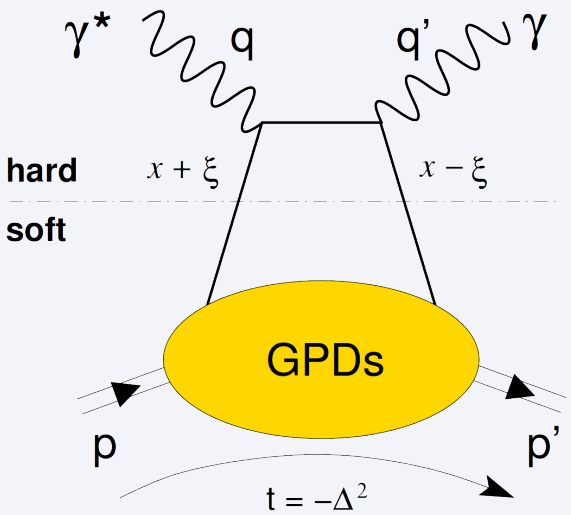

Future Meas.: Generalized Parton Distributions (2015-16)

Access via DVCS and HEMP

- *Goal:* 3D image of partonic structure of nucleon
- $\mu^{+\leftarrow}$ and $\mu^{-\rightarrow}$ beams on unpolarized ℓH_2 target
  - Measure beam-charge/spin cross section sum

$$\frac{d\sigma_{DVCS}}{d|t|} \propto e^{-B|t|}; \quad B(x_{Bj}) \propto \langle r_\perp^2(x_{Bj}) \rangle$$

  - Transverse imaging of the nucleon
  - Contraint GPDs via azimuthal dependence of beam-charge/spin sum and difference